MITOCHONDRIAL DNA MUTATIONS IN CANCER

THE PHENOTYPIC IMPACT OF MITOCHONDRIAL DNA MUTATIONS IN CANCER

By

ADAM GEMIN, B.Sc.

A Thesis

Submitted to the School of Graduate Studies

in Partial Fulfillment of the Requirements

for the Degree

Masters of Science

McMaster University

MASTERS OF SCIENCE (2003) McMaster University

(Biochemistry) Hamilton, Ontario

TITLE: The Phenotypic Impact of Mitochondrial DNA Mutations in Cancer

AUTHOR: Adam Gemin, B.Sc. (Guelph University)

SUPERVISOR: Professor G. Singh (Dalhousie University)

NUMBER OF PAGES: xiv; 132

BIBLIOGRAPHY

Abstract:

Gemin, A. and Singh, G. 2002. Retention of mitochondrial morphological and biochemical phenotype in cybrids. Mitochondria and Choloroplast Gordon Research Conference, Oxford, England.

Abstract

Mitochondrial DNA (mtDNA) aberrations have been detected in a large proportion of tissue samples isolated from human tumours, although the functional significance of these mutations is yet to be determined. Proponents of the selective advantage mtDNA defect acquisition model believe these mutations arise spontaneously, but propagate because they afford some benefit to overall neoplastic cell proliferation. The most tantalizing of these growth advantage properties is an elevation of electron transport chain (ETC) generated reactive oxygen species (ROS), which are already associated with some pathogenic mtDNA defects. However, others theorize that these mutations may arise spontaneously and expand through the ambivalent process of genetic drift alone. The 2008 human ovarian cancer cell line and its cis-platinum(II)-diammine-dichloride (CDDP) resistant C13* cell variant have divergent phenotypes when mitochondrial morphology, membrane potential ($\Delta\Psi_M$), ROS production, and rate of oxygen consumption are considered. Furthermore, the increased $\Delta\Psi_M$ observed in C13* cells has been implicated in its CDDP resistant characteristic. In order to determine if mtDNA mutations were responsible for these phenotypic variations, the complete mitochondrial genomes of both cell lines were directly sequenced. Two novel mtDNA mutations were identified within cytochrome c oxidase subunit II (COXII) and the d-loop of 2008 and C13* cells respectively, however the functional significance of these defects were not obvious. To expunge the effects of nuclear DNA (nDNA) cybrids were created by transferring the mtDNA of 2008 and C13* cells to a common 143B TK^- nDNA background, creating 2008cyb and C13cyb cells. C13*cyb cells did not demonstrate

CDDP resistance, decrease in rate of oxygen consumption or increase in $\Delta\Psi_M$ when compared to 2008cyb cells. However, C13*cyb cells did retain mitochondrial morphological properties as well as increased Rh123 sensitivity and ROS production. This data would imply that mtDNA mutations are responsible for a proportion of mitochondrial-associated changes in the context of carcinogenesis.

Acknowledgements

I would first like to thank my supervisor, Dr. Gurmit Singh for his support and guidance throughout the course of my graduate work. I would also like to thank both Dr. Mark Tarnopolsky and Dr. Radhey Gupta who served as helpful members of my supervisory committee. Arkan Abadi, Nisha Anand, Leigh Wilson, Scott Su, and Dr. Tom Preston, all past and present McMaster graduate students, also deserve a great deal of thanks for their intellectual input and more importantly their friendship both in and out of the laboratory. The helpful scientific advice I have received from Paul Northcott, Grace Trentin, Dr. Hong Wang, and Dr. Subir Chowdhury, was also indispensable and greatly appreciated. Operating grants to Dr. G. Singh from the Canadian Institutes of Health Research (CIHR) were responsible for the financial support of this work.

Most importantly, I would like to thank my parents and siblings Daniella and Eric for their support (of all kinds) throughout both my undergraduate and graduate studies.

List of Abbreviations

ε	Extinction cofficient
ρ^o	mtDNA deficient
$\Delta\psi_M$	Mitochondrial membrane potential
$(NH_4)_2SO_4$	Ammonium sulfate
12S rRNA	12S ribosomal RNA
16S rRNA	16S ribosomal RNA
95% CI	95% Confidence Interval
AD	Alzheimer's Disease
ADP	Adenosine 5'-diphosphate
ANT	Adenine Nucleotide Translocator
ATP	Adenosine 5'-triphosphate
ATPase 6	ATP synthase subunit 6
ATPase8	ATP synthase subunit 8
BRDU	5-bromo-2'-deoxyuridine
CCCP	Carbonyl cyanide m-chlorophenylhydrazone
CDDP	Cis-platinum(II)-diammine-dichloride
CO_2	Carbon Dioxide
CoQ	Coenzyme Q_{10}
COX	Cytochrome c Oxidase
COXI	Cytochrome c Oxidase subunit I
COXII	Cytochrome c Oxidase subunit II
COXIII	Cytochrome c Oxidase subunit III
CPEO	chronic progressive external ophthalmoplegia
CS	Citrate Synthase
CSBI	Conserved Sequence Block I
CSBII	Conserved Sequence Block II
CSBIII	Conserved Sequence Block III
CuZnSOD	Copper Zinc Superoxide Dismutase
d-loop	Displacement loop
DMEM	Dulbecco's minimal essential medium
DMSO	Dimethyl sulfoxide
DNA	Deoxyribonucleic acid
DTT	Dithiothreitol
EDTA	Ethylenediaminetetraacetic acid
EMSA	Electromobility Shift Assay
ERK	Extracellular signal-regulated kinases
ETC	Electron Transport Chain
FCS	Fetal Calf Serum
GCCR	Glycerophosphate cytochrome c reductase
GPx	Glutathione Peroxidase
H_1	Heavy strand promoter 1
H_2	Heavy strand promoter 2

H_2O_2	Hydrogen peroxide
HRP	Horseradish Peroxidase
IC50	Inhibitory Concentration of 50% of population
JNK	c-Jun N-terminal Kinases
KCl	Potassium Chloride
KSS	Kearns-Sayre syndrome
LHON	Leber's hereditary optic neuropathy
MAPK	Mitogen-activated protein kinases
MELAS	Mitochondrial encephalomyopathy, lactic acidosis with stroke-like episodes
$MgCl_2$	Magnesium Chloride
MnSOD	Manganese Superoxide Dismutase
mtDNA	Mitochondrial DNA
mTERF	Mitochondrial transcription termination factor
mtRNApol	Mitochondrial RNA polymerase
mtTFA	Mitochondrial Transcription Factor A
NaCl	Sodium Chloride
NAD^+	Nicotinomide adenine dinucleotide (oxidized form)
NADH	Nicotinomide adenine dinucleotide (reduced form)
NAO	10-N-Nonyl acridine orange
NaOH	Sodium Hydroxide
NARP	Neurological muscle weakness, ataxia, and retinitis pigmentosa
ND1	NADH Dehydrogenase Subunit 1
ND2	NADH Dehydrogenase Subunit 2
ND3	NADH Dehydrogenase Subunit 3
ND4	NADH Dehydrogenase Subunit 4
ND4L	NADH Dehydrogenase Subunit 4L
ND5	NADH Dehydrogenase Subunit 5
ND6	NADH Dehydrogenase Subunit 6
nDNA	Nuclear DNA
NTH1	Endonuclease III homolog
$O_2.-$	Superoxide anion
OGG1	8-Oxoguanine glycosylase 1
O_H	Heavy strand origin of replication
$OH^·$	Hydroxl radical
O_L	Light strand origin of replication
OXPHOS	Oxidative Phosphorylation
PBS	Phosphate Buffered Saline
PCR	Polymerase Chain reaction
PD	Parkinson's disease
PEG	Polyethylene glycol
RFLP	Restriction Fragment Length Polymorphism
Rh123	Rhodamine 123
RNA	Ribonucleic Acid

RNAse	Ribonuclease
ROS	Reactive Oxygen Species
RRFs	Ragged Red Fibers
rRNA	Ribosomal RNA
SCCR	Succinate cytochrome c reductase
SDS	Sodium dodecyl sulfate
TASs	Termination Associated Sequences
TK^-	Thymidine Kinase deficient
TMRM	Tetra-methyl rhodium methyl ester
tRNA	Transfer RNA
TTGE	Temporal temperature gradient gel electrophoresis
TUNEL	Tat-mediated dUTP nick-end labeling
UDG	Uracil-DNA glycosylase

Table of Contents

List of Figures

1.0 Introduction

2.0 Materials and Methods

3.0 Results

List of tables

1.0 Introduction

1.1 Mitochondrial OXPHOS and mtDNA genomics

Organelles of eukaryotic cells, mitochondria are hypothesized to have arisen 1.5 billion years ago when aerobic bacteria capable of oxidative phosphorylation (OXPHOS) took up residence within an anaerobic eukaryotic host cell (Wallace 1999; Carew and Huang 2002). These organelles are approximately 1 μm in diameter with variable length and comprise up to 15% of the total cellular protein (Schatz 1995). Similar to gram-negative bacteria, the mitochondrion is enclosed by two membrane bilayers. The outer membrane is permeable to small molecules and ions. Transmembrane pores composed of the protein porin span the outer membrane, allowing passage of molecules with a molecular weight of less than 5,000 to the inner membrane space (Lehninger et al. 1997). In contrast, the inner membrane is relatively impermeable, precluding the movement of molecules without specific transporters. The inner membrane is folded into cristae that increase the surface area available for insertion of electron transport chain proteins needed for OXPHOS. This membrane also serves to surround the matrix which house mitochondrial DNA (mtDNA), ribosomes and enzymes used in the citric acid cycle and fatty acid oxidation (See Figure 1.1) (Lehninger et al. 1997).

Regarded as the powerhouse of the cell, mitochondria produce 90% of the cellular adenosine triphosphate (ATP) through OXPHOS (Wallace 1997). However, this molecule is not easily manufactured, and ATP produced by the process of OXPHOS involves the transfer of electrons between a series of enzymes that form the electron transport chain (ETC). The ETC is comprised of five protein complexes (Complex I to V) that serve to

oxidize hydrogen derived from the oxidation of organic acids such as pyruvate and fatty acids with atomic oxygen to generate water (Wallace 1999). Electrons carried on NAD^+ (nicotinamide adenine dinucleotide) are transferred to complex I (NADH dehydrogenase) and then to coenzyme Q_{10} (CoQ), while electrons from succinate produced in the tricarboxylic acid (TCA) cycle are transferred through complex II (Succinate dehydrogenase, SDH) to CoQ (Coenen et al. 2001). Electrons bound to CoQ are transferred to complex III and from there to complex IV (cytochrome c oxidase, COX) by way of cytochrome c (Borisov 2002). Once at complex IV electrons are donated to $½ O_2$ to render H_2O. The energy released during this process is harnessed to pump protons (H^+) out of the inner membrane of the mitochondria, thus creating an electrochemical gradient ($\Delta\Psi_M$) that is negative on the matrix side (Wallace 1992). The resulting unequal proton distribution across the inner membrane is essentially a capacitor whose energy may be dissipated with reentry of protons into the matrix, which occurs mainly through a proton channel in the F_0 portion of ATP synthase (complex V) (Hatefi 1985). This well orchestrated movement of protons in and out of the mitochondrial matrix drives the condensation of ADP (adenosine diphosphate) and P_i (inorganic phosphate) to produce ATP (Wallace 1999). The ANT (adenine nucleotide translocator) then transports ATP into the cytosol in exchange for spent ADP (Buck et al. 2003). In this fashion, oxygen consumed by the ETC is coupled to ADP phosphorylation by way of ATP synthase through the electrochemical gradient, $\Delta\Psi_M$ (Mandavilli et al. 2002) (See Figure 1.1).

The human ETC is comprised 87 proteins that are assembled to form five enzyme complexes depicted in Figure 1.1 (Grossman 1995). The majority of these proteins are

translated from genes on nDNA, while only 13 are translated from genes located within mtDNA (Penta et al. 2001; Liu et al. 2001). It is believed that the bifurcation of ETC genes occurred following the symbiotic relationship between a glycolytic proto-eukaryotic cell and an oxidative bacterium (Wallace 1999). Presumably, non-essential mtDNA genes were lost, while essential exons were transferred to the nucleus where they are transcribed into mRNAs, translated on cytoplasmic ribosomes and imported into the mitochondrion (Tully and Levin 2000). Today the human mitochondrial genome has been stripped down to a mere 16569 base pairs, which allows its rapid replication and ensures transmission to daughter cells at cytokinesis (Liu et al. 2001).

Located within the inner mitochondrial matrix, mtDNA is double stranded, circular, and comprises 0.1 to 1.0% of the total DNA in most mammalian cells(Singh et al. 1992). Each mitochondrion contains 2-10 copies of mtDNA, with each human cell containing in excess of 1000 copies (Wei 1992). The large number of mtDNA molecules per cell permits a state of mtDNA heteroplasmy in which both wild type and mutated genomes may exist within a given cell, tissue, or organ. Conversely, mitochondria that contain an exclusively wild-type or mutated population of mtDNA are termed homoplasmic (Penta et al. 2001). The occurrence of homoplasmy or degree of heteroplasmy within a population of cells may greatly impact phenotypic properties when mitochondrial diseases are considered (Disscussed further in mtDNA mutations in disease) (Schmiedel et al. 2003).

Human mtDNA contains a total of 37 genes coding for 22 tRNAs and 2 rRNAs, which are needed to synthesize the 13 electron transport chain proteins also located in the

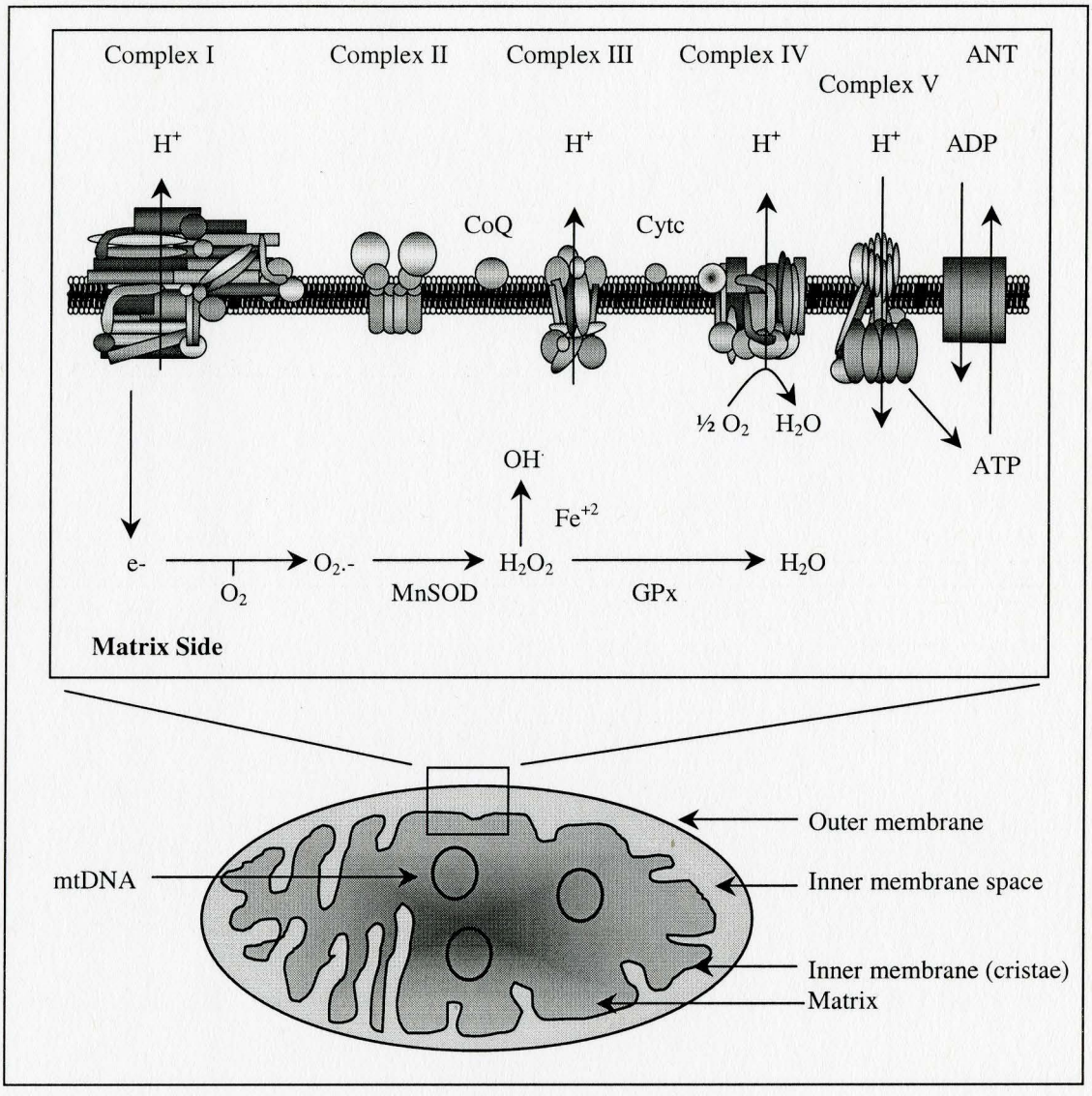

Figure 1.1: Schematic of the mitochondrion. Mitochondrial DNA is located within the matrix of the mitochondrion. The electron transport chain spans the inner membrane, transporting electrons that enter at complex I and II to complex IV where they react with atomic oxygen and hydrogen to form H_2O. Hydrogen ions pumped out of the matrix reenter through complex V. ATP produced at complex V is pumped out of the matrix through the ANT. MnSOD and GPx detoxify superoxide produced during OXPHOS.

genome (See Figure 1.2). Seven of these polypeptides (ND1, ND2, ND3, ND4, ND4L, ND5, and ND6) will assemble with 36 nDNA encoded proteins to form complex I (NADH dehydrogenase) (Weiss et al. 1991). Cytochrome b, also encoded by mtDNA, makes up one of 11 proteins comprising complex III(Coenen et al. 2001). Complex IV contains 13 protein subunits, 3 of which are translated from mtDNA (COXI, COXII, COXIII) (Coenen et al. 2001). Complex V (ATP synthase) contains the final 2 polypeptides (ATPase 6 and ATPase 8) encoded by the human mitochondrial genome (Hatefi 1985). Unlike the other complexes, complex II of the ETC is composed of four protein subunits all of nuclear origin (Mandavilli et al. 2002).

Mitochondrial gene products are transcribed from both sides of the double stranded mtDNA molecule by mitochondrial RNA polymerase (mtRNApol). Twenty-eight of the genes use the purine-rich heavy strand (H strand) as a template while the remaining nine are located on the pyrimidine-rich light strand (L strand) (Tully and Levin 2000). Genes are transcribed from both the H and L strand as polycistronic RNA products (Clayton 1991). It is believed that transcription of the heavy strand is mediated by the heavy strand promoter, which is actually two closely located initiation sites (H_1 and H_2) (Montoya et al. 1982; Bogenhagen et al. 1984). However, *in vitro* transcription assays have failed to show any detectable H_2 activity indicating that transcription initiation of both strands may occur at the same promoter (Fernandez-Silva et al. 2003). The upstream H_1 site produces a transcript of both 12S and 16S rRNAs, in addition to two tRNAs (Montoya et al. 1983). The downstream H_2 site results in the synthesis of a longer polycistronic transcript that spans the entire length of the heavy strand and contains 12

tRNAs, and 12 mRNAs. The shorter heavy strand transcript is produced at a 25-fold greater rate than the full-length transcript, ensuring that adequate quantities of 12S and 16S rRNAs will be available for protein translation (Montoya et al. 1983). The light strand promoter (L) is more active than the heavy strand promoter(s) and serves as the transcription start site of the light strand to produce eight tRNAs and one protein (ND6) (Tully and Levin 2000). Transcription of both heavy and light strands occurs in opposite directions and is controlled by mitochondrial transcription factor A (mtTFA) (Sewards et al. 1994). This 25kDa protein is nDNA encoded and binds, as a dimer, to heavy or light strand promoters, unwinding mtDNA (Clayton 1991). Binding of mtTFA introduces negative supercoils upon mtDNA, which increases the efficiency of transcription (Tully and Levin 2000). Heavy strand promoter activation occurs after multiple mtTFA molecules are bound, whereas binding of a single molecule is sufficient to initiate transcription of the light stand (Tully and Levin 2000). The mechanisms that cause transcription termination of H_2 and L RNA products are yet to be elucidated (Attardi and Schatz 1988). However, arrest of the H_1 RNA product is brought about at the 16 rRNA-$tRNA^{UUR}$ boundary in the presence of both a $tRNA^{UUR}$ 13 base pair sequence and a specific protein factor, human mitochondrial transcription termination factor (mTERF) (See Figure 1.2) (Christianson and Clayton 1988).

The interspersion of tRNA genes between both mRNA and rRNA genes facilitates the release of individual transcripts and involves four enzymatic reactions. First, RNase P acts to cleave heavy strand polycistronic transcripts on the 5' side of the tRNA (Rossmanith et al. 1995;Doersen et al. 1985). Next a 3' endonculease enzyme, yet to be

identified, cleaves transcripts on the 3'side of tRNA sequences (Fernandez-Silva et al. 2003). A stretch of adenine residues are then added to the 3' end of mRNA and rRNA molecules (~55 and 1-10 respectively) by poly(A)polymerase, and CCA is added to tRNAs through the action of tRNA nucleotidyl transferase (Tully and Levin 2000). Polyadenylation of mRNA stabilizes these molecules and generates stop codons on some mRNAs that are critical in their proper translation (Ojala et al. 1981). Most mature poly(A)-RNAs encode a single gene product, however the mRNA for ND4 and ND4L and ATPase 6 and ATPase 8 contain two overlapping reading frames (Fernandez-Silva et al. 2003).

Translation of mitochondrial ETC polypeptides takes place within the mitochondria on mitochondrial ribosomes. The genetic code within the mitochondrion diverges from the "Universal Genetic Code" in several ways. For instance, TGA is a tryptophan codon within the mitochondria while in the universal code it represents a stop codon. Furthermore, the genetic code within nuclear DNA contains 32 tRNAs, while the mitochondrial genetic code is much simpler having only 22 tRNAs (Wei 1998).

In addition to the coding region, human mtDNA also contains a 1122 base pair noncoding region located between $tRNA^{Phe}$ and $tRNA^{Pro}$ (See Figure 1.2). This area contains three hypervariable regions and a displacement loop. The displacement loop is often referred to as the d-loop and was labeled as such because a nascent H strand DNA segment (500-700 nt) remains annealed to the parental L-strand forming a triplex in metabolically active cells (Fernandez-Silva et al. 2003). The d-loop contains the transcription initiation sequences for both the heavy and light strands as well as

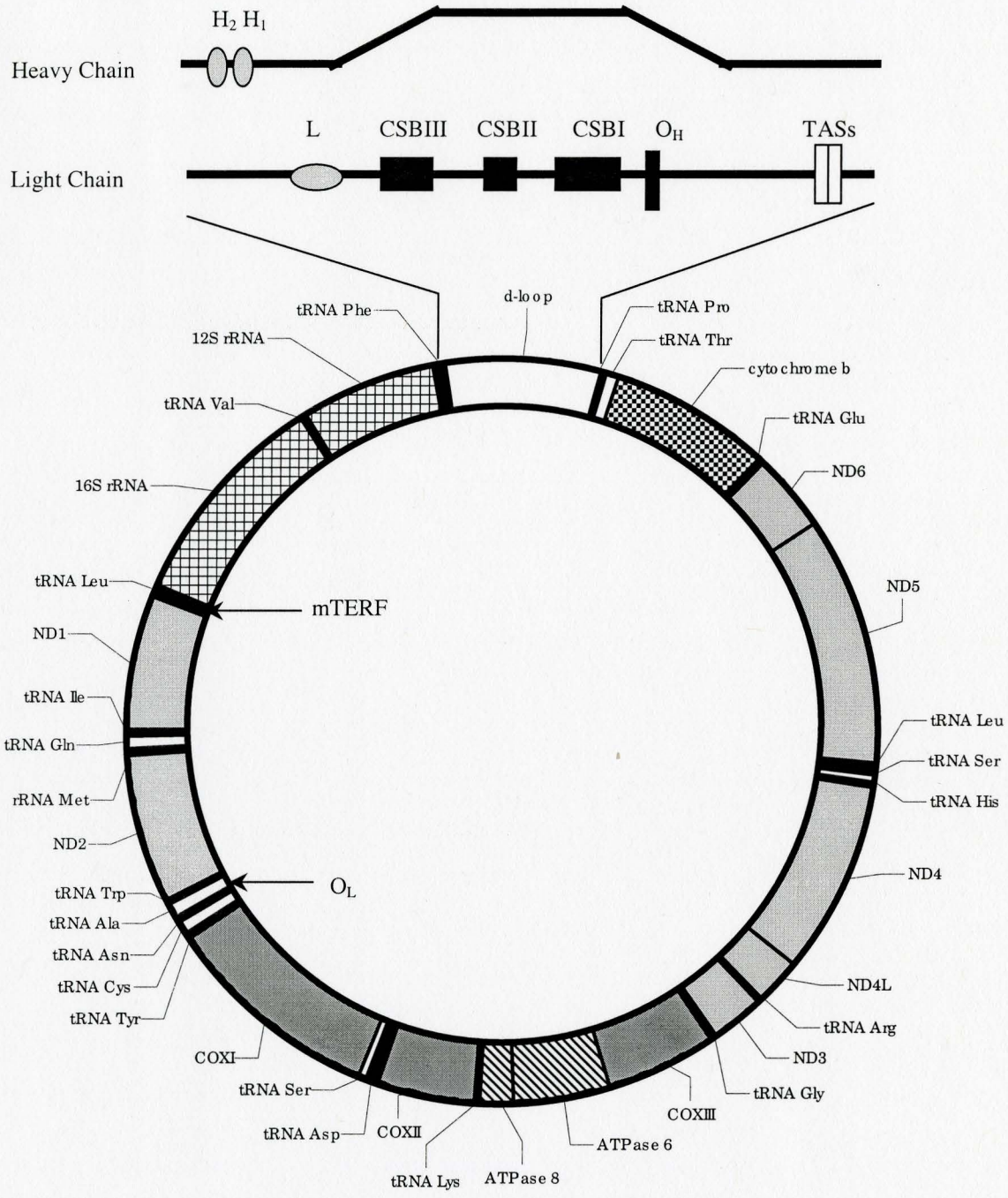

Figure 1.2: **Map of the human mitochondrial genome**. Protein, tRNA and rRNA genes are represented by boxes. H_1 and H_2: Heavy strand promoters; L: Light strand promoter; CSB: Conserved Sequence blocks; TASs: Termination Associated Sequences; mTERF: mitochondrial transcription termination factor; O_L: Orign of light strand replication; O_H: Origin of heavy strand replication

regulatory sequences for replication of mtDNA. The origin of replication for H strand synthesis (O_H) is also located within the d-loop making it a critical region in the process of mtDNA replication (Clayton 1991).

Like mitochondrial transcription and translation, replication of the mitochondrial genome involves the participation of both nuclear and mtDNA. Replication begins at O_H and is catalyzed by mtDNA polymerase γ, a protein of nuclear origin that is imported into the mitochondrion (Schon 1993). Replication of the heavy strand proceeds in a clockwise direction from O_H until it reaches the termination-associated sequences (TASs), where two outcomes may occur. In most cases mtDNA replication is arrested creating the triplex d-loop structure (Clayton 1982). In a minority of events replication of the H-strand proceeds, eventually reaching the light strand origin of replication (O_L) 2/3 of the way around the genome. At this point, synthesis of the light strand begins in the opposite, counterclockwise, direction (Clayton 1982; Lestienne and Bataille 1994). Replication of both strands is carried to completion, resulting in a catenated pair of circles (Tully and Levin 2000). The linked rings are then cut and resealed by mtDNA ligase, another nDNA encoded protein imported into mitochondrion. The replication of one mtDNA molecule requires approximately 1-2 hours to complete (Schon 1993; Graves et al. 1998). Replication has been observed in non-dividing cells and may occur more than once during the cell cycle, indicting that mtDNA synthesis is somewhat autonomous (Attardi and Schatz 1988). It is not yet known what function the d-loop serves or what mechanisms lead to full or partial replication of the mitochondrial genome (Brown and Clayton 2002).

Although mtDNA replication is independent of nDNA synthesis and the cell cycle, mitochondria must be transmitted to daughter cells. During mitosis mitochondria randomly segregate into daughter cells through a process known as replicative segregation. Because this process is indeed random, cells containing heteroplasmic populations of mtDNA may transmit different proportions of each mtDNA to daughter cells. Conversely, during meiosis in oogenesis, mtDNAs experience a bottleneck phenomenon by which only a small proportion of mtDNA molecules are amplified and inherited by offspring (Marchington et al. 1998). It is widely believed that mtDNA is strictly maternally inherited in the context sexual reproduction, with paternal sperm mtDNA being actively eliminated following fertilization (Fernandez-Silva et al. 2003). However, recent data has demonstrated that paternal mtDNA may escape destruction and has been observed in the muscle of offspring at relevant levels (Schwartz and Vissing 2002). One or a combination of these mtDNA transmission patterns may greatly impact cell phenotype from the perspective of disease (Discussed further in mtDNA mutations in disease).

1.2 OXPHOS generated ROS and mitochondrial DNA damage

Production of Reactive Oxygen Species During OXPHOS

Although the process of OXPHOS is responsible for the production of vast amounts of energy, an undesirable byproduct is produced in the process. As electrons travel through the electron transport chain approximately 1% escape and react with molecular oxygen to form superoxide anions ($O_2^{\cdot -}$) (Wallace 1999; Raha and Robinson 2001). The inadvertent escape of these electrons occurs predominantly at complex I and

III (Saybasili et al. 2001; Staniek et al. 2002). Fortunately, detoxification systems have evloved within the cell to convert superoxide anions to innocuous compounds. Superoxide anions maybe processed by mitochondrial manganese superoxide dismutase (MnSOD, SOD2) or cytoplasmic copper zinc superoxide dimutase (CuZnSOD, SOD1) to hydrogen peroxide (H_2O_2) (Rhee et al. 1994; Fridovich 1995). The hydrogen peroxide produced on either side of the mitochondrial membrane may be converted to the more harmful hydroxyl radical (OH^-) by free cupric or ferric ions through the fenton reaction or detoxified by glutathione peroxidase (GPx) to water (Raha et al. 2000;Esworthy et al. 1997). All three species ($O_2^{\cdot-}$,OH^-, H_2O_2) make up a group of molecules termed reactive oxygen species (ROS), which are capable of damaging biomolecules.

Reactive oxygen species that are not detoxified by cellular systems may interact with proteins, lipids, and nucleic acids with devastating consequences. For instance, superoxide has been shown to cause damage to the (4Fe-4S) type of iron center (Pryor 1986; Flint et al. 1993). Specifically, the cytosolic enzyme aconitase is forced to release ferrous iron after exposure to superoxide and the de-activated enzyme binds the mRNA of ferritin. This interaction increases the half-life of the mRNA ensuring an increase in ferritin synthesis to bind free iron (Pryor 1986; Flint et al. 1993). Hydrogen peroxide is capable of damaging mtDNA in retinal pigment epithelial, endothelial, and smooth muscle cells (Ballinger et al. 2000; Ballinger et al. 1999). This molecule also inhibits mitochondrial protein synthesis, reduces cellular ATP, alters redox function and increases lipid peroxidation (Ballinger et al. 1999; Sousa et al. 2003). OH^- radicals also have

negative effects on biomolecules resulting in mtDNA damage and lipid peroxidation (Mohanan and Yamamoto 2002; Yamamoto and Mohanan 2003).

Indirect evidence of ROS damage can be studied by experimentally eliminating detoxification systems. For instance, homozygous MnSOD (*sod2*$^{-/-}$) knockout mice rarely survive one week post birth and display extensive damage to iron sulfur centers contained in mitochondrial aconitase, complex I and succinate dehydrogenase (Lebovitz et al. 1996; Li et al. 1995). Eventually enzyme function becomes so impaired that there is a lack of mitochondrial ATP generation and an increase in lactic acid production. *sod2*$^{-/-}$ mice also suffer more mtDNA damage in the liver and lung when compared to wild-type littermates. Furthermore, treatment of these knockout mice with an SOD mimetic, MnTBAP extended their lifespan by several weeks (Melov et al. 2001). Conversely, homozygous cytosolic CuZnSOD knockout mice only demonstrated a small decrease in life span, indicating that mitochondrial generated ROS plays an important role in cell homeostasis (Carlsson et al. 1995).

ROS and the mitochondrion are also intimately linked through the process of programmed cell death or apoptosis. Although many of the intricate details, precise chain of events, pathways, and players of apoptosis are still to be fully elucidated, ROS have proven to be potent inducers of this process. For example, ROS are strong activators of the tumour suppresser protein p53 (Martindale and Holbrook 2002). A universal sensor of genotoxic stress, p53 plays a critical role in regulating the expression of genes that mediate growth arrest and cell death. ROS activated p53 induces the production of the pro-apoptotic protein Bax leading to release of cytochrome c from the mitochondrion and

loss of $\Delta\Psi_M$ (Nakamura and Sakamoto 2001; Raha and Robinson 2001). Released cytochrome c triggers the apoptotic cascade by activating enzymes that degrade cellular proteins and DNA. Release of cytochrome c can also be directly triggered by ROS (Raha and Robinson 2001). These observations are strengthened by the finding that elimination of p53 function enhances survival of hydrogen peroxide treated cells (Yin et al. 1998). ROS is generally considered to elicit an apoptotic response when it places a cell in conditions of oxidative stress, while low levels of ROS are actually mitogenic (Cheng et al. 2003). For a more comprehensive review of ROS and apoptosis please refer to Martindale and Holobrook (2002).

ROS inflicted mtDNA Damage

The mutation rate of mtDNA exceeds that of nDNA by 10-fold (Brown et al. 1979). It is thought that this increase in mtDNA damage reflects differences in the maintenance and environment of these two gene pools. The location of mtDNA within the inner mitochondrial matrix places it within close proximity to the ETC and hence ROS byproducts of OXPHOS (Jones et al. 2001). Furthermore, the mitochondrial genome lacks protective histones present in nDNA (Carew and Huang 2002). Additionally, the enzyme responsible for catalyzing mtDNA replication, mtDNA polymerase γ, is relatively error prone with replication errors occurring in 1 out of every 7000 bases (Kunkel and Loeb 1981). It was also suggested a lack of mitochondrial repair enzymes might also contribute to the high mtDNA mutation rate (Clayton et al. 1974). However, it was later discovered that mitochondria are capable of base excision and

possibly mismatch repair, but lack enzymes responsible for nucleotide excision repair (Bogenhagen 1999; Mason et al. 2003).

The process of BER corrects oxidative damage incurred by the mitochondrial genome. In general, repair is initiated by the action of a glycosylase and sometimes involves the supplemental action of an endonuclease and DNA polymerase γ to complete the process. Glycosylase enzymes such as 8-oxoguanine glycosylase 1 (OGG1) and endonuclease III homolog (NTH1) are present in humans and play a primary role in the removal of 8-oxoguanine DNA lesions brought about by oxidative damage in mtDNA (Nakabeppu 2001). Another glycosylase, uracil DNA glycosylase (UDG), is critical in the removal of uracil from mtDNA resulting from deamination of cytosine or misincorporation of dUMP by DNA polymerase γ (Anderson and Friedberg 1980). Recent research has demonstrated that although mitochondria are capable of removing oxidative damage they appear to lack the enzymatic machinery needed to remove bulky lesions from their DNA (LeDoux et al. 1999). Ineffective repair of mtDNA lesions may contribute to the propagation of mutant mitochondrial genomes.

1.3 mtDNA mutations in Disease

As previously mentioned, the polyploid nature of the mitochondrial genome permits a state of heteroplasmy in which two genetically distinct populations of mtDNA molecules exist within a given cell, tissue or organ. Conceptually this heterogeneous population of genomes might be inherited maternally or acquired postzygotically during development. mtDNA heteroplasmy might also occur in some instances through the transfer of paternal mtDNA to offspring, although this is still controversial (Schwartz and

Vissing 2002). Once present, the proportion of each mtDNA molecule present in a given cell population may fluctuate with time due to replicative segregation and the stochastic nature of mitochondrial genomics. All of these issues are of great importance if an individual harbors a population of mtDNA with mutations affecting the product encoded. Initially phenotypic effects of this mutation may not be observed, but with the passage of time the number of mutant mtDNA molecules may increase. As this proceeds the cellular energy capacity decreases until it falls below the bioenergetic threshold, the minimum energy output necessary for a cell or tissue to function normally (Wallace 1999). Below this boundary, disease symptoms appear, and may become worse with the passage of time. This degenerative process is known as the threshold effect (DiMauro and Andreu 2000).

The first of these pathogenic mutations was reported in 1988 when large-scale deletions were detected in a patient with mitochondrial myopathy and a point mutation in ND4 was described in a family with Leber's hereditary optical neuropathy (LHON) (Holt et al. 1988; Wallace et al. 1988). By the year 2000, a further 96 putative pathogenic point mutations had been identified (DiMauro and Andreu 2000). The unpredictable nature of mitochondrial genetics makes both inheritance and symptoms of these diseases highly variable. In fact, members of the same family who harbor the identical mtDNA mutation may manifest dramatically different symptoms, resulting from chance fluctuations in the percentage of mutant mtDNA inherited by each individual and tissue affected (Chinnery et al. 2001). Furthermore, the underlying decrease in cellular energy capacity, which is common to all mitochondrial diseases, produces similar symptoms in patients with

different mutations. Consequently, it has proven more effective to diagnose mitochondrial diseases on the basis of genetic defect rather than by symptoms presented (Wallace 1999).

The mutation at position 3243 of the mitochondrial genome has been studied extensively and demonstrates great heterogeneity in regard to the phenotype presented. The mitochondrial genomic defect in this case is an adenine to guanine transition mutation that occurs within $tRNA^{Leu}$. Normally this tRNA is responsible for bonding a leucine molecule to form an aminoacyl-tRNA that later recognizes leucine codons present on mitochondrial mRNAs. Studies have demonstrated that this mutation results in a drop in steady-state levels of $tRNA^{Leu}$ and also has been associated with impaired tRNA aminoacylation (El Meziane et al. 1998a). This mutation displays the typical threshold effect of mitochondrial diseases. Cells containing 60%-90% mutant DNA exhibit a mild complex I defect, while cells with greater than 90% mutant DNA display a general impairment of respiratory function (Dunbar et al. 1996). When a mutational load of 98% or greater is reached protein synthesis is diminished almost to the point of cessation (El Meziane et al. 1998b). Another study has also demonstrated that cells with >90% mutant mtDNA are under a greater amount of oxidative stress, consume less oxygen and produce less ATP (Pang et al. 2001). The impact these findings in the laboratory translate well to the clinic where broad ranges of patient symptoms are observed. When mutant $tRNA^{Leu}$ is present at high levels (>85%) a condition known as MELAS or mitochondrial encephalomyopathy with lactic acidosis and stroke like episodes are often observed (Goto et al. 1990). As the name implies, MELAS is characterized by recurrent stroke like

episodes, myopathy (muscle disorder), lactic acidosis (drop in blood pH), and encephalopathy although all may not be present simultaneously. Sometimes patients may also experience migraine headaches, limb weakness, and short stature (Huang et al. 2002). Affected tissue generally displays both COX positive and negative abnormal muscle fibres (ragged red fibres, RRFs) (DiMauro and Andreu 2000). When the $tRNA^{Leu}$ mutation occurs in 5-30% of mtDNA molecules disease symptoms are less severe resulting in diabetes mellitus or deafness (Goto 1995).

The thymine to adenine mutation at position 14459 has also been well characterized. This nucleotide substitution converts a highly conserved alanine residue in ND6 (subunit of complex I) to a valine (Wallace 1999). The physical effects of this mutation on subunit function are still not fully understood, but it is hypothesized that the alteration affects CoQ binding to complex I (Jun et al. 1996). The same study observed a 60% decrease in complex I activity in cells harboring the mutation when compared to control cells. Patients with this mutation generally present with either Leber's hereditary optic neuropathy (LHON) or dystonia. LHON and dystonia are generally associated with lower and higher mutational loads respectively (Novotny, Jr. et al. 1986; Jun et al. 1994; Shoffner et al. 1995). Individuals with LHON experience sudden-onset blindness at approximately 20 years of age brought about by death of the optic nerve (Schmiedel et al. 2003). Conversely, symptoms of dystonia manifest early in life with generalized movement disorder, mental retardation, and short stature. This condition is also frequently accompanied by degeneration of the basal ganglia of the brain (Tully and Levin 2000).

A third point mutation that results in variable disease outcome occurs at position 8993 of the mitochondrial genome. This thymine to guanine transition occurs at codon 156 of ATPase 6 and converts a conserved leucine residue to an arginine. Biochemical analysis revealed that cells harboring this mutation display a blockage of the ATPase F_0 proton channel (Trounce et al. 1994). This mutation is exclusively heteroplasmic and symptom presentation is also dependent on mutational load. When the defect is present in <75% of mtDNA molecules it can cause neurogenic muscle weakness, ataxia, and retinitus pigmintosa (NARP) (Tatuch et al. 1992). These individuals may also experience a combination of developmental delay, dementia, seizures and sensory neuropathy (Tully and Levin 2000). However, when the mutational load is higher (>90%), it causes an early-onset disease known as Leigh's syndrome. Patients afflicted with this condition demonstrate ataxia, hypotonia, spasticity, developmental delay, optic atrophy, and ophthalmoplegia (paralysis of the extra-ocular eye muscle) (Schmiedel et al. 2003). Leigh's syndrome is progressive, degenerative and frequently lethal with accompanied degeneration of the basal ganglia under some circumstances (Shoffner and Wallace 1995). The inheritance pattern of this disease has also been well documented and shows great variability in mutational load, tissue distribution and offspring symptoms (Tatuch et al. 1992; Shoffner et al. 1992). It should also be noted that this defect has been rectified *in vitro* through the targeting of a nDNA encoded ATPase 6 gene to the mitochondria (Manfredi et al. 2002).

In addition to point muations, a large-scale mtDNA deletion which results in a number disease phenotypes has also been extensively studied. The 4977 base pair

deletion results in the partial removal of ND5 and ATPase 8 as well as the full removal of ATPase 6, COXIII, ND3, ND4, ND4L, and 5 tRNAs (DiMauro and Andreu 2000). Recent biochemical investigations have revealed that this abnormality also displays a threshold effect. If the deleted molecules comprise >55% of the total population, the $\Delta\Psi_M$ and rate of ATP synthesis was equivalent to control cells. However, once the mutation exceeded this proportion the $\Delta\Psi_M$ and rate of ATP synthesis decreased (Porteous et al. 1998). This deletion is associated with three related diseases, namely chronic progressive external ophthalmoplegia (CPEO), Kearn-Sayre syndrome (KSS), and Pearsons syndrome (Porteous et al. 1998). Patients with CPEO experience ophthalmoplegia (paralysis of the eye muscles), ptosis (droopy eyelids), mitochondrial myopathy, and RRFs (Wallace 1999; Tully and Levin 2000). Subsets of patients also have cardiac defects, renal problems and diabetes mellitus (Wallace 1999). KSS is a more severe syndrome, manifesting at an early age and including symptoms such as atypical retinitis pigmentosa, and mitochondrial myopathy (Schmiedel et al. 2003). Individuals may additionally display cerebellar syndrome, increased cerebral-spinal fluid, or cardiac conduction abnormalities (Schmiedel et al. 2003). The accumulation of deleted mtDNA genomes in bone marrow precursor cells results in Pearson's syndrome and includes symptoms of pancytopenia and pancreatic dysfunction (Brown and Wallace 1994). The occurrence of large-scale deletions is generally a sporadic event, meaning that the deleted genomes are undetectable in the mother, siblings and children of the affected individuals (Larsson et al. 1992). However, these deletions may be transmitted

maternally and oocytes from healthy women have been found to contain such deletions (Chen et al. 1995).

These four examples of mtDNA defects resulting in disease only represent a small subset of the pathological mitochondrial genomic aberrations identified to date. Mitochondrial mutations have also been implicated in Parkinson's disease (PD) and Alzheimer's disease (AD), both late-onset degenerative diseases(Castellani et al. 2002; Beal 2003). As in mtDNA diseases, cells containing PD and AD mtDNA defects display decreased complex I activity and increased ROS generation (Swerdlow et al. 1996;Ghosh et al. 1999; Gu et al. 1998; Bijur et al. 1999). However, work in this field is ongoing. For a more comprehensive study of mtDNA mutations and disease please refer to Tully and Levin (2000) and DiMauro and Andreu (2000).

Although the clinical symptoms of mtDNA defects are not uniform, the underlying cause appears to be a decrease in electron transport chain function and subsequent decrease in energy production (Mandavilli et al. 2002). If the mutation(s) represent a small proportion of the total mtDNA population, or energy demands of the tissue are still met, no disease symptoms are observed. However, if the energy production drops below the metabolic threshold symptoms are manifested. Another common finding is that organs with the highest oxygen demands, such as muscular and neuronal tissue, also display the highest mutational load (DiMauro and Andreu 2000; Oldfors et al. 1995;Lombes et al. 1992). It is hypothesized that the heterogeneity of disease phenotype observed in patients with identical mtDNA mutations is attributable to different mutational loads in individual tissues (DiMauro and Andreu 2000). These

authors also speculate that specific mutations may accumulate in very specific areas of the brain such as the choroid plexus or discrete cortical areas. Another theory proposes that tissues such as leukocytes which undergo rapid division possess the ability to expunge cells with mutations, whereas non-dividing tissues such as the brain and skeletal muscle do not eliminate these cells and may favor the accumulation of mutant mtDNA (Tully and Levin 2000; Swerdlow et al. 1996).

The decrease in electron transport chain function brought about by mtDNA defects is also presumed to cause an increase in ROS production and oxidative stress (Borisov 2002; Ito et al. 1999). It is believed these genomic changes elicit the inefficient transfer of electrons through the ETC resulting in their premature release and reaction with molecular oxygen to form superoxide, which subsequently leads to other ROS species (See section 1.2). The idea behind this theory is essentially the same as that for ETC related ROS production under normal circumstances except the yield of ROS is greater in circumstances of disease. Experimental evidence supports this assertion demonstrating that cells carrying mtDNA defects do show increased levels of ROS when compared to control cells (Swerdlow et al. 1997; Sheehan et al. 1997; Di Giovanni et al. 2001). Other studies have also demonstrated that mtDNA defects result in increased mtDNA lesions and lipid peroxidation (Wei et al. 2001; Pang et al. 2001).

Both inhibition of the electron transport chain and ROS are capable of initiating apoptotic events (Chomyn and Attardi 2003; Plas and Thompson 2002). Several studies have looked at the levels of apoptosis in cells harboring mtDNA mutations with mixed results. Mirabella *et al.* (2000) observed TUNEL positive staining in 75% or more of

muscle fibres in patients with a high proportion (>40%) of mtDNA deletions or tRNA mutations (>70%). Conversely, the same study found no change in apoptosis in individuals with mtDNA mutations in structural genes. 25-75% of the muscle fibres isolated from patients carrying a high proportion (>70%) of the A3243G mutation in $tRNA^{Leu}$ exhibited TUNEL positive staining, while, patients afflicted with the T8993C mutation of the ATPase 6 gene showed no TUNEL positive nuclei (Mirabella et al. 2000). However, an additional study determined that fibroblast cells harbouring the 8993 mutation underwent massive apoptosis when glucose in the media was replaced with galactose (Geromel et al. 2001). The authors hypothesized that the induction of apoptosis in this case may be the result of oxidative stress rather than a defect in OXPHOS as both mitochondrial and cytosolic SOD was increased. The variable results of these studies may reflect cell specific responses to the same mutations.

Although it was mentioned earlier that mtDNA randomly segregate during mitosis, there is experimental evidence to support the theory that mtDNAs harbouring pathogenic mutations have a replicative advantage over wild-type molecules. For instance, Diaz *et al.* (2002) created cells that contained a heteroplasmic mtDNA population comprised of an approximately equal proportion of both wild-type molecules and those with the common 4977 bp deletion. Following partial mtDNA depletion, molecules containing the 4977 bp deletion repopulated cells at a faster rate, increasing their numbers by 6% after 10 days. This implies that mitochondrial genomes with the 4977 bp deletion have a replicative advantage over wild-type mtDNA molecules during repopulation (relaxed copy number) conditions (Diaz et al. 2002). These authors

speculate this advantage is most likely due to the faster completion of these shorter molecules during replication when compared to longer wild-type mtDNA. This large-scale deletion is found in increasing amounts with age, and in the context of mtDNA disease and cancer, which may in itself point to an advantage or possible common defect in mtDNA replication (Tully and Levin 2000).

In another study by Chinnery et al. (1999) the tissue distribution of the A3243G mtDNA point mutation was examined in multiple tissue types from four siblings and one offspring of the same family afflicted with maternally inherited diabetes and deafness. Mutational loads in the hair follicles, buccal mucosa, and blood were analyzed from all family members, while the proportion of mutation in skeletal muscle was evaluated in three individuals. The mutational load corresponded to rate of cell turnover of each tissue in all individuals. The highest proportion of mutant mtDNA was detected within the skeletal muscle, with decreasing levels occurring in the hair follicles, buccal mucosa, and blood respectively. The increased mutational load in the muscle when compared to the blood is observed not only in 90% of patients with the A3243G mutation, but also in 91% of the individuals harbouring the A8344G mutation (Chinnery et al. 1997). Furthermore, Schon et al. (1997) created cells with a heteroplamic population of wild-type and A3243G mutant DNA. Of the 13 clones 5 displayed a shift towards total mutant mtDNA homoplasmy. The other 8 cells lines maintained a stable mutant mtDNA population with 6 exhibiting nearly homoplasmic mutant mtDNA. Subcloning and growth rate measurements indicated that an intracellular replicative advantage was responsible for the dramatic shift towards the mutant genotype (Schon et al. 1997). Dunbar *et al.* (1995)

corroborated these findings, but also demonstrated that the presence of the same heteroplasmic mtDNA population in cells with a different nucleus resulted in a shift towards wildtype homoplasmy indicating that nuclear genetic background of cells can influence the segregation of mtDNA. Alternatively Chinnery *et al.* (1997) speculate that the segregative or replicative advantage of the A3243G mutation may be the result of a yet unidentified *cis*-acting factor possibly within the d-loop. The results of these experiments are difficult to understand because pathogenic mutations are believed to confer a phenotype that is energetically inferior to that of wild-type mtDNA and in some cases incompatible with life. However, these observations will prove to be important in the subsequent chapter.

1.4 mtDNA mutations and cancer

In addition to their implication in myopathies, Parkinson's disease and Alzheimer's disease, mitochondria, and more recently mtDNA have been implicated in the process of carcinogenesis. As early as the 1930's it was hypothesized that alterations in oxidative phosphorylation played a role in cancer growth (Warberg 1930; Warburg 1956). 73 years later, numerous mitochondrial aberrations have been noted in cancer cells when compared to quiescent cells. Perhaps the most important feature as it relates to mitochondrial function is the energy derivation pathway shift from the process of aerobic OXPHOS to that of aerobic glycolysis (Torroni et al. 1990;Lu et al. 2002). Normally 90% of cellular ATP is produced through OXPHOS, but one study has demonstrated that this value drops to 40% in transformed cells with the remainder coming from glycolysis (Nakashima et al. 1984). Many tumor cells also display increased levels of total

hexokinase activity, the first enzyme involved in the commitment to glycolysis, as well as elevated levels of the mitochondrial outermembrane bound protein hexokinase II (Mathupala et al. 1995; Penso and Beitner 1998).

Transformed cells produce greater amounts of ROS than their non-transformed counterparts, placing tumour cells under persistent oxidative stress (Toyokuni et al. 1995; Burdon 1995). Studies have also demonstrated that protective systems such as MnSOD which reside in the mitochondria are inversely correlated with tumour aggressiveness indicating that lower oxidative defenses in the mitochondria of neoplastic cells may be advantageous to these cells (Korenaga et al. 2003; Soini et al. 2001). These observations are intriguing as ROS molecules and antioxidant defenses must be balanced to prevent a state of oxidative stress, which may lead to cell death (Martindale and Holbrook 2002). Additionally, increased ROS may damage the electron transport chain which is consistent with observations that decreased OXPHOS correlates with tumour aggressiveness and more recent reports of mtDNA mutations in tumor tissue (Simonnet et al. 2002).

A number of studies have examined the occurrence of mtDNA mutations in various types of cancers including tumours isolated from the breast, ovary, kidney and stomach to name a few. Depending on the method used, mtDNA mutations were found in 40-80% of the tumours examined when compared to adjacent tissue. In one report temporal temperature gradient electrophoresis (TTGE) was used to identify mutations in 19 tumor samples. Fourteen tumours (74%) displayed mutations with 22 of the 27 (81%) occurring within the d-loop (Tan et al. 2002). Furthermore, 3 of the d-loop mutations

occurred within the D310 tract of conserved sequence block II (CSBII). A study conducted by Baillet *et al.* (1995) used restriction enzymes to identify mutations within 7 breast tumours and compared them to the adjacent normal tissue. The common 4977 bp deletion implicated in CPEO was found in the normal tissue sample of one patient and the tumour tissue of the two others. Mitochondrial mutations in ovarian cancers have also been investigated by Liu et al. (2001). The d-loop of 15 tumours were directly sequenced and compared to adjacent normal tissue with 3 of the 15 tumour samples (20%) containing mutations one within the D310 tract of CSBII. The same study sequenced the entire mitochondrial genome of 10 pairs of tumours and control tissue revealing somatic mutations in 6 (60%). Most of these mutations were T to C or G to A transitions and the vast majority of these mutations were homoplasmic. The complete mtDNA sequence of 8 renal cell carcinomas were also sequenced and compared to control tissue. Of the eight samples five (62%) displayed a mutation, one of which was in D310 tract of CSBII. In one final example, PCR-SSCP analysis was used to detect mtDNA mutations in 32 tumours isolated from the stomach. Of these 26 (81%) displayed mutations, mainly in the d-loop and ND1 and ND5 of complex I. The common 4977 bp deletion was detected in 17 samples and other insertions or deletions were detected in 10 samples(Maximo et al. 2001).

With exception of the 4977 deletion detected in a number of cancer cell lines, only a few aberrations have been previously associated with mtDNA diseases. For example, Jones *et al.* (2001) revealed a total of 49 mtDNA variations after sequencing the complete mitochondrial genome of 10 pancreatic cell lines. Of these variations one adenine to

thymine mutation at position 9804 had been previously associated as a secondary mutation in LHON. In a separate study, 32 gastric carcinomas were analyzed. Although the common 4977 mutation was detected in 17 samples none displayed $tRNA^{Leu}$ or $tRNA^{Ser}$ mutations common to mtDNA diseases (Maximo et al. 2001). Parrella *et al.* (2003) sequenced 84% of the mitochondrial genome of 18 primary breast tumors revealing 11 mutations. Of these, only one mutation at position 13708 was previously described as a secondary LHON mutation. Mutations found in neoplastic cells are often detected as homoplamic aberrations, unlike those of mitochondrial disease which are invariably present in a state of heteroplasmy (Jones et al. 2001). With such a high mutational load and low correspondence with mutations of mtDNA disease, the true functional consequence of these mitochondrial genomic aberrations is currently at best speculative.

In the field of carcinogenesis, a great deal of attention has recently been focused on the D310 tract of the d-loop(Sanchez-Cespedes et al. 2001;Parrella et al. 2003). The D310 tract is part of CSBII which is located 92 bp from the heavy strand origin of replication and contains a stretch of cytosines and one thymine (C[5-10]TC[6]) (Mambo et al. 2003). It is well established that CSBII cooperates with CSBI and CSBII to contribute to form a persistant RNA-DNA hybrid, termed the R-loop, which primes the initiation of mtDNA replication (Fernandez-Silva et al. 2003). The insertion or deletion of cytosines in the D310 tract has been observed in 42% of cancer cells screened when compared to non-neoplastic tissue controls (Parrella et al. 2003). A separate investigation also demonstrated that the D310 tract is more susceptible to oxidant damage when

compared to the rest of the d-loop and other portions of the mitochondrial genome (Mambo et al. 2003). Despite evidence that the D310 tract might play some role in carcinogenesis, it is still not clear what effect these variations have on mitochondrial genomic function (Sanchez-Cespedes et al. 2001).

The observation that a high proportion of neoplastic cells display mitochondrial mutations has lead some to the hypothesis that these mutations may provide an advantage to cancer cells through the upregulation of ROS. To this point, ROS have been discussed in terms of molecules that interact negatively with biomolecules to cause damage and induce programmed cell death. However, low levels of ROS, in particular H_2O_2, are known to be mitogenic and promote cell growth. A number of proliferation pathways are induced by ROS including the phosphoinositide 3-kinase/protein kinase B (PI3KL/Akt), extracellular signal-regulated kinase (ERK), p38 MAPK, and c-Jun N-terminal kinase pathways (JNK) (Dong-Yun et al. 2003; Cheng et al. 2003). However, the JNK pathway is also involved in ROS induced events leading to cell death indicating that the amount of ROS, or perhaps more precisely the level of oxidative stress, dictates whether cell proliferation or death occurs (see Martindale *et al.* 2002 and references therein). Moreover, ROS is known to function in both the initiation and promotion of cancer, and this moelcule is in fact critical to cell survival, as ROS scavenging actually leads to cell death (Preston et al. 2003; Penta et al. 2001).

As already mentioned, some mtDNA mutations are capable of decreasing the efficiency of the ETC, consequentially increasing OXPHOS produced ROS in the context of disease. Currently some hold the hypothesis that among the high background of

random mtDNA mutations that provide no selective advantage in carcinogenesis, there are a smaller number of mutations that that provide a survival advantage. After their spontaneous occurrence, mutated genomes are preferentially selected and with time expand to make up a substantial proportion of the mtDNA population or even reach a state of homoplasmy. Computer modeling of mtDNA mutations has estimated that approximately 30% of all homoplasmic mutations may occur through this process and *in vivo* data supported this estimate (Coller et al. 2001). Other evidence supporting this theory is the observation that upon fusing two neoplastic cells with different mtDNA, one quickly dominated that of the other, indicating that similar to pathogenic mtDNA mutations, mitochondrial or nuclear genomic factors influence the mtDNA compliment (Polyak et al. 1998). Furthermore, it has also been demonstrated that mutations within the D310 loop may confer a replicative advantage to cells (Mambo et al. 2003). However, others believe that these mutations occur through the more ambivalent process of random drift.

A random mitochondrial genomic drift might instead explain the appearance of mtDNA mutations seen in neoplastic cells. In this model mutations to the mitochondrial genome would arise during development to create a situation of intracellular heteroplasmy. Through population genetics alone, a number of these mutations reach a state of homoplasmy (Jones et al. 2001). The premise behind this model has also been tested using mathematical modeling. Using this model Jones *et al.* (2001) began with one mtDNA mutation and observed that 1% of daughter cells displayed the mtDNA mutation in a state of homoplasmy after 2000 cell divisions. These authors also claim that if the

parental cell contained >50 different mutant DNA molecules the probability of generating a state of homoplasmy for any of the mutations is greater than 40% after 2000 divisions. The notion of random drift is partially supported by a study in which laser microdisection was used to obtain tissue from two sites within a tumour and a sample of benign control tissue (Chen et al. 2002). Fourteen of the sixteen cases (90%) showed mutations however, 4 individual mutations were only detected in one of the two neoplastic samples isolated from the same tumour. Furthermore, 2 of these 4 mutations were homoplasmic mutations. This leads to the conclusion that the mtDNA population, even within a tumour, may change with a function of location and reach a state of homoplasmy. However, it still does not establish if these mutations occurred through random drift or selection processes.

Some fundamental properties of cancer cell biology make it difficult to determine if mtDNA mutations in tumors arise through a selection process or through random drift. Unlike mtDNA disease there is no particular phenotype to indicate potential candidate cells that might be used to test this hypothesis. For instance, some mitochondrial genomic defects in the case of disease reduce ETC efficiency and OXPHOS derived ATP, while producing more ROS and lactic acid. However, hallmarks of cancerous tissue are a switch to aerobic glycolysis and increased ROS production from several cellular sources. Furthermore, no studies have correlated glycolytic rate and ROS production to the occurrence of mtDNA mutations. Without a good candidate cell line to test the null hypothesis that mtDNA mutations occur through random drift, one could be looking for a needle in the proverbial haystack.

The 2008 human ovarian cancer cell line and its cis-Platinum(II)-diammine-dichloride (CDDP) resistant C13* variant might prove useful in establishing a mode of mtDNA defect acquisition in cancer cells. C13* cells were derived from the 2008 ovarian cancer cell line through 13 consecutive exposures to CDDP(Andrews et al. 1988). CDDP contains two chloride groups and two amine groups all covalently bonded to a platinum atom core to form a molecule with the configuration:

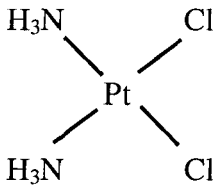

cis-Platinum(II)-diammine-dichloride
(CDDP)

Once internalized within the cell, the chloride ions are shed and replaced by water molecules (Kartalou and Essigmann 2001). This positively charged aquatic species is now capable of reacting with nucleophillic sites present on intracellular biomolecules (Kartalou and Essigmann 2001). Although this anticancer drug interacts with proteins and RNA, its main cytotoxic effect is believed to occur through direct interaction with DNA to form platinum adducts (Kartalou and Essigmann 2001). These lesions evidently occur at a higher frequency in mtDNA following treatment with CDDP (Olivero et al. 1997; Murata et al. 1990). Furthermore, fewer numbers of platinum adducts are removed from mtDNA, likely because mitochondria lack nucleoside excision repair mechanisms, hypothesized to be the main pathway by which these lesions are removed (Kartalou and Essigmann 2001; Olivero et al. 1997; Tully and Levin 2000). CDDP also generates ROS, and has a toxic effect on non-target kidney proximal tubule cells, impairing the ETC and damaging mtDNA (Chang et al. 2002; Satoh et al. 2003; Davis et al. 2001). Damage to

these cells may be reversed with antioxidants or ETC inhibitors indicating that ROS also contributes greatly to the poisonous effects of CDDP (Yoshida et al. 2003; Biroccio et al. 2001; Miyajima et al. 1999).

Derived C13* cells were found to be 12-fold more resistant to cisplatin and the mitochondria within 2008 and C13* cells displayed striking differences in terms of mitochondrial morphology and positioning within the cell (Andrews et al. 1985; Andrews and Albright 1992). Electron micrographs concluded that the cristae in C13* cells were thicker and more irregular, or absent in many cells. C13* cells also displayed a 2-fold increase in $\Delta\Psi_M$ and were 5-fold more sensitive to the $\Delta\Psi_M$ dependent poison rhodamine 123 (Rh123) when compared to their 2008 counterpart (Andrews and Albright 1992). C13*cells also have higher levels of heat shock proteins (HSPs) including HSP27, HSP70 and HSP60 (Yamamoto et al. 2001; Kimura et al. 1993). It was theorized that the elevated mitochondrial membrane potential in C13* cells played a direct role in the observed CDDP resistance phenotype. To try and address this hypothesis, C13* cells were exposed to 4 rounds of Rh123 and the surviving cells (termed RH4) had a 2-fold lower $\Delta\Psi_M$ and were only 2-3 fold resistant to CDDP treatment when compared to 2008 cells (Zinkewich-Peotti and Andrews 1992). It was also observed that C13* and RH4 cells had similar mitochondrial morphological features. Both C13* and RH4 cells accumulated 2.5-fold less CDDP meaning less of this drug would interact with, and damage, intracellular biomolecules. Furthermore, both had elevated levels of glutathione (GSH), which forms a covalent bond with CDDP and is transported out of the cell by the ATP-dependent glutathione-S-conjugate export pump (Zinkewich-Peotti and Andrews

1992; Kartalou and Essigmann 2001). Although the elevated GSH levels and decreased CDDP accumulation could not account for the complete CDDP resistance phenotype in C13* cells, they may afford some protection as observed from RH4 cell survival data (Zinkewich-Peotti and Andrews 1992). The only clear observable difference between C13* and RH4 cells was a difference in $\Delta\Psi_M$, however it was not apparent how an increase in mitochondrial membrane potential was capable of modulating the cellular response to CDDP. It was hypothesized that the changes to mitochondrial morphology and elevation in $\Delta\Psi_M$ might have arisen through mtDNA mutations incurred during CDDP treatment (Zinkewich-Peotti and Andrews 1992).

In keeping with the hypothesis that an mtDNA mutation might play some role in the phenotype of C13* cells, it was also determined that these cells produce 2-fold more H_2O_2 and consume one half of the oxygen when compared to 2008 cells (Doward 1999). The same study also determined through the use of mitochondrial electron transport inhibitors that this H_2O_2 was emanating from the mitochondria of C13* cells. Furthermore, C13* cells display a 2.4 fold resistance to exogenously applied H_2O_2, which is in agreement with the idea that C13* cells are able to resist the damaging effects ROS produced through OXPHOS or through other chemically derived means, such as CDDP treatment (Doward 1999; Chang et al. 2002).

However, if the phenotypic impact of the mtDNA of 2008 and C13* cells are to be evaluated, the nucleus of each cell line must be normalized to expunge differences in the nDNA compliment. Currently the delivery of mtDNA to the mitochondria is unfeasible and the polypoid nature of mitochondrial genomics would pose problems if

this procedure were possible. Fortunately, the cytoplasmic hybrid model or cybrid model pioneered by Attardi provides a way of normalizing the nuclear background and has been used extensively to study aberrant mitochondrial DNA molecules in disease (King and Attardi 1989 Swerdlow et al. 1996; Hayashi et al. 1991; Ito et al. 1999). In this procedure cells are exposed to low levels of ethidium bromide that inhibits γ DNA polymerase, thus preventing replication of mtDNA. With each cell division the mtDNA copy number drops by half until some cells contain no mtDNA. These mtDNA-less cells (ρ^0) have to be supplemented with pyruvate, however their need for this compound is not obvious because these cells should be able to generate sufficient amounts of pyruvate from the glycolytic breakdown of glucose (Attardi and Chomyn 1996). Cells lacking mtDNA must also be supplemented with a source of pyrimidines because the enzyme dihydrooratate, which is involved in the pyrimidine biosynthetic pathway, requires the ETC for normal function (Gregoire et al. 1984).

After creating ρ^0 cells, another group of cells containing the mtDNA defect of interest are enucleated through centrifugation and fused to cells that lack mtDNA using polyethylene glycol (PEG). Cybrid cells are selected through their ability to survive without pyrimidine supplemention or through drug resistance properties. The surviving cybrid cells presumably now share a common nuclear background, differing only with respect to mtDNA compliment. Thus, the utilization of cybrid cells containing the mtDNA compliment of 2008 and C13* cells will help to elucidate what impact mtDNA mutations have on observed cancer cell phenotype (See Figure 2.2).

1.5 Hypothesis

Mitochondrial genomic differences between the human 2008 ovarian cancer cell line and the CDDP resistant C13* variant are responsible for the phenotypic divergence observed between these cells.

1.6 Objectives

1. Sequence the mitochondrial genomes of the 2008 ovarian cancer cell line and its cisplatin resistant C13* variant to determine if aberrations between mitochondrial genomes exist.
2. Create cybrid cell lines that contain the mitochondrial genomes of 2008 and C13* cells, but share a common nuclear background.
3. Determine if phenotypic differences observed within the 2008/C13* model system is also observed within cybrid cell lines containing their respective mitochondrial genomes.

2.0 MATERIALS AND METHODS

Cell Culture

2008, C13*, and RH4 cells were obtained from Dr. Paul Andrews (Georgetown University, Rockville MD) and cultured in RPMI 1640 medium supplemented with 1% penicillin-streptomycin and 5% fetal calf serum (FCS) at 37°C in 5% CO_2 in air. Cybrid lines (2008cyb and C13*cyb) with a 143B TK^- human osteosarcoma nuclear background were created by Xianhua Yin (Hamilton Regional Cancer Centre, Hamilton, Ontario, Canada) and grown in DMEM supplemented with 1% penicillin-streptomycin and 5% FCS at 37°C in 5% CO_2 in air. 143B $TK^- \rho^o$ cells were obtained from Dr. Eric Shoubridge (McGill University, Montreal, Quebec, Canada) and grown in DMEM medium with 1% penicillin-streptomycin, 5% FCS and 50 µg/ml uridine at 37°C in 5% CO_2 in air. Media, FCS and penicillin-streptomycin were all obtained from Gibco BRL. Uridine and all other compounds listed below were supplied by Sigma unless stated otherwise.

Total Cellular DNA Extraction

Subconfluent monolayers of cells were removed from a single 150 x 20mm tissue culture plate (Corning) using 2% trypsin-EDTA (2% trypisn, 3 mM EDTA in Phosphate Buffered Saline) (Gibco BRL). Cells were suspended in PBS and centrifuged at 1000 rpm for 5 min. PBS was aspirated and the cell pellet was suspended in lysis buffer (100 mM Tris (pH 8.3), 5 mM EDTA, 0.2%SDS, 200 mM NaCl, 2.4 mg/ml RNase A) and incubated for 2 min at room temperature. Proteinase K was added at a final concentration of 0.4 mg/ml and incubated overnight at 55°C. One lysate volume of chloroform and NaCl (420 mM) was added and vortexed for 30 s. The mixture was then centrifuged for

10 min at 10000 rpm. The supernatant was collected and added to two supernatant volumes of absolute ethanol. Samples were gently agitated for 5 s. Precipitated DNA was spooled out with a 16.5 gauge needle. DNA was placed in a solution of 500 mM Tris (pH 8.3)/100 mM EDTA. The solution was incubated for 30 min at 65°C with the lid open and an additional 2 hr at 4°C.

Direct Sequencing of the mtDNA Genome

Direct sequencing of the mitochondrial genome was conducted by applying a nested primer strategy. In the first stage, forward and reverse primers were designed to facilitate the amplification of eight large portions of the human mitochondrial genome (See Table 2.1). 15 ng of total cellular DNA was added to a 50 µl PCR reaction containing 1x PCR buffer, 1.5 mM $MgCl_2$, 0.2 mM dNTP mix, 1 U of Taq DNA polymerase (All supplied by Gibco BRL) and 100 pmoles of each specific primer (Mobix, Hamilton, Ontario, Canada). The thermocycler (Perkin-Elmer GeneAmp 2400) PCR protocol was: one initial 5 min hot start at 94°C followed by 30 consecutive cycles consisting of a 30 s denaturation step at 94°C, a 30 s annealing step at 55°C, a 2.5 min extension step at 72°C, and one single 7 min polishing step at 72°C. PCR products were separated by electrophoresis on a 1% agarose gel and stained with 1 µg/ml ethidium bromide. Primer specificity to mtDNA was confirmed by the absence of a product utilizing 143B TK^- ρ^o template DNA. Amplified PCR products were extracted from the gel through the use of a Qiagen Gel Extraction kit according to the manufacturer's protocol.

Nested primers were created to prime within regions of the amplified mtDNA sequences (See Table 2.2). For this second PCR reaction 15 ng of PCR amplified DNA was added to a PCR reaction containing 1x PCR buffer, 1.5 mM $MgCl_2$, 0.2 mM dNTP mix, 100 pmoles of each specific primer and 1 U of Taq DNA polymerase (50 µl reaction volume). The thermocycler was programmed to carry out one initial 5 min hot start at 94°C followed by 30 consecutive cycles consisting of a 30 s denaturation step at 94°C, a 30 s annealing step at 55°C, a 40 s extension step at 72°C, and one single 7 min polishing step at 72°C. 2 µl of the PCR sample was separated by electrophoresis on a 1% agarose gel and stained with 1 µg/ml ethidium bromide to ensure the correct product was amplified. The remaining PCR product was purified using a Qiagen PCR Purification Kit according to the manufacturer's protocol. Purified samples were sequenced in the forward and reverse direction using their respective primers (Mobix, Hamilton, Ontario, Canada). Sequences were compared to each other as well to wild-type mtDNA sequences listed in pubmed and mtDNA polymorphisms/mutations reported in the Mitomap database (www.mitomap.org). Any suspected mutations were confirmed by repeating the reactions described above with a new sample of genomic template DNA (See Figure 2.1).

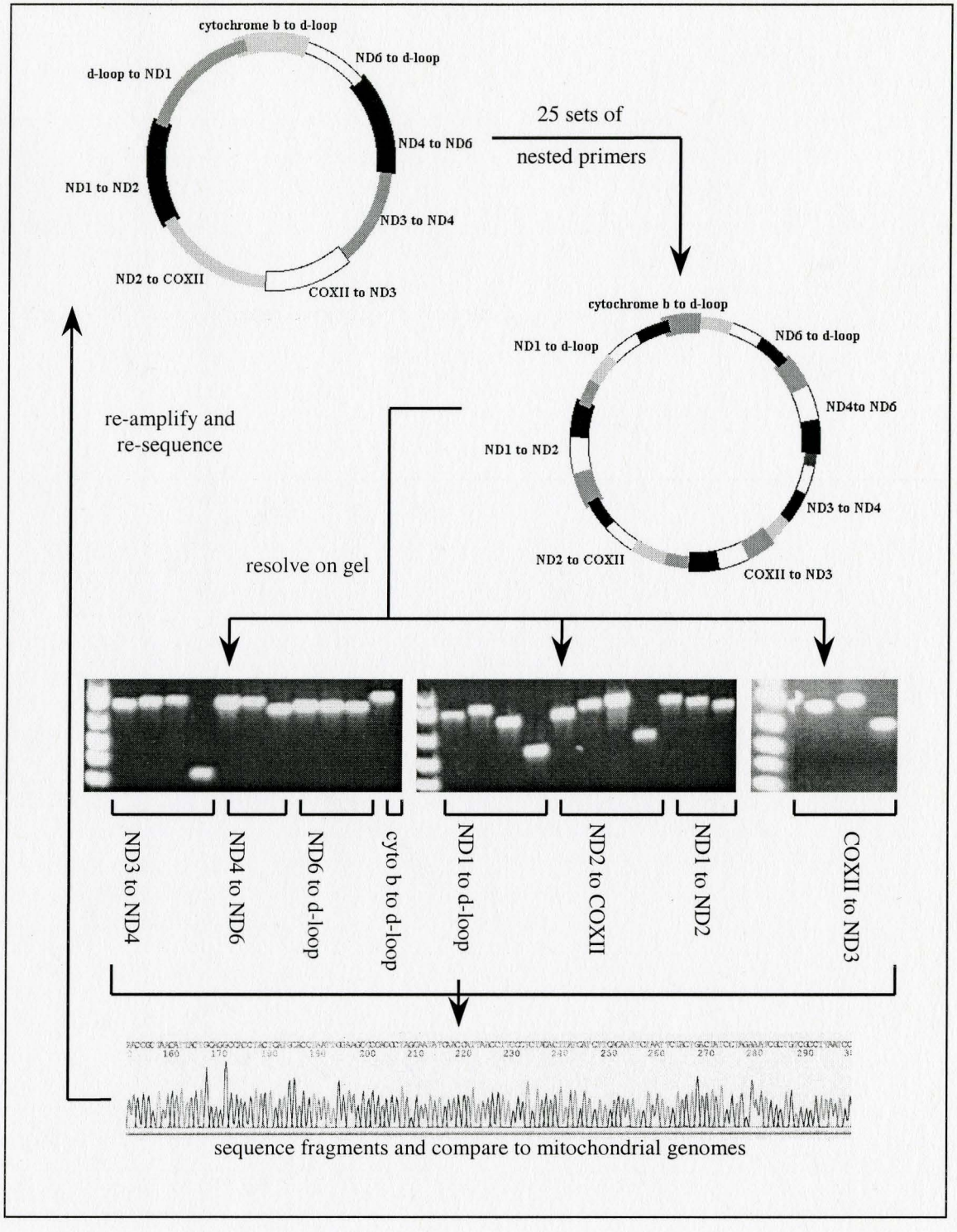

Figure 2.1: Overview of the nested primer strategy to sequence human mtDNA

Region	Forward (F) or Reverse (R) Primer	5' to 3' Sequence	Region of MtDNA Genome Amplified	Length of Product (Kb)
ND1 to ND2	F	CCCGGTAATCGCATAAAACT	5550 to 3242	2.308
	R	GGCTTTGAAGGCTCTTGGTC		
ND3 to ND4	F	TCTCCATCTATTGATGAGGGTCT	9964 to 12237	2.273
	R	GGGCACGAGTTAGCAGTTCT		
ND4 to ND6	F	CAGAGGCTTACGACCCCTTA	14377 to 12179	2.198
	R	AGGTAGGATTGGTGCTGTGG		
ND6 to d-loop	F	CCACCACCCCATCATACTCT	14326 to 16520	2.194
	R	ATGGCCCTGAAGTAGGAACC		
cytochrome b to d-loop	F	TCGGAGGACAACCAGTAAGC	15757 to 740	1.545
	R	CCCTTTTGATCGTGGTGATT		
d-loop to ND1	F	TTAGACGGGCTCACATCACC	617 to 3320	2.703
	R	TGGCCATGGGTATGTTGTTA		
ND2 to COXII	F	CCACGCTACTCCTACCTATCTCC	8209 to 5465	2.744
	R	ATGGGCATGAAACTGTGGTT		
COXII-ND3	F	CGGGGGTATACTACGGTCAA	10100 to 8158	1.942
	R	AGGCTCTAGGAAGGGTGTTGATT		

Table 2.1: Primers for long range amplification of human mtDNA. All primers were based on the human M2 haplotype mtDNA sequence (pub-med nucleotide AF382013)

Region	Forward (F) or Reverse (R) Primer	5' to 3' Sequence	Region of MtDNA Genome Amplified	Length of Product (Bps)
ND1 to ND2	F	CCCGGTAATCGCATAAAACT	3242 to 4070	830
	R	TGTAGAGTTCAGGGGAGAGTGC		
	F	CCCTCACCACTACAATCTTCC	4011 to 4809	798
	R	TCAGAAGTGAAAGGGGGCTA		
	F	AGGAATAGCCCCCTTTCACT	4804 to 5550	746
	R	GGCTTTGAAGGCTCTTGGTC		
ND3 to ND4	F	TCTCCATCTATTGATGAGGGTCT	9964 to 10726	762
	R	GGCCATATGTTTGGAGATTG		
	F	AGCCAATATTGTGCCTATTGC	10631 to 11419	788
	R	ACATGGGCTTTAGGGAGTCA		
	F	TCACTCTCACTGCCCAAGAA	11292 to 12093	801
	R	GGAGAATGGGGGATAGGTGT		
	F	AACCACGTTCTCCTGATCAAA	11905 to 12237	332
	R	GGGCACGAGTTAGCAGTTCT		
ND4 to ND6	F	CAGAGGCTTACGACCCCTTA	12179 to 12982	803
	R	GAGGCCTAGTAGTGGGGTGA		
	F	TCCAACTCATGAGACCCACA	12911 to 13705	794
	R	CAGGCGTTTAATGGGGTTTA		
	F	CGCTTCCCCACCCTTACTA	13640 to 14377	737
	R	AGGTAGGATTGGTGCTGTGG		
ND6 to d-loop	F	CCACCACCCCATCATACTCT	14326 to 15104	778
	R	CAGGAGGATAATGCCGATGT		
	F	CGGACGAGGCCTATATTACG	15038 to 15810	772
	R	CGGATGCTACTTGTCCAATG		
	F	TCGGAGGACAACCAGTAAGC	15757 to 16520	763
	R	ATGGCCCTGAAGTAGGAACC		
cytochrome b to d-loop	F	CCATAACACTTGGGGGTAGC	16457 to 740	859
	R	CCCTTTTGATCGTGGTGATT		
d-loop to ND1	F	TTAGACGGGCTCACATCACC	617 to 1422	805
	R	TCCACCTTCGACCCTTAAGTT		
	F	TGGCAAGAAATGGGCTACAT	1348 to 2193	845
	R	AATTGGTGGCTGCTTTTAGG		
	F	GAGGAACAGCTCTTTGGACA	2102 to 2853	751
	R	ATGTACTGCTCGGAGGTTGG		
	F	CCCACAGGTCCTAAACTACCA	2759 to 3320	561
	R	TGGCCATGGGTATGTTGTTA		
ND2 to COXII	F	CCACGCTACTCCTACCTATCTCC	5465 to 6242	777
	R	GCGAGCAGGAGTTAGGAGAGA		
	F	GGAGGCTTTGGCAACTGACT	6127 to 6957	830
	R	GCCACCTACGGTGAAAAGAA		
	F	CCGGCGTCAAAGTATTTAGC	6847 to 7709	862
	R	GGGCATACAGGACTAGGAAGC		
	F	TCCCCTATCATAGAAGAGCTTATCA	7622 to 8209	587
	R	ATGGGCATGAAACTGTGGTT		
COXII-ND3	F	CGGGGGTATACTACGGTCAA	8158 to 8918	760
	R	AAGTGGGCTAGGGCATTTTT		
	F	CATGGCCATCCCCTTATG	8832 to 9629	797
	R	CTCCTGAGCGAGTAATACGG		
	F	TTCGCAGGATTTTTCTGAGC	9483 to 10100	617
	R	AGGCTCTAGGAAGGGTGTTGATT		

Table 2.2: Nested primers for sequencing human mtDNA. All primers were based on the human M2 haplotype mtDNA sequence (pub-med nucleotide AF382013)

Creation of Cytoplasmic Hybrid (Cybrid) Cell Models

2008 or C13* cells ($2.5x10^3$ cells) were allowed to adhere to circular pieces of 150 mm tissue culture plates (Corning) cut out with a heated No. 15 hole cutter. Following adherence, these disks were placed in centrifuge tubes (cells facing down) containing serum free DMEM and 10 ng/ml cytochalasin B (Calbiochem). Tubes with disks inside were centrifuges at 10000 g for 15 min to enucleate cells. Disks were retrieved, placed in tissue culture plates, and incubated at 37°C for 2 hr in fully supplemented media. 143B TK^- ρ^o cells were then plated on top of enucleated cells at a ratio of 3:1 (143B TK^- ρ^o:enucleated cells) and allowed to grow to confluence overnight in 143B TK^- ρ^o media (DMEM, 5% FBS, 50 μg/ml uridine, 100 μg/ml bromodeoxyuridine). Disks were then rinsed in three changes of Hank's Balanced Salt Solution (Gibco BRL, calcium and magnesium free) and exposed to a 90% polyethylene glycol, 10% DMSO (v/v) solution for 1 min with light agitation. Disks were washed three times with serum free DMEM containing 10% DMSO and one time in DMEM containing 10% serum. Disks were placed in 100 mm tissue culture plates and incubated at 37°C for 5hr in 143B TK^- ρ^o media. Cells were trypsinized from disks and plated in 150 mm tissue culture plates containing 143B TK^- media (DMEM without pyruvate, 5% concentrated FBS, 100μg/ml bromodeoxyuridine and gentamicin). Over 2 weeks the plates were scanned for colonies (See Figure 2.2).

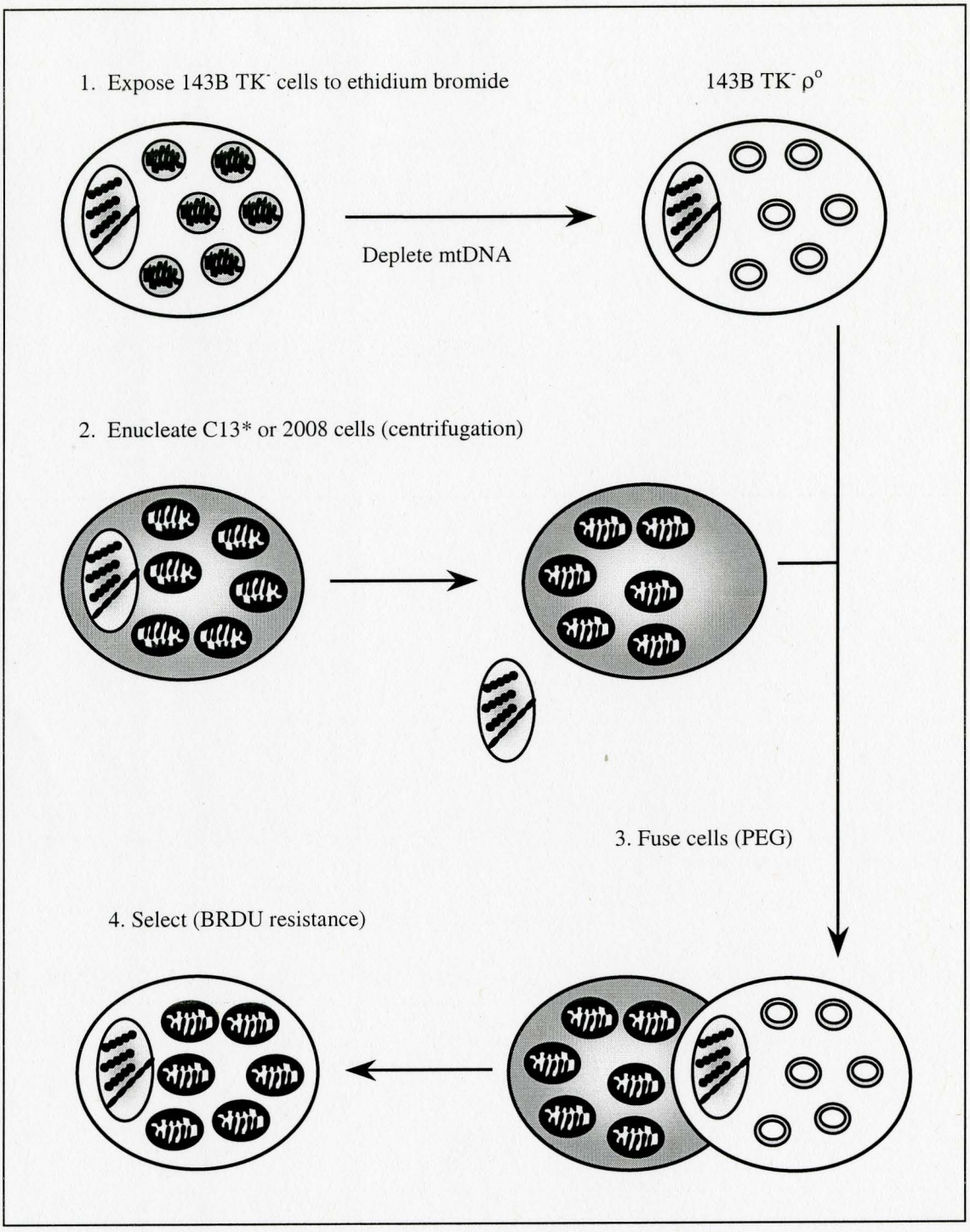

Figure 2.2: Overview of the cybrid creation process

RT-PCR

RT-PCR was used to screen cybrid cell clones for the presence of ATPase 6 RNA and the absence of thymidine kinase RNA. RNA was extracted from cells using a Qiagen RNA Easy kit according to the manufacturer's protocols. Forward and reverse primers used in the reverse transcription and subsequent polymerase chain reaction were as follows: ATPase 6 forward 5' ACCTACCTCCCTCACCAAAGC 3', ATPase 6 reverse 5' GGACGTGCTGTTGTGTATTACTG 3', thymidine kinase forward 5' CGCAATGAGCTGCATTAACCTG 3' and thymidine kinase reverse 5' TCAGTTGGCAGGGCTGCATTG 3'. 2 μg of RNA and 100 pmoles of reverse primer in a total volume of 10 μL were incubated at 70°C for 10 min after which time the full volume was added to an equal volume of reverse transcription mixture (2x first strand buffer, 10 mM DTT, 40 U RNAse out, 2 mM dNTPs and 15 U of Reverse Transcriptase) (Gibco BRL). This mixture was incubated at 25°C for 10 min and then for 1 hr at 50°C. After a 10 min incubation at 85°C, RNase H was added (2 U) and the solution was incubated at 37°C for 20 min. 2 μL of this solution was added to 48 μL of PCR reaction mixture (1xPCR buffer, 1.5mM $MgCl_2$, 0.2 mM dNTPs, 100 pmoles forward and reverse primer and 1 U of Taq polymerase), and amplification was conducted under the following conditions; one initial 5 min hot start at 94°C followed by 30 consecutive cycles consisting of a 30 s denaturation step at 94°C, a 30 s annealing step at 50°C, a 40 s extension step at 72°C, and one single 7 min polishing step at 72°C. PCR products were analyzed by electrophoresis through a 1% agarose gel containing 1 μg/ml ethidium bromide.

Confirmation of mtDNA Mutations in Cybrid Models

Confirmed mutation sites in 2008 and C13* mtDNA donor cells were also analyzed within cybrid models to ensure that the respective mitochondrial genomes were properly transferred into 143B TK^- ρ^o cells. DNA extraction and direct sequencing analysis was carried out as described above.

Cytotoxicity Assays

Subconfluent monolayers of cells were removed from tissue culture plates using trypsin-EDTA (2%). Cells were centrifuged at 1000 rpm for 5 min and resuspended in complete medium at a concentration of $4.0x10^5$ cells/ml. Cells were plated on 96-well plates (Falcon) at a concentration ranging from $4.0x10^4$ cells/well to 0 cells/well to generate a cell number standard curve. $2.0x10^3$ cells/well were also plated on separate 96-well plates. All cells were allowed to adhere overnight. Standard cell curve plates were washed once with PBS and replaced with 100 µl of H_20 per well. Plates containing $2.0x10^3$ cells/well were exposed to different concentrations of CDDP in media (prepared fresh) for 1 hr. The drug solution was removed and replaced with fresh fully supplemented drug-free media. Other plates containing $2.0x10^3$ cells/well were continually exposed to the mitochondrial poison rhodamine 123 (in 100% DMSO) in fully supplemented media. Following a 96 hr growth period plates were washed with PBS and replaced with 100 µL of H_20. Following 2 freeze-thaw cycles Hoescht dye No. 33258 (10 µg/ml, Calbiochem) in TNE (1 mM Tris, 0.1 mM EDTA, 0.1 M NaCl, pH 7.4)

was added to each well and Fluorescent emission was detected using a Series 4000 PerSeptive Biosystems CytoFluor ($\lambda_{excit.}$=350nm, $\lambda_{emiss.}$=460nm).

Assessment of Mitochondrial Mass

The fluorochrome 10-N-Nonyl acridine orange (NAO) was used to determine mitochondrial mass based on its affinity for the inner mitochondrial membrane specific phospholipid cardiolipin (Maftah et al. 1989;Petit et al. 1992). Mitochondrial uptake of this dye is essentially independent of mitochondrial energetic state and membrane potential (Leprat et al. 1990). Several groups have assayed cardiolipin content as an indirect indicator of mitochondrial mass through the use of NAO (Kluza et al. 2002; Pieri et al. 1992).

Subconfluent cultures of cells were removed from monolayers using trypsin-EDTA. Cells were centrifuged at 1000 rpm for 5 min and resuspended in complete medium at a concentration of $5.0x10^5$ cells/ml. NAO was added at a final concentration of 5 μM from a stock solution dissolved in DMSO. Cell suspensions were gently agitated by hand for 15 s and incubated at 37°C for 45 min. Samples were then centrifuged at 1000 rpm for 5 min and resuspended in fresh medium. After incubation on ice for 5 min, the individual fluorescence of $5x10^3$ cells was determined on a Coulter Epics Flow Cytometer using FL1 ($\lambda_{excit.}$=480nm, $\lambda_{emiss.}$=530nm). The mean NAO fluorescence of this population was then calculated.

Measurement of Intracellular ROS Production

The cell membrane permeable fluorochrome 2',7'-dichlorodihydrofluorescein-diacetate (2',7'-dichlorofluorescin diacetate; H_2DCFDA; DCFH-DA) was employed to determine intracellular hydrogen peroxide production (Bass et al. 1983; Cathcart et al. 1983). DCFH-DA is a stable, non-fluorescent, molecule that is converted to non-fluorescent DCFH by alkaline hydrolysis while penetrating the cell membrane (Miyajima et al. 1997). DCFH is then rapidly oxidized to the fluorescent compound DCF by ROS (Miyajima et al. 1997).

Subconfluent cultures of cells were removed from monolayers using trypsin-EDTA. Cells were centrifuged at 1000 rpm for 5 min. and resuspended in serum and antibiotic free medium at a concentration of 5.0x 10^5 cells/ml. DCFH-DA was added at a final concentration of 10 μM from a stock solution dissolved in DMSO. Cell suspensions were gently agitated for 15 s and incubated at 37°C for 15 min. Samples were then centrifuged at 1000 rpm for 5 min and resuspended in fresh serum and antibiotic free medium. At this point H_20_2 dissolved in H_20 was added to the media of positive controls at a final concentration of 10 μM. Cells were then incubated for an additional 20 min. After incubation for 5 min on ice, the individual fluorescence of 5x10^3 cells was determined on a Coulter Epics Flow Cytometer using FL1 ($\lambda_{excit.}$= 480 nm, $\lambda_{emiss.}$ = 530 nm).). The mean NAO fluorescence of this population was then calculated.

Protein Quantitation

Purified bovine serum albumin (BSA) was dissolved in water to create standard solutions of known protein concentrations (0 to 0.5 mg/ml). Standard BSA solutions were added to Biorad Protein Assay solution (20% in H_2O) at a final concentration range of 0 to 25μg/ml in a 96-well plate. Prepared cellular lysates of unknown protein concentrations were added to separate wells containing Biorad Protein Assay solution and the absorbance of all samples were measured at 570 nm in a 96-well microplate reader (Bio-Tek instruments). Absorbance values of BSA standards were plotted to create a standard curve and linear regression was used to obtain an equation of the line. Absorbance values of cellular lysates were substituted into the equation to obtain a protein concentration.

Western Blot Analysis of Antioxidant Defences

MnSOD Expression

Cellular lysates were made from the following cell lines: 2008, C13*, 2008cyb, C13*cyb, and 143B TK^- ρ^o. Briefly, cells were washed twice with ice cold PBS, pelleted through centrifugation, and resuspended in ice cold NP40 lysis buffer (15% NP40, 50 mM Tris (pH 7.4), 5mM EDTA, 0.4M NaCl) supplemented with 1x protease inhibitor (Boringer-Manheim). The mixture was put on ice for 30 min and rocked for an additional 15 min at 4°C. Samples were then spun at 10000 rpm for 5 min. and supernatant collected. The protein concentration of each sample was determined by the process described in the above section. 25 μg of protein was added to SDS sample buffer (3% SDS, 125mM Tris (pH 6.8), 10% glycerol, 5% β-Mercaptoethanol), boiled for 5 minutes,

loaded onto a 12% polyacrylamide gel containing 0.1% SDS and electrophoresis was carried out. Separated proteins were electroblotted onto Hybond ECL membranes (Amersham Pharmacia Biotech) and nonspecific binding of the antibody was blocked using 5% skim milk in TBST (0.1% Tris (pH 7.3), 1.5M NaCl, 0.5% Tween 20). The membrane was incubated in the presence of rabbit anti-human MnSOD polyclonal Ab (1:5000, Upstate), in 5% skim milk in TBST, and washed 3 times in TBST (10 min each). Membranes were incubated with HRP-conjugated anti-rabbit antibody (1:10000, Santa Cruz) and washed 3 times in TBST (10 min each). Membranes were visualized on X-OMAT AR film (Kodak) after reaction with ECL plus according to manufacturer's protocols.

CuZnSOD Expression

CuZnSOD expression was analyzed in a similar manner described above with a few exceptions. Membranes were incubated with sheep anti-human CuZnSOD polyclonal Ab (1:5000, Upstate) followed by a 1 hr incubation with HRP-conjugated anti-sheep antibody (1:10000, Molecular Probes). Membranes were visualized on X-OMAT AR film (Kodak) after reaction with ECL plus according to manufacturer's protocols.

Catalase expression

Catalase expression was analyzed in a similar manner described above with a few exceptions. Membranes were incubated with rabbit anti-human Catalase polyclonal Ab (1:5000, AbCam) followed by a 1 hr incubation with HRP-conjugated anti-rabbit antibody (1:10000, Santa Cruz). Membranes were visualized on X-OMAT AR film (Kodak) after reaction with ECL plus according to manufacturer's protocols.

Mitochondrial Membrane Potential ($\Delta\Psi_M$)

The fluorescent compound tetramethylrhodamine methylester (TMRM) was utilized to evaluate mitochondrial membrane potential. This compound is a fluorescent dye which is internalized by mitochondria in proportion to mitochondrial membrane potential and has been used to measure this parameter in a number of studies (Bell et al. 2003; Wong and Cortopassi 2002; Floryk and Houstek 1999).

Subconfluent cultures of cells were removed from monolayers using trypsin-EDTA. Cells were centrifuged at 1000 rpm for 5 min and resuspended in serum and antibiotic free medium at a concentration of 1.0x 10^6 cells/ml and divided into two aliquots. TMRM was added to both at a final concentration of 100 nM from a stock solution dissolved in 100% DMSO. Cell suspensions were gently agitated by hand for 15 s and incubated at 37°C for 30 min. After the 30 min incubation period, oligomycin, an ATPase inhibitor, and the mitochondrial protonophore carbonyl cyanide m-chlorophenyl hydrazone (CCCP) were added to one cell suspension at a final concentration of 100 ng/ml and 50 μM respectively. Cell suspensions were again agitated by hand for 15 s and incubated at 37°C for 30 min. Cells were placed on ice for 5 min and analyzed by flow cytometry using FL2 ($\lambda_{excit.}$= 549 nm, $\lambda_{emiss.}$ = 573 nm).

Preparation of Cells for Electron Microscopic Analysis

2008, C13*, C13cyb, 2008cyb and 143B TK$^-$ ρ^0 were grown to subconfluence in 6-well tissue culture dishes (Falcon). The media was aspirated, replaced with 2% glutaraldehyde in 200 μM sodium cacodylate buffer (pH 7.4) and incubated for 30 min at

room temperature. This solution was removed and the cells were washed twice in 200 μM sodium cacodylate buffer (pH 7.4) for 5 min each. After the second wash, cells were incubated in a 1% osmium tetroxide in 100 μM sodium cacodylate buffer for 30 min at 4°C. After removal of the osmium tetroxide solution, cells were dehydrated through a series of graduated ethanol exposures (50%, 70%, 90% ethanol, twice each for 3-5 min, and 100% ethanol three times for 5-10 min). Cells were then lifted from 6-well plates with propylene oxide and transferred to 2.0 ml conical tubes. Cells were exposed to propylene oxide:spur resin (50:50) for 45 min, propylene oxide:spur resin (25:75) for 45 min, and finally 100% spur resin (twice 30 min each). Cells in spur resin were embedded in capsules and polymerized overnight at 60°C. Sections of embedded cells (90 nm thick) were cut on a Reichart Ultracut E Ultramicrotome. Sections were fixed to copper-palladium grids and stained with uranyl acetate and lead citrate. Stained samples were examined on a Biosystem transmission electron mircroscope at 12000 times magnification.

Electrophoretic Mobility Shift Assay (EMSA)

Cell Lysates were prepared as described in Manley *et al.* (1980) with slight modifications. Briefly, 2008 lysates were prepared by harvesting subconfluent monolayers of cells from five 150 x 20 mm tissue culture plates using trypsin-EDTA (2%). All further operations were carried out at 4°C. Cells were washed in PBS and resuspended in four packed cell volumes of 10 mM Tris, (pH 7.9), 1 mM EDTA, 5 mM DTT. After 20 min cells were homogenized by passing the cell solution 10 times through a 20.5 gauge needle. Four packed cell volumes of 50mM Tris, pH 7.9, 10 mM $MgCl_2$, 2

mM DTT, 25% sucrose, 50% (vol/vol) glycerol were added to the mixture and gently agitated. One packed cell volume of saturated $(NH_4)_2SO_4$ was added and the lysate gently agitated for an additional 20 min. The extract was centrifuged at 52000 rpm for 3 hr using a Beckman 70 Ti/70.1Ti rotor. The supernatant was decanted and precipitated by addition of solid $(NH_4)_2SO_4$ (0.33g/ml of suspension). After the solid $(NH_4)_2SO_4$ was dissolved, 0.01 ml of 1 M NaOH per 10 g of $(NH_4)_2SO_4$ was added and the suspension was stirred for an additional 30 min The precipitate was collected by centrifugation at 14800 rpm for 20 min and resuspended with one tenth the volume of the high-speed supernatant in a buffer containing 50 mM Tris, pH 7.9, 6 mM $MgCl_2$, 40 mM $(NH_4)_2SO_4$, 0.2 mM EDTA, 1mM DTT, and 15% glycerol. This suspension was dialyzed for 8 hrs. against 2 changes of 100 volumes of dialysis buffer (20 mM HEPES, pH 7.9, 100 mM KCl, 12.5 mM $MgCl_2$, 0.1 mM EDTA, 1 mM DTT and 17% glycerol).

Portions of the human mtDNA d-loop were PCR amplified using three sets of forward and reverse primers (See Table 2.3). 15 ng of total cellular DNA was added to a 50 µl PCR reaction containing 1x PCR buffer, 1.5 mM $MgCl_2$, 0.2 mM dNTP mix, 1 U of Taq DNA polymerase and 100 pmoles of each specific primer. The thermocycler carried out one 5 min hot start at 94°C followed by 30 consecutive cycles consisting of a 10 s denaturation step at 94°C, a 10 s annealing step at 45°C, a 15 s extension step at 72°C, and one single 1.5 min polishing step at 72°C. 4 µL of this reaction was analyzed by electrophoresis in a 1% agarose gel containing 5 µg/µl ethidium bromide. The remaining volume was PCR purified using a Qiagen PCR purification kit and manufacturer's protocol. 100 ng of purified DNA was end labeled with $\gamma^{32}P$ (Perkin Elmer) in a 20 µL

reaction mixture (33pmol γ^{32}P ATP, 1xT4PNK buffer, 20 units T4 polynucleotide kinase) and incubated at 37°C for 40 min.

Protein extracts (5 μg) were added to a reaction mixture containing 20 mM Hepes (pH 7.9), 50 mM KCl, 50 mM NaCl, 2 μg of poly(dI.dC), 0.5 mM DTT, 0.2 mM EDTA, and 8% glycerol in a total volume of 8 μL. After 10 min on ice 1 μL of end-labeled DNA fragments were added, and the mixture was incubated at room temperature for 30 min. For competition studies various amounts of unlabeled DNA were added 15 min prior to the addition of labeled probe. This reaction mixture was loaded on a pre-run (180V for 1.5 hrs.) 1 mm thick 5% nondenaturing polyacrylamide gel (0.25xTBE, 1.25% glycerol) and electrophored at 180 V for 2 hr. Gels were transferred to filterpaper (VWR) and dried for 1 hr at 80°C under vacuum in a gel drier (Biorad). Dried gels were autoradiographed through the use of a phosphoimager screen (Molecular Dynamics) and analyzed with a phosphoimager and Imagequant 5.0 (Molecular Dynamics).

DNA Probe Name	Primer Sequence (5' to 3')	Position on mtDNA	Protein Binding Sites Present on Probe	Specific Protein-DNA Binding Sequence(s)
Mt43	TGGCCACAGCACTTAAACAC	321 to 340	mt3	ATCTGGTT
	AAATTTGAAATCTGGTTAGG	400 to 381	mt4	TGGTGTTAG
Mt4	TGGCCACAGCACTTAAACAC	321 to 340	mt4	TGGTGTTAG
	TAGGCTGGTGTTAGGGTTCT	365 to 384		
Mt4m	TGGCCACAGCACTTAAACAC	321 to 340	mt4	AGGTGTTAG*
	TAGGCAGGTGTTAGGGTTCT*	365 to 384		

Double underlined letters represent the position in the d-loop which was mutated in C13 cells alone.

Table 2.3: Primers for electrophoretic mobility shift assay probes

Polarographic Measurements

Oxygen consumption of cell lines was determined at 30°C using the OROBOS oxygraph 2K (Innsbruck, Austria). For each measurent, subconfluent monolayers of cells were removed from a single 150 x 20mm tissue culture plate using trypsin-EDTA (2%). Cells were centrifuged at 1000 rpm for 5 min and resuspended in KCl medium (80 mM KCl, 10 mM Tris-HCl, 3 mM $MgCl_2$, 1 mM EDTA, 5 mM potassium phosphate, pH 7.2) at a concentration of 1-2.5x10^6 cells/ml. Cells were permeabilised by digitonin (12.5 µg/1x10^6 cells) and various respiratory substrates and inhibitors were added in the order listed in Table 2.4. Oxygen consumption was expressed as pmol oxygen/s/1x10^6 cells.

Compound	Substrate or Inhibitor	Complex Effected	Function	Final Concentration
Glutamate	Substrate	I	Provides NADH to complex I[❖]	10 mM
Malate	Substrate	I	Provides NADH to complex I[❖]	5 mM
ADP	Substrate	I-III	Increases mitochondrial oxygen consumption and NADH formation[❖]	2 mM
Rotenone	Inhibitor	I	Prevents utilization of NADH as a substrate[❖]	1 μM
Succinate	Substrate	II	Provide electrons to complex II through FAD by way of succinate dehydrogenase[❖]	10 mM
Antimycin A	Inhibitor	III	Prevents electron transfer from cytochrome b to cytochrome c[❖]	1 μg/mL

[❖]From Principles of Biochemistry 2nd Edition. 1992. Lehninger, Nelson and Cox.

Table 2.4: Electron transport chain substrates and inhibitors

Reduction of Cytochrome C

Purified bovine cytochrome c was dissolved in 10 mM phosphate buffer (pH 7.8) at a concentration of 100 mg/ml. Sodium dithionite was added to the cytochrome c solution until the absorbance reached a maxima at 550 nm, indicating that the vast majority of cytochrome c had been reduced. Hydrated sepharose G-25 was loaded into a gel filtration column (5 cm diameter) to a height of 20 cm and equilibrated with 10 mM phosphate buffer (pH 7.8). Reduced cytochrome c was loaded onto the column and sodium dithionite was separated from reduced cytochrome c by elution of cytochrome c with 10 mM phosphate buffer (pH 7.8). Reduced cytochrome c was collected and the absorbance of a small aliquot was measured at 550 nm. Potassium ferricyanide was added to the aliquot to re-oxidize cytochrome c and the absorbance was again measured at 550 nm. The concentration (mM) of cytochrome c was then calculated by utilizing the following equation:

$$\frac{\mathbf{abs_{550}\ of\ reduced\ cytochrome\ c - abs_{550}\ of\ oxidized\ cytochrome\ c}}{\mathbf{19.1}}$$

where 19.1 is the extinction coefficient of cytochrome c.

Spectrophotometric Measurements

Methods for spectrophotometric analysis of ETC complexes were adapted from Chowdhury *et al.* 2000 and Rustin *et al.* (1994). Subconfluent monolayers of cells were removed from a single 150 x 20mm tissue culture plate using trypsin-EDTA. Cells were centrifuged at 1000 rpm for 5 min, washed twice, and resuspended in PBS. Each cell

suspension was divided into two equal volumes with one aliquot being sonicated twice for 20 sec. Protein content was determined as described above. Whole cell suspensions were used to determine citrate synthase (CS) and cytochrome c oxidase activities (COX, complex IV), while sonicated cell samples were used to determine succinate cytochrome c reductase (SCCR, complex II and III) and glycerophosphate cytochrome c reductase (GCCR, glycero-3-phosphate plus complex III) activities. All spectrophotometric measurements were conducted at 30°C using a Beckman 640 spectrophotometer adapted with a temperature control unit. Enzymatic activity was expressed as nmol of product/min/mg of protein.

Citrate synthase (ε = 13.6) activity was evaluated in a medium containing 150 mM Tris-HCl, pH 8.2, 8 mg of lauryl maltoside/mg of protein, 0.1 mM dithionitrobenzoic acid and 0.2 mg of cell protein. The reaction was initiated with the addition of 300 µM acetyl CoA and changes in absorbance at 412 nm were measured for 1 min. This rate was subtracted from the rate obtained after the subsequent addition of 0.5 mM oxalacetic acid. Absorbance values were recorded for a total of 5 min.

Cytochrome c oxidase (ε = 19.1) activity was measured by monitoring the rate of oxidation of reduced cytochrome c at 550 nm. Cytochrome c was reduced by sodium dithionite and excess sodium dithionite was removed by filtration through a Sephadex G-25 column as described above. The proportion of cytochrome c reduced and autoxidation rate were controlled. COX activity measurements were accomplished using 30 µM cytochrome c, 20 mM phosphate buffer, 0.1 mg of protein from cultured cells and 8 mg of lauryl maltoside/mg protein. Absorbance values were recorded for 5 min.

SCCR and GCCR activities were measured in medium containing 10 mM potassium phosphate (pH 7.8), 2 mM EDTA, 0.01% fatty acid free bovine serum albumin, 0.2 mM ATP, 1mM KCN, 5 μM rotenone and 10 mM succinate or 20 mM glycerophosphate respectively. Sonicated cells (0.2 mg protein) were incubated in medium for 2 min at 30°C, after which time the reaction was initiated by the addition of 40 μM oxidized cytochrome c. Changes in absorbances were monitored for 5 min at 550 nm.

Statistical Analysis

Standard error for all biological parameters are displayed in appropriate Tables and Figures. The unpaired student's t test was used to determine significant difference (95% probability) between different sample populations. Probit analysis was used to determine the concentration of CDDP and Rh123 which was required to inhibit cell proliferation by 50% (IC50) between sample groups (Lai and Singh 1995; Papermaster et al. 1974).

3.0 RESULTS

Direct Sequencing of the mtDNA Genome

To explore the role of mtDNA mutations in the phenotypic differences between the mitochondria of 2008 and C13* ovarian cancer cells, the complete mitochondrial genome of each cell line was PCR amplified and sequenced. Direct sequence analysis of 2008 and C13* cells revealed three mtDNA sequence variations when compared to the human mtDNA sequences reported in pubmed and polymorphisms or mutations reported within mitomap (www.mitomap.org). A heteroplasmic A379T mutation occurred only in C13* cells. This mutation occurred within the d-loop, a region responsible for both replication of mtDNA and transcription of encoded gene products. Position 379 of the d-loop is the last base pair of a nine base pair mtDNA-protein binding sequence. This binding sequence has demonstrated the ability to bind a poorly characterized protein termed mt4 (Suzuki et al. 1991).

A second heteroplasmic G7859A mutation was found only in 2008 cells. This mutation resulted in an amino acid change that converted amino acid residue 92 of COXII from an aspartic acid to asparagine. The amino acid sequence of 2008 COXII was compared its bovine protein counterpart to deduce the effect of the mutation on complex IV activity. Bovine COXII shares 74.5% homology with the human polypeptide and the crystal structure of bovine COXII has been previously analyzed (Tsukihara et al. 1996). Comparison of the two amino acid sequences revealed that this mutation occurred in close proximity to a putative transmembrane α-helix. It should also be noted that residue 92 of bovine COXII is normally asparagine which is identical to the residue found in the

mutated 2008 polypeptide, so the functional consequences of this mutation on the human protein are not obvious (See Figure 3.1).

A third homoplasmic T15287C mutation was found in both 2008 and C13*cells. This mutation resulted in an amino acid change that converts amino acid residue 181 in cytochrome b from a phenylalanine to a leucine. The amino acid substitution occurs directly beside a histidine that anchors the heme group (b_{566}) closest to the cytoplasmic side of cytochrome b (Esposti et al. 1993) (See Table 3.1 and Figure 3.1).

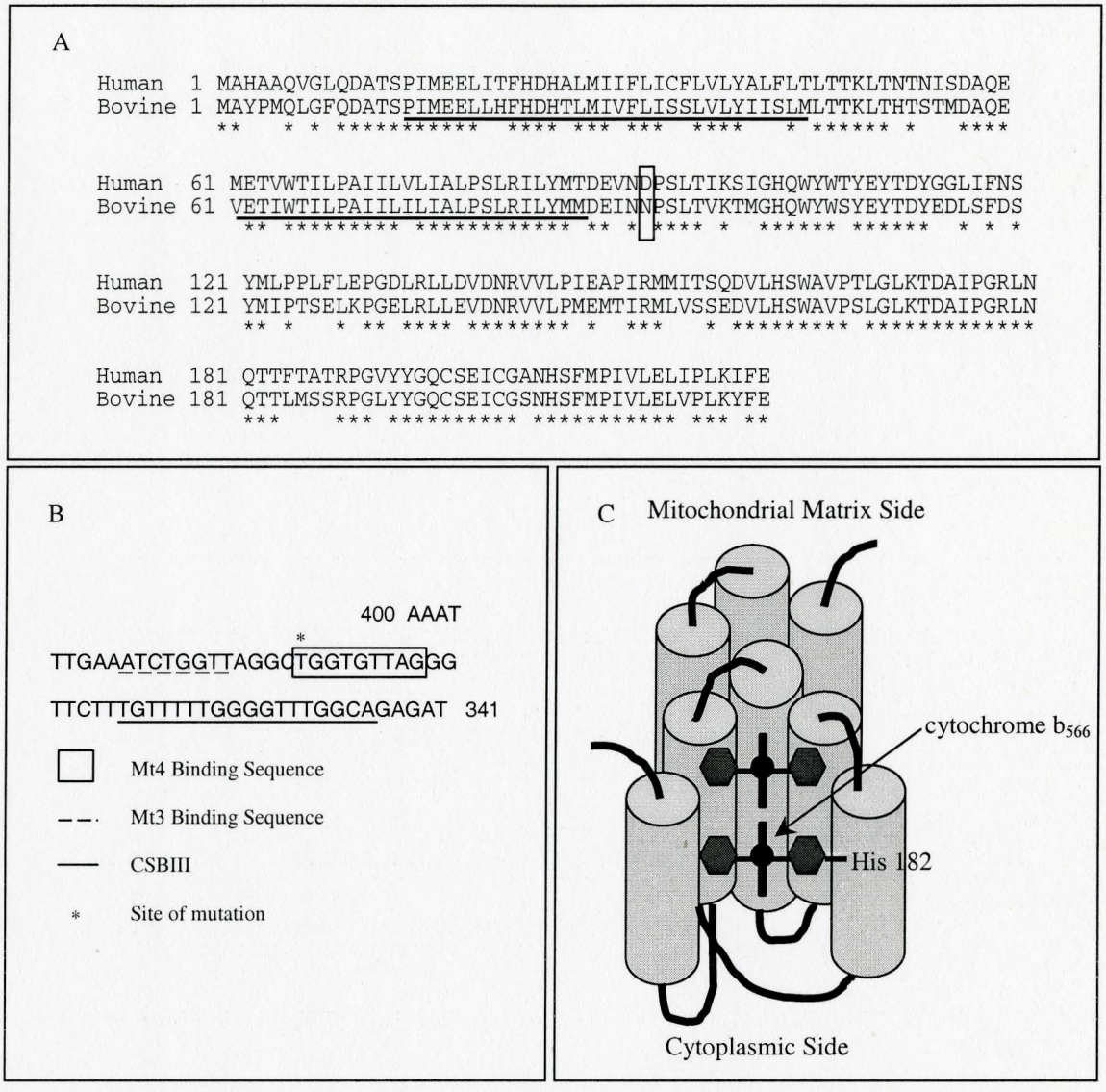

Figure 3.1: **Sequence Alignment of COX II, Schematic Diagram of d-loop, and Diagram of Cytochrome b.** A, sequence alignment of human COXII with the analogous bovine protein. Underlined portions represent α-helical transmembrane domains identified in bovine COXII from Tsukihara *et al.* (1996). A box surrounds the position of the amino acid substitution in 2008 cells. B, mutation at position 379 of the mitochondrial genome in relation to mt3 and CSBIII. C, diagram of human cytochrome b. Mutation in both 2008 and C13* cells occurred at amino acid residue 181 directly beside His 182 (from Espoti *et al.*, 1993).

Position in mtDNA	Base Change	Amino Acid Change	Protein Effected	Cell Line	
				2008	C13*
379	A to T	N/A*	N/A*	✗	✓
7859	G to A	phenylalanine to leucine	COXII	✓	✗
15287	T to C	asparagine to aspartic acid	cytochrome b	✓	✓

*Position 379 is contained within the d-loop of mitochondrial DNA and hence does not encode a protein product

Table 3.1: mtDNA Mutations Identified in 2008 and C13* Cells.

Confirmation of Cybrid Models

In order to expunge the impact of nuclear encoded gene products, 2008 and C13* cells were enucleated and fused with 143B TK^- ρ^0 cells which lack mitochondrial DNA. The resultant 2008cyb and C13*cyb cybrid cell lines share a common 143B TK^- nuclear background, but vary with respect to their mtDNA compliment. In order to confirm that true cybrid cell lines were indeed created, RT-PCR was performed on all cell lines involved to determine their thymidine kinase cDNA status. No detectable levels of thymidine kinase cDNA were present in cybrid cell lines or 143B TK^- ρ^0, confirming that cybrids do indeed contain the correct thymidine kinase null (143B TK^- ρ^0) nuclear background. As expected thymidine kinase cDNA products (708 bps) were detected in both 2008 and C13* cells (Figure 3.2). With the exception of 143B TK^- ρ^0 which lack mtDNA, a portion of ATPase6 cDNA (750 bps) was detectable in all other cells confirming that mitochondrial DNA was indeed transferred to cybrid cell lines (Figure 3.2).

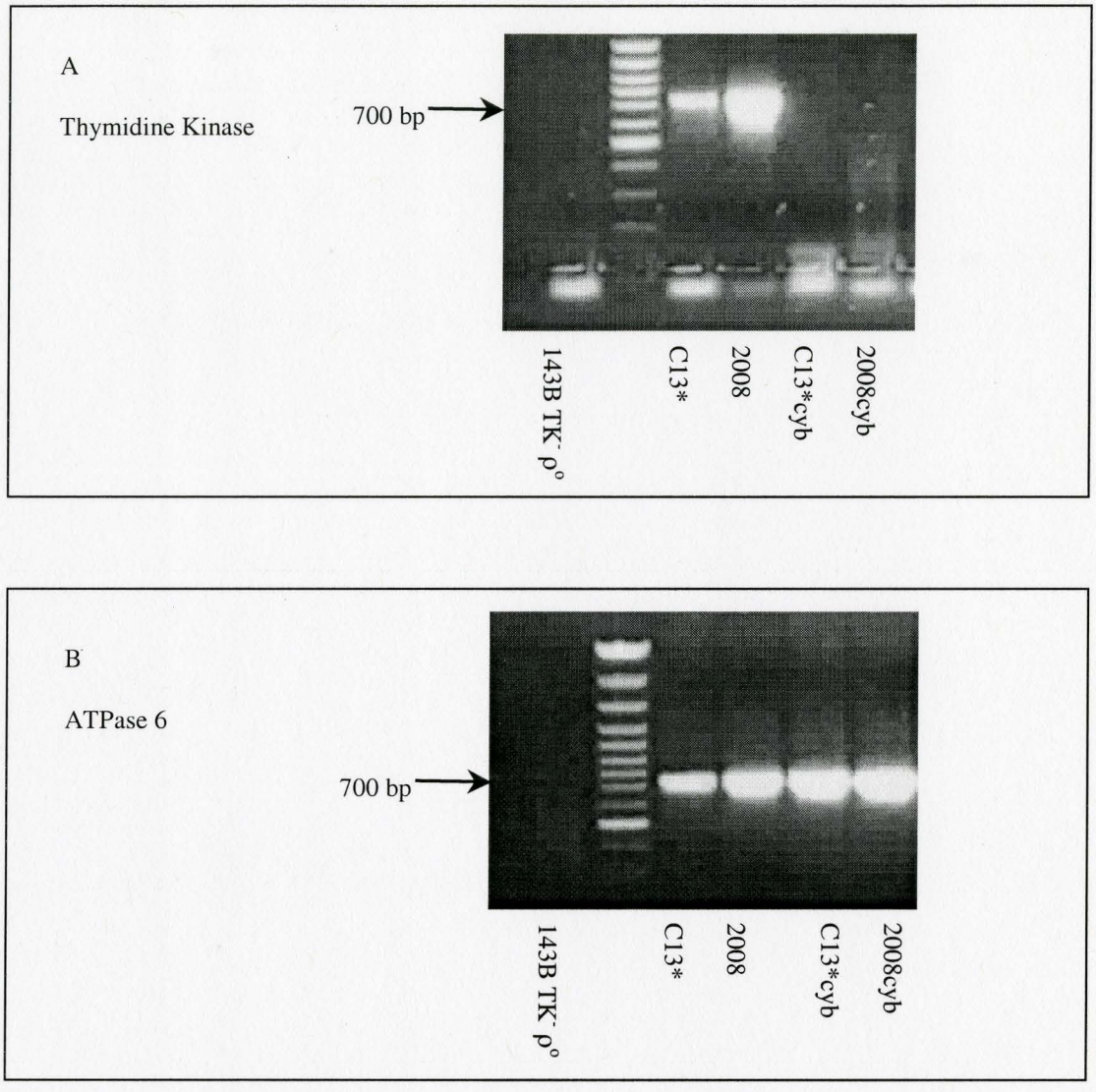

Figure 3.2: RT-PCR of Thymidine Kinase and ATPase 6 mRNA. A, RT-PCR amplification of a segment of thymidine kinase (708 bp), a nucelar encoded gene. B, RT-PCR amplification of a segment of ATPase 6 (750 bp), a nucelar encoded gene.

Confirmation of mtDNA Transfer to Cybrid Models

In order to determine if the correct mtDNA compliment was delivered to 143B TK^- ρ^o cells, mutations were characterized in cybrid cell lines. The A379T mutation which occurred exclusively in the d-loop of C13* cells created a BspMI restriction site making it possible to characterize this mutation in 2008, C13*, 2008cyb and C13*cyb cells through restriction fragment length polymorphism (RFLP) analysis. A 1545 bp fragment of mtDNA encompassing a portion of cytochrome b and the d-loop was PCR amplified and cut with BspMI. Restriction with this enzyme results in the production of 1189 bp and 356 bp fragments. The mutation at position 379 was indeed detected only in C13* and C13*cyb cells, producing DNA fragments of the expected size. The human ovarian cancer cell line SKOV-3 and three prostate cancer cell lines (DU145, PC3 and CL1) all failed to display this mutation through restriction with BspMI (Figure 3.4). The mutation at position 379 was also detected in RH4 cells (data not shown). The heteroplasmic A7859G mutation present solely in 2008 cells was also detected in 2008cyb cells through direct sequence analysis. Finally, the homplasmic T15287C mutation found in both 2008 and C13*cells was also detected in 2008cyb and C13*cyb cells lines through direct sequence analysis (See Table 3.2).

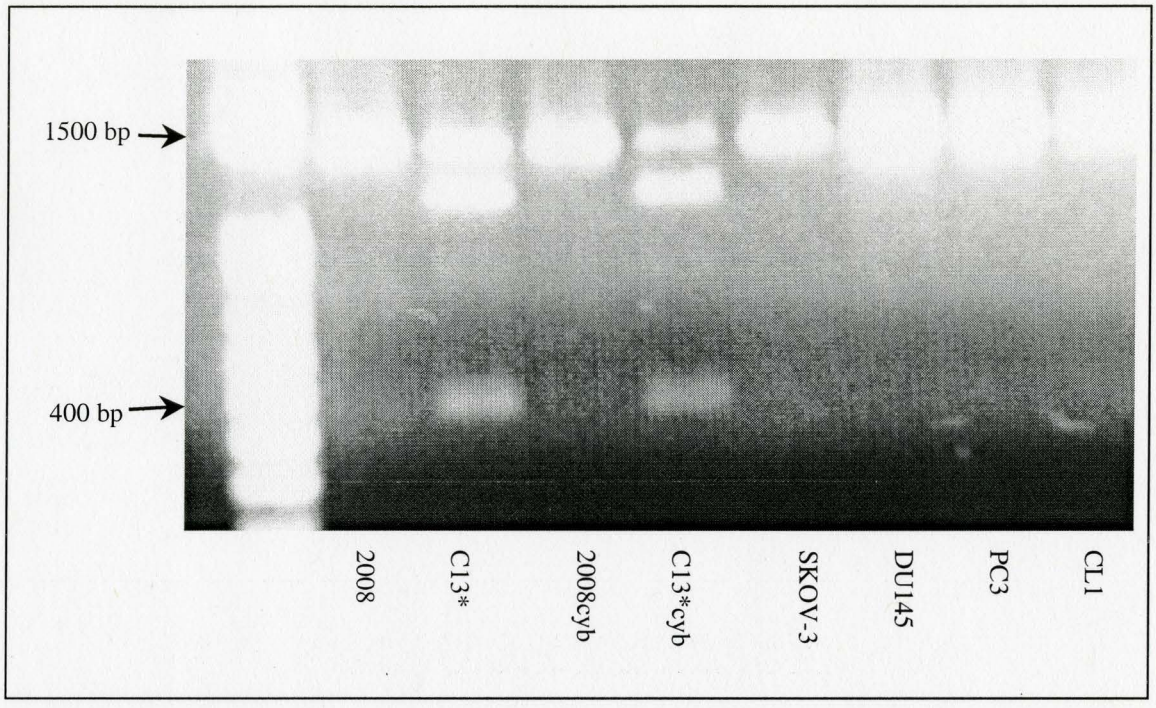

Figure 3.4: Restriction of d-loop fragment with BspMI

Position in mtDNA	Base Change	Protein Effected	Cell Line			
			2008	2008cyb	C13*	C13*cyb
379	A to T	N/A*	✗	✗	✓	✓
7859	A to G	COXII	✓	✓	✗	✗
15287	T to C	cytochrome b	✓	✓	✓	✓

*Position 379 is contained within the d-loop of mitochondrial DNA and hence does not encode a protein product

Table 3.2: mtDNA Mutations Identified in 2008, C13*, 2008cyb and C13*cyb Cells.

Microscopic Analysis

A previous study has observed that the organization of the cristae within the mitochondria of 2008 and C13* cells are quite dissimilar. Electron micrographs revealed that 2008 cells presented mitochondria with highly pronounced cristae, while the mitochondria of C13* cells contained cristae which were thicker and more irregular (Andrews and Albright 1992). In order to ascertain if the identified mtDNA mutations are associated with these structural differences, electron micrographs of 2008 and C13* cells as well as their cybrid counterparts and the mtDNA deficient 143B TK^- ρ^0 cell line were obtained and analyzed.

Electron micrographs of 2008 and C13* cells confirmed previous observations that 2008 mitochondria contain highly pronounced cristae, while C13* cells have thicker more irregular cristae (Figure 3.4). These distinct morphological characteristics were also apparent in 2008cyb and C13*cyb cell lines. Like their 2008 mtDNA donor cell, 2008cyb cells also display mitochondria with highly pronounced cristae (Figure 3.5). In the same respect, C13*cyb cells contain mitochondria with thicker more irregular cristae, characteristic of the C13* mtDNA donor cell (Figure 3.5). The organization of the cristae in 143B TK^- ρ^0 cells was also unique demonstrating circular cristae or none at all, which is typical of cells lacking mtDNA (Figure 3.6) (Gilkerson et al. 2000).

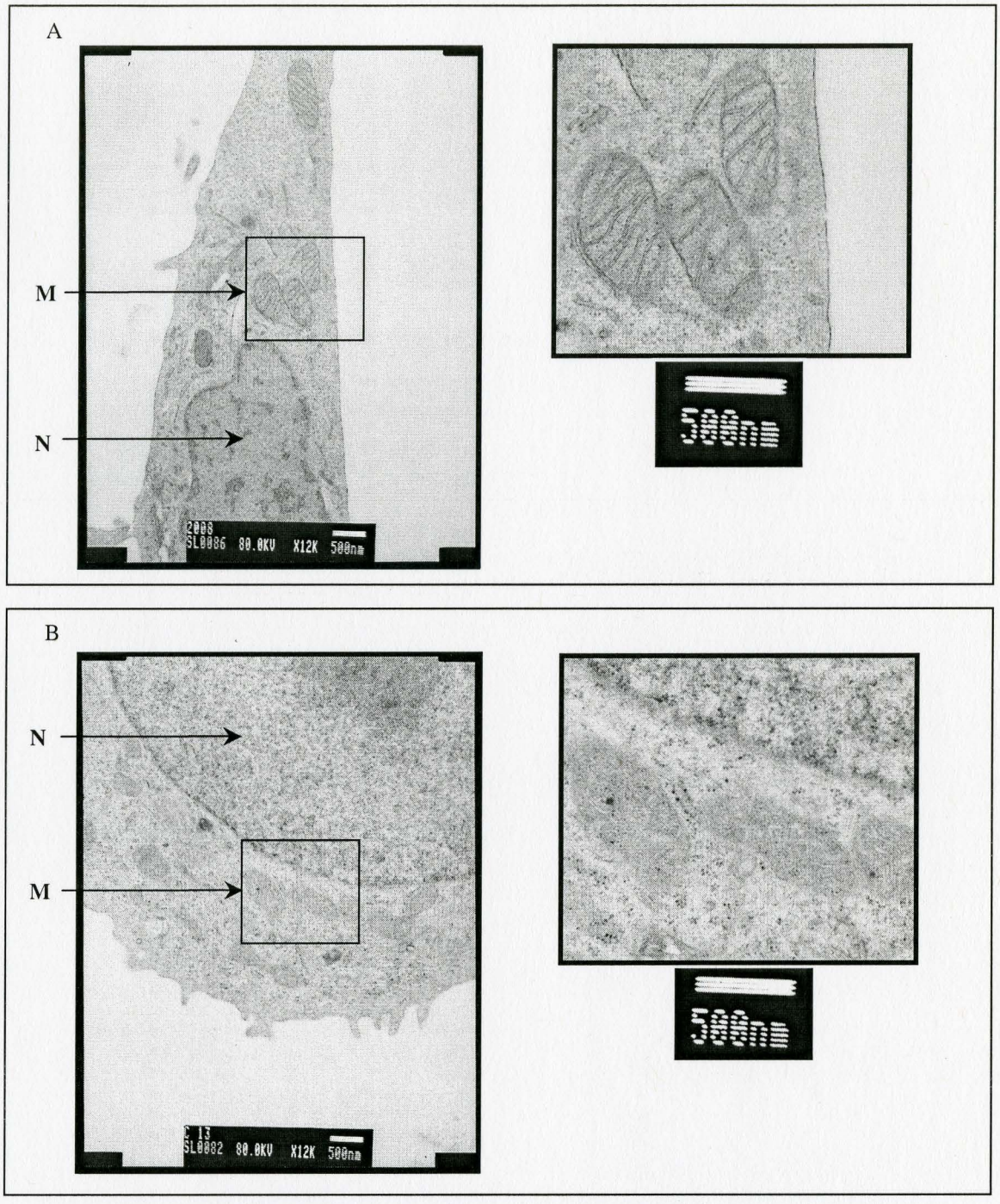

Figure 3.4: Electron Micrographs of 2008 and C13* Cell Lines. A, electron micrograph of 2008 cell. B, electron micrograph of C13* cell (both 12000 times magnification). Organelles labeled N and M are the nucleus and mitochondria respectively. Rectangular inlays are enlarged an additional 300% and appear to the right their respective micrograph.

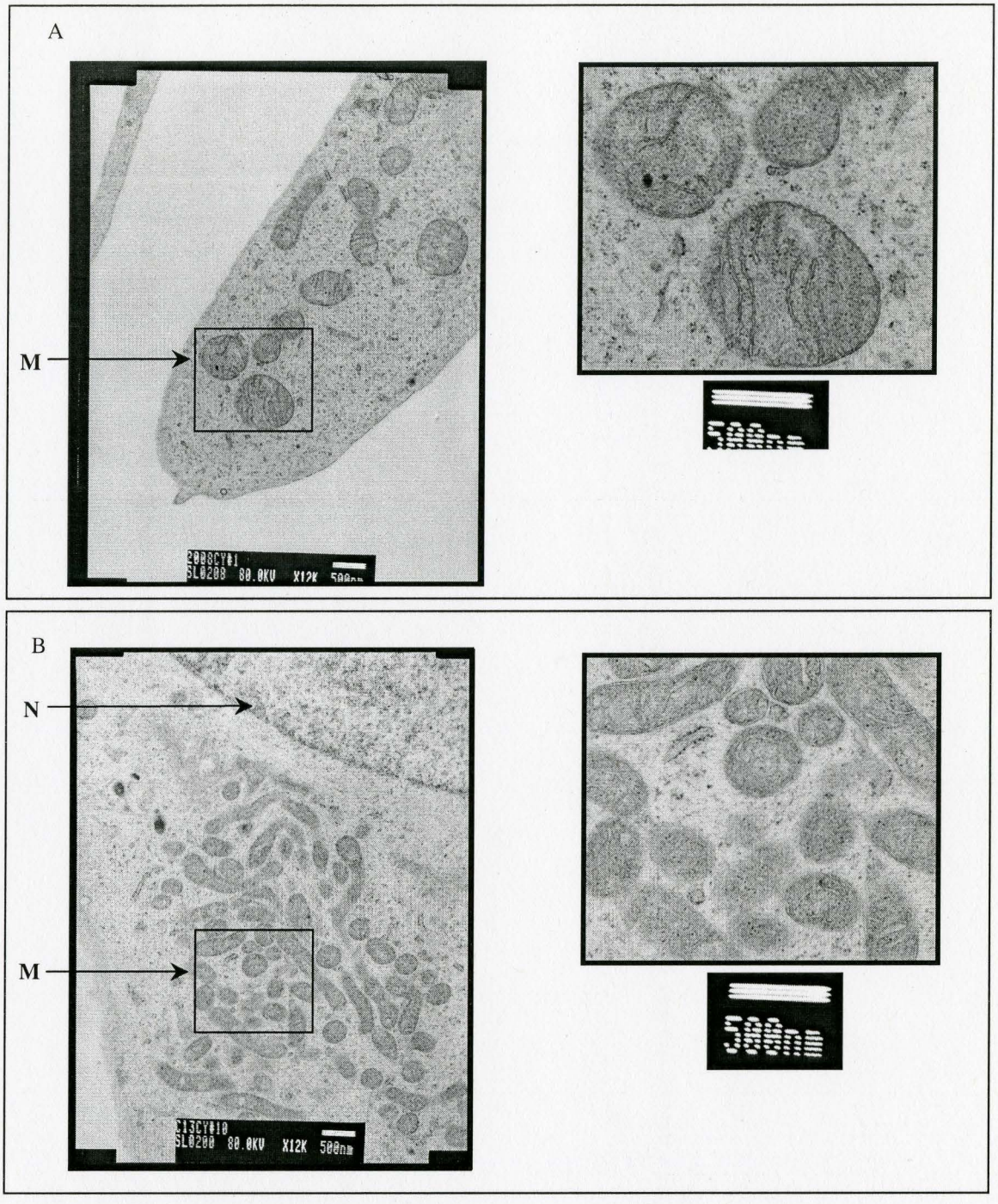

Figure 3.5: Electron Micrographs of 2008cyb and C13*cyb Cell Lines. A, electron micrograph of 2008cyb. B, electron micrograph of C13*cyb cells (both 12000 times magnification). Organelles labeled N and M are the nucleus and mitochondria respectively. Rectangular inlays are enlarged an additional 300% and appear to the right their respective micrograph.

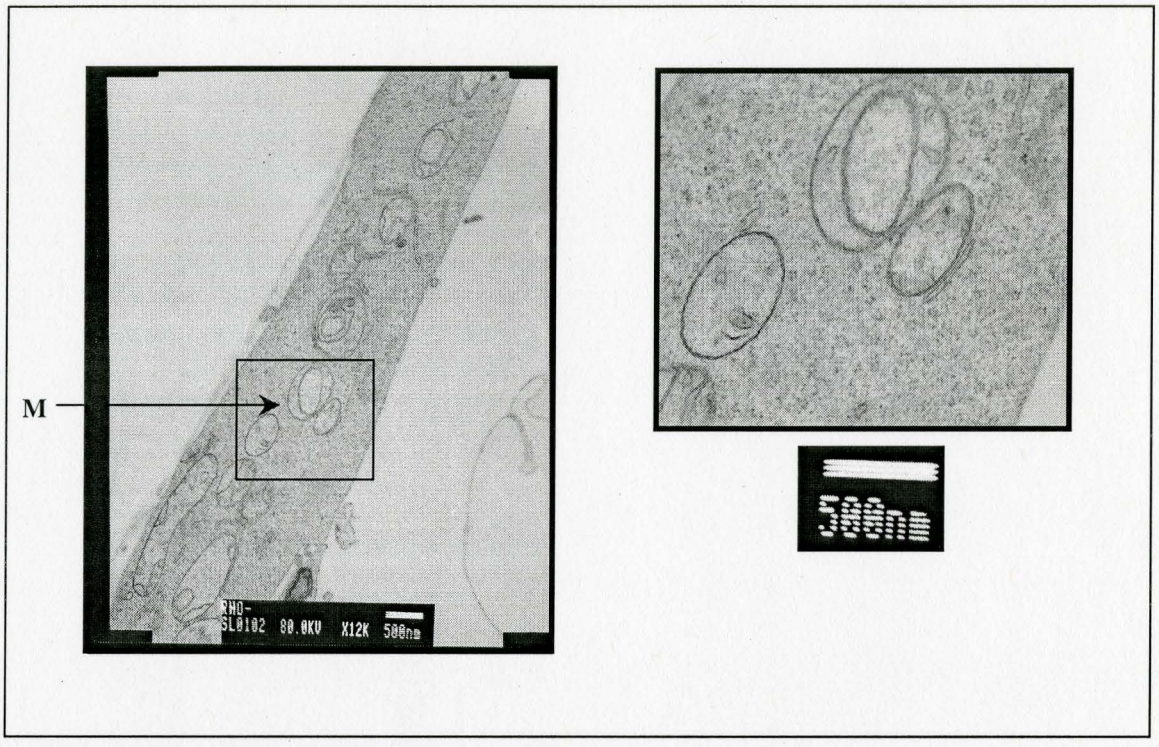

Figure 3.6: Electron Micrograph of 143B TK$^-$ ρ^o Cell. Electron micrograph of 143B TK$^-$ ρ^o cell (12000 times magnification). Organelles labeled M are mitochondria. Rectangular inlay is enlarged an additional 300% and appears to the right of the micrograph.

CDDP Induced Growth Inhibition

Growth Inhibition of C13*, 2008 and RH4 cells following CDDP treatment has been evaluated in a previous study (Andrews et al. 1985). Nevertheless, CDDP was administered to these cell lines to ensure characteristic responses to this chemotheraputic agent were retained. As portrayed in Figure 3.7, C13* cells were resistant to a 1 hr pulse of CDDP when compared to 2008 or RH4 cells. The IC50 value of C13* cells was 24.0 μM (95% CI 27.1-21.3 μM), while the IC50 value of 2008 and RH4 cells were 3.7 μM (95% CI 4.9-2.8 μM) and 3.1 (95% CI 4.0-2.7 μM) respectively. Identical methods were used to evaluate the growth inhibition of C13*cyb, 2008cyb and 143B TK^- ρ^o following exposure to CDDP. Unlike C13* cells, C13*cyb cells did not display any resistance to a 1 hr. pulse of cisplatin when compared to either 2008cyb or 143B TK^- ρ^o (Figure 3.8). The IC50 value of C13*cyb cells was 9.3 μM (95% CI 11.1-7.6 μM), while the IC50 value of 2008cyb and 143B TK^- ρ^o cells were 15.4μM (95% CI 17.2-13.7 μM) and 20.22μM (95% CI 23.8-17.0 μM) respectively (See Figure 3.8 and Appendix Table 6.1).

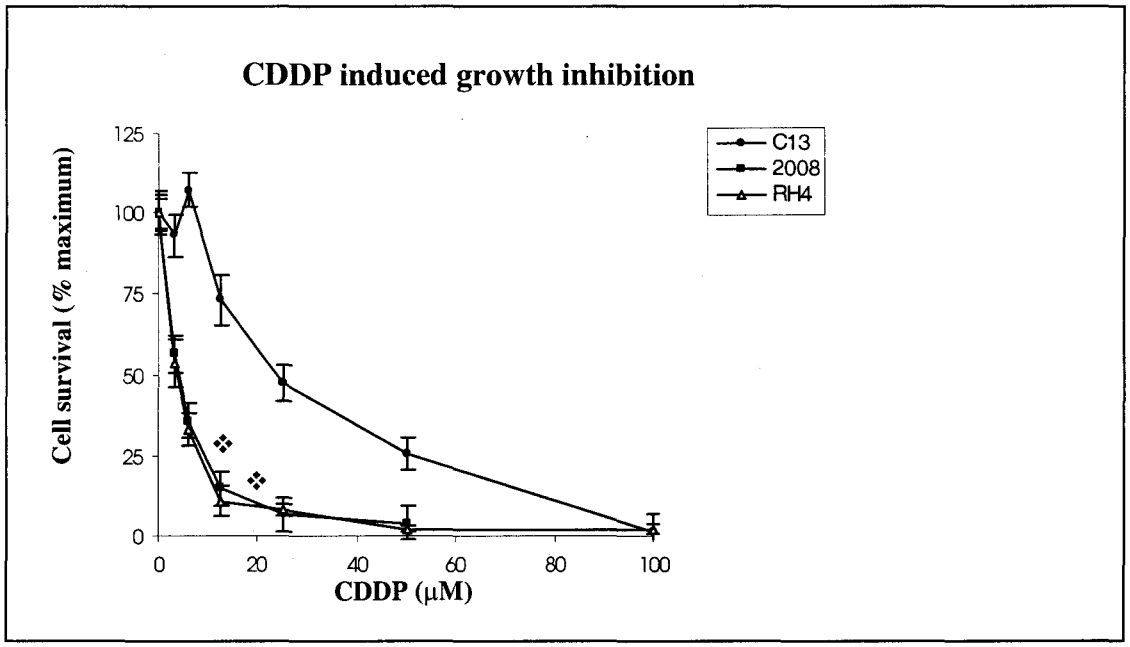

Figure 3.7: 2008, C13*, RH4 Induced Growth Response to CDDP. Lines marked with a (❖) indicate values that are significantly different from C13* cells. Error bars represent the mean ± SEM.

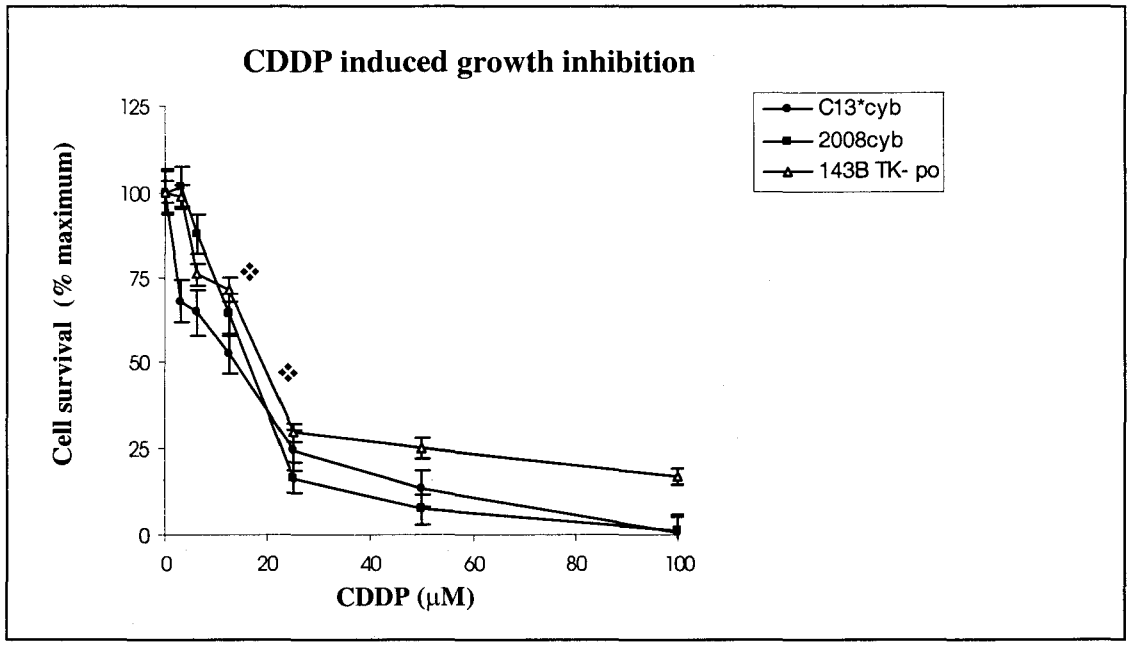

Figure 3.8: 2008cyb, C13*cyb and 143B TK$^-$ ρ^o Induced Growth Response to CDDP. Lines marked with a (❖) indicate values that are significantly different from C13*cyb cells. Error bars represent the mean ± SEM.

Rh123 Induced Growth Inhibition

The effect of Rh123 on the growth of C13*, 2008 and RH4 cells has also been previously evaluated (Zinkewich-Peotti and Andrews 1992). 2008 and RH4 IC50 values were 5.33 μM (95% CI 6.7-4.0 μM) and 4.57 μM (95% CI 5.4-3.7 μM) respectively, while C13* cells were quite sensitive to continuous exposure to Rh123 having an IC50 value less then 4.57, confirming previous findings (Figure 3.9). IC50 values could not be reliably calculated for C13* cells as the lowest concentration of Rh123 used resulted in a large decrese in cell numbers. Similarly, 2008cyb and 143B TK^- ρ^o cells showed resistance to Rh123 having IC50 values of 16.38 μM (95% CI 14.77-18.07 μM) and 21.03 μM (95% CI 18.44-24.26 μM), while C13*cyb cells had an IC50 value of 6.56 μM (95% CI 5.74-7.43 μM) (Figure 3.10).

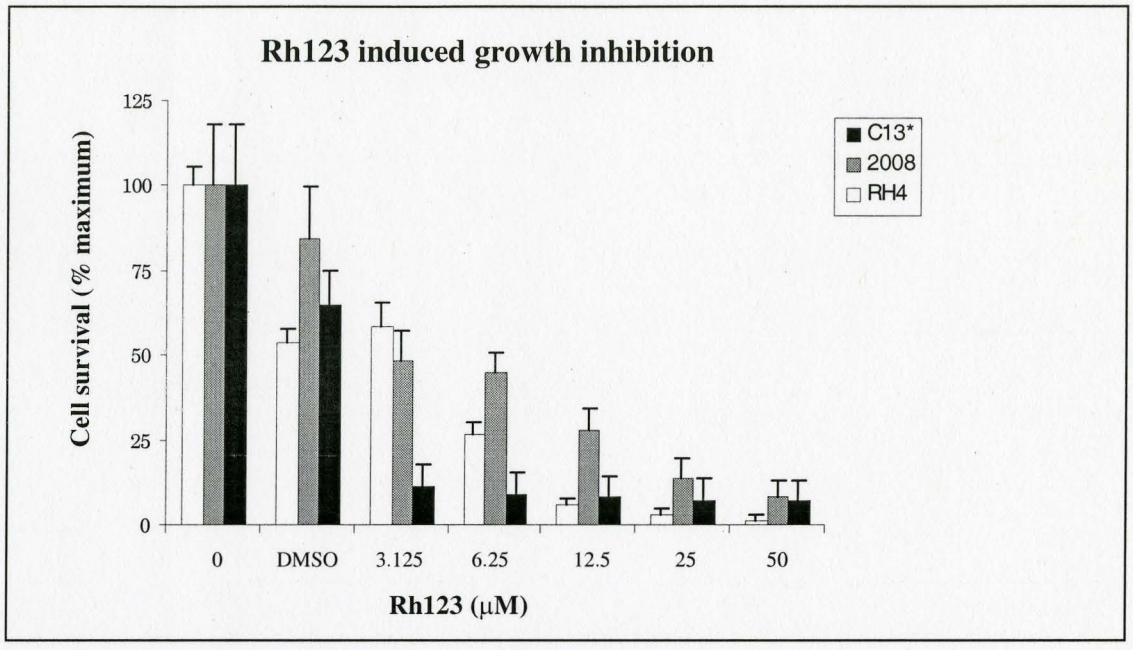

Figure 3.9: 2008, C13* and RH4 Induced Growth Response to RH123. Error bars represent the mean ± SEM.

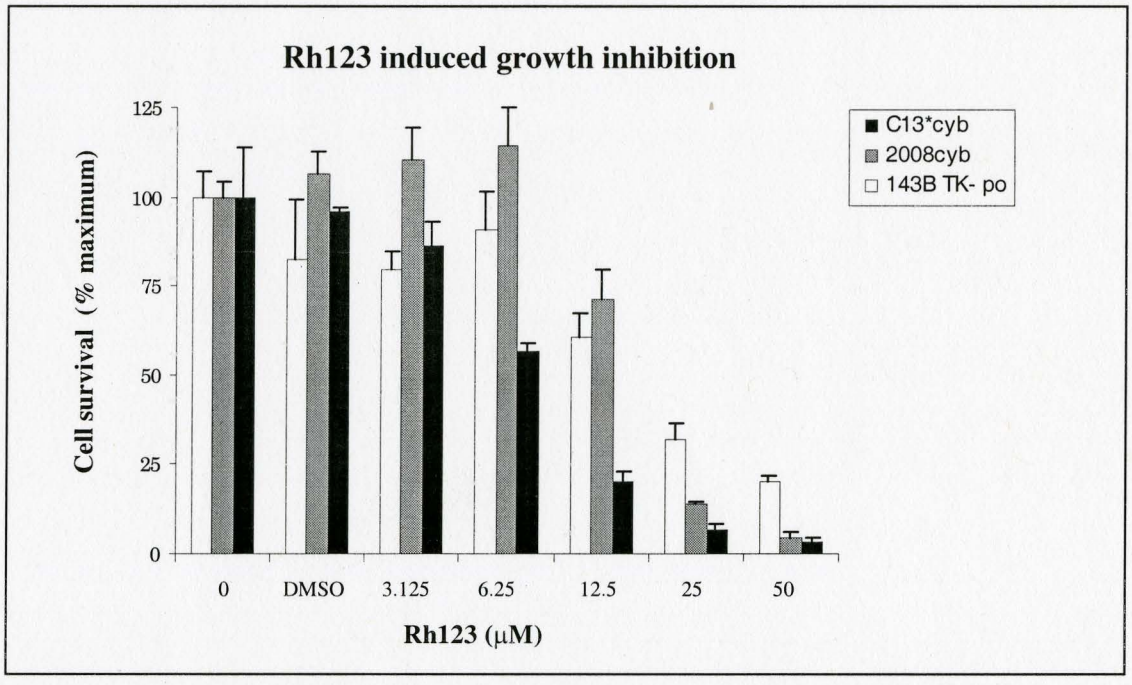

Figure 3.10: 2008cyb, C13*cyb and 143B TK$^-$ ρ^o Induced Growth Response to Rh123. Error bars represent the mean ± SEM.

Assessment of Mitochondrial Mass

NAO is a cardiolipin specific fluorescent dye which has been previously used to evaluate mitochondrial mass (Maftah et al. 1989; Petit et al. 1992). Cardiolipin binding of NAO was not significantly different in 2008 and C13* cells, indicating that the mitochondrial mass of these cells are equal. Likewise, the mitochondrial masses of cybrid cell lines were equal as indicated by the fluorescence readings in Figure 3.11. The mitochondrial mass of 143B TK$^-$ ρ^0 lacking mitochondrial DNA was significantly higher than C13*cyb and 2008cyb which share a common 143B TK$^-$ nuclear background. All cells which share a 143B TK$^-$ nuclear background had significantly higher NAO fluorescence when compared to 2008 or C13* cells, indicating that the nucleus must influence mitochondrial mass to some extent.

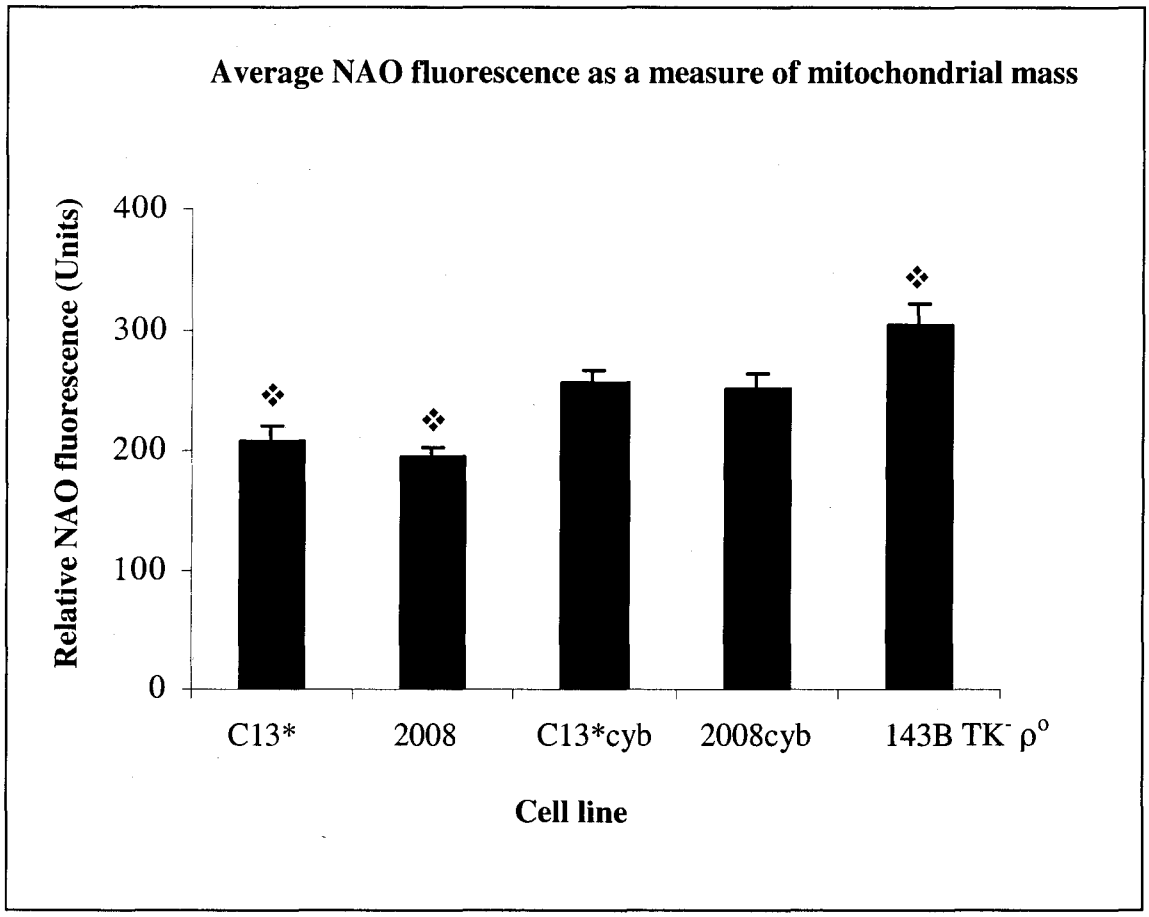

Figure 3.11: Mitochondrial Mass Assessment of C13*, 2008, C13*cyb, 2008cyb and 143B TK$^-$ ρ^o Cell Lines. Bars marked with a (❖) indicate values that are significantly different from 2008cyb cells. Values are mean ± SEM and are representative of n=3 independent experiments.

Measurement of Intracellular ROS Production

DCFH-DA was used to measure intracellular ROS production. This molecule is non-flourescent, but upon entering the cell and reacting with ROS it is converted to the fluorescent compound DCF (Bass et al. 1983; Cathcart et al. 1983; Miyajima et al. 1997). Previous studies have determined that mtDNA mutations are capable of inhibiting the electron transfer chain, resulting in increased energy byproducts in the form of reactive oxygen species (Swerdlow et al. 1996; Luo et al. 1997; Pitkanen and Robinson 1996). C13* extracellular ROS production has been found to be 2-fold that of 2008 cells, however the intracellular ROS production of both these cells had not been previously determined (Doward 1999).

Intracellular ROS levels of C13* cells were 2.7-fold higher than that of 2008 cells, which correlates well with extracellular ROS production values. Intracellular ROS levels were evaluated in cells with a 143B TK^- nuclear background to validate the hypothesis that the observed mtDNA mutations might be responsible for the increased ROS production in C13* cells. C13*cyb displayed 1.6-fold higher DCF fluorescence when compared to 2008cyb or 143B TK- ρ^o cells (Figure 3.12). Extracellularly applied H_20_2 (10 μM) was used as a positive control in C13*cyb cells which displayed the highest overall DCF fluorescence to ensure that all of the dye had not been oxidized and the dye was responsive to changes in ROS. This treatment had the effect of further raising DCF fluorescence values, indicating that ROS was indeed being measured and not all of the DCFH had been oxidized in the samples (data not shown). 143B TK- ρ^o cells produced a substantial amount of ROS which is contradictory to the findings of previous studies

(Leach et al. 2001) that noted a 2-fold decrease in ROS when compared to their 143B TK$^-$ ρ^+ counterpart (Figure 3.12).

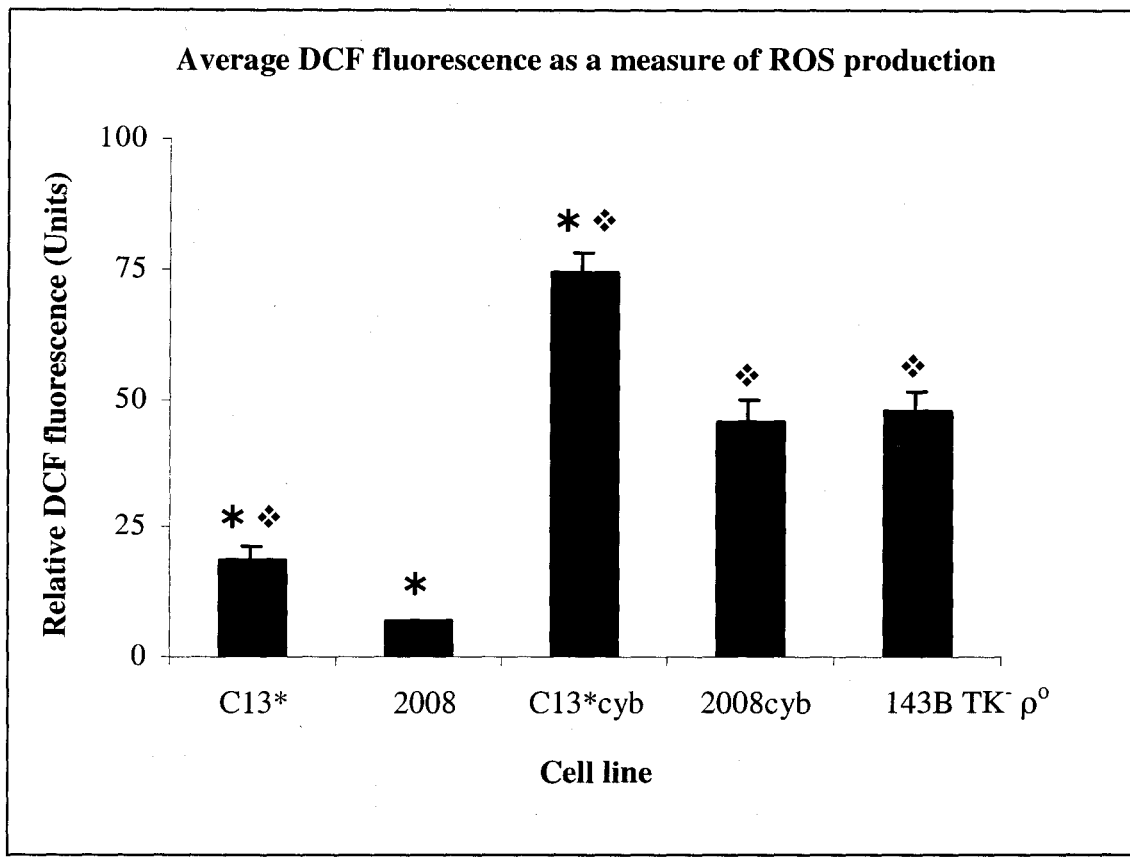

Figure 3.12: Intracellular ROS Assessment of C13*, 2008, C13*cyb, 2008cyb and 143B TK⁻ ρ° Cell lines. Bars marked with a (❖) indicate values that are significantly different from 2008 cells. Bars marked with a (✱) indicate values that are significantly different from 2008cyb cells. Error bars represent the mean ± SEM.

Antioxidant Protein Expression

MnSOD Expression

Electrons which escape the electron transport chain prematurely may react with molecular oxygen to form reactive superoxide anions (O_2^{-}.). Superoxide anions are detoxified by mitochondrial MnSOD to yield H_2O_2, which is metabolized to H_2O by GPx and catalase (Wallace 1999). Moreover, tissues isolated from patients diagnosed with mitochondrial diseases show increased MnSOD both at the mRNA and protein level presumably in response to increased ROS(Ohkoshi et al. 1995; Pitkanen and Robinson 1996). It was hypothesized that intracellular levels of ROS would directly correlate with MnSOD protein expression. Western blot analysis revealed that MnSOD protein expression was highest in 2008 cells, while C13* cells expressed lower levels of MnSOD (Figure 3.13). Cells with a 143B TK^- background expressed low levels of MnSOD when compared to 2008 cells, which produce much smaller amounts of ROS. On the other hand, MnSOD levels did correlate well with ROS production in cybrid and ρ^o cells. C13*cyb cells expressed the highest level of MnSOD, followed by 2008cyb and 143β $TK^- \rho^o$ (Figure 3.13).

CuZnSOD Expression

Superoxide anions present in the cytoplasm are detoxified by CuZnSOD to H_2O_2, which is converted by GPx to H_2O (Raha and Robinson 2001). Expression of this protein is also found in tissue isolated from patients with mitochondrial diseases (Filosto et al. 2002). Similar to MnSOD, it was hypothesized that protein levels of CuZnSOD would correlate directly with intracellular ROS. However, western blot analysis revealed that

CuZnSOD protein expression was highest in 2008 and C13* cells, while cybrid cell lines expressed lower levels of CuZnSOD. 143B TK$^-$ ρ^0 expressed the lowest levels of CuZnSOD (Figure 3.13).

Catalase Expression

Catalase scavenges cytoplasmic H_2O_2, converting it to innocuous H_2O. It was hypothesized cellular ROS levels would correlate directly with protein levels of catalase. Western blot analysis revealed that catalase protein expression was highest in 2008 cells. C13* catalase expression was considerably lower than 2008 cells, but still extremely high when compared to cells with a 143B TK$^-$ background (Figure 3.13).

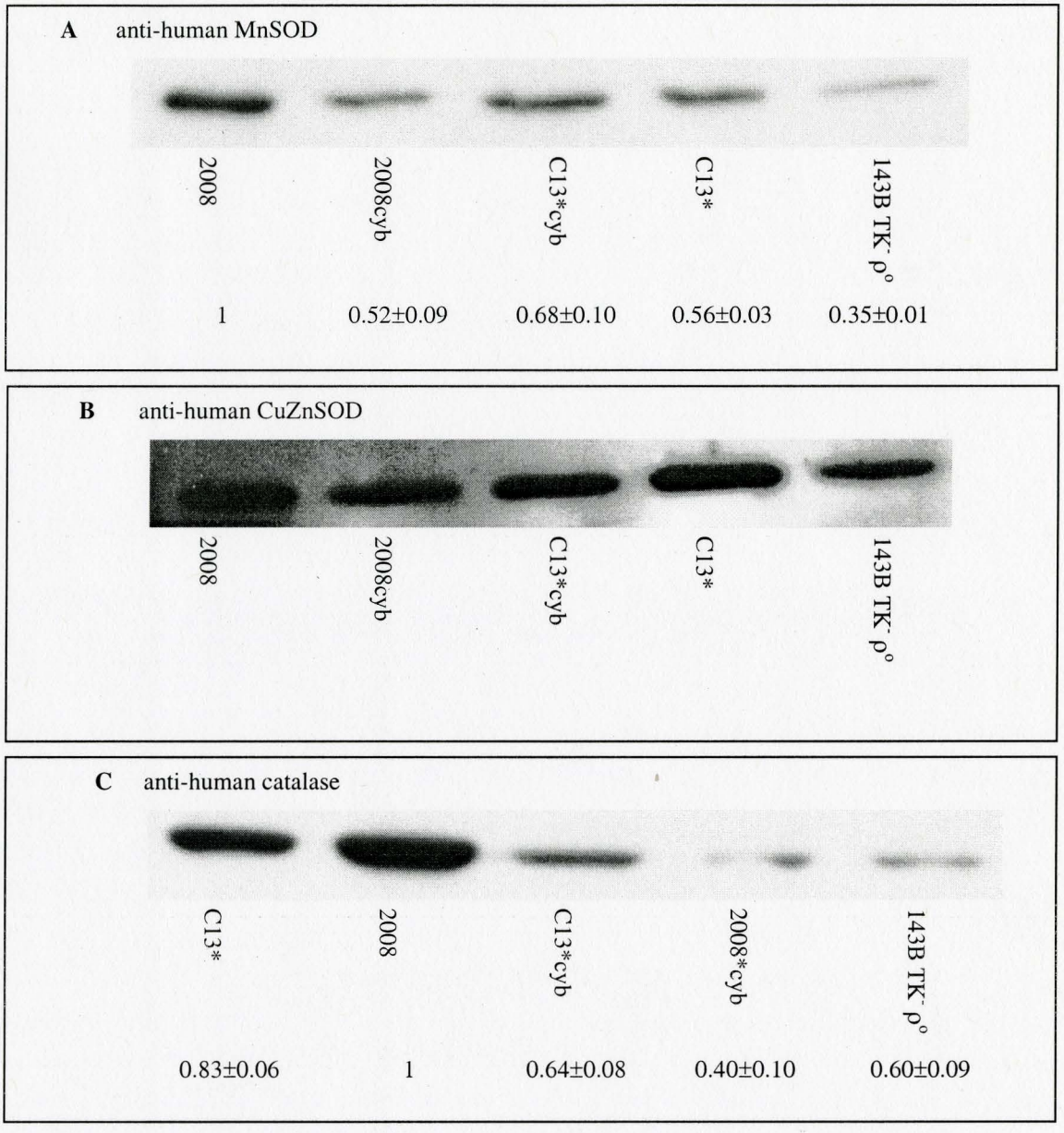

Figure 3.13: Western blot analysis of antioxidant protein expression. Figures A, B and C were incubated in the presence of anti-human MnSOD, anti-human CuZnSOD, and anti-human catalase respectively. Blots are representative of n=3 independent experiments using independent cell lysates. Numbers under blots represent the mean signal density as a fraction of the signal density of 2008 lysates±SEM. Densities could not be calculated for anti-CuZnSOD blots due to high uneven background.

Mitochondrial Membrane Potential ($\Delta\Psi_M$)

Previous studies have indicated that C13* cells displayed an approximate 2.3-fold higher mitochondrial membrane potential when compared to their 2008 parental counterpart (Andrews and Albright 1992). In order validate these results, the $\Delta\Psi_M$ was reevaluated in these cell lines. TMRM fluorescence was measured in both the presence and absence of the complex V inhibitor oligomycin and protonophore CCCP. $\Delta\Psi_M$ values were expressed as ratios of fluorescence values in the absence of inhibitors (coupled) to fluorescence values in the presence of inhibitors (uncoupled). Under these conditions the $\Delta\Psi_M$ value of C13* cells was determined to be 1.4-fold higher than that of 2008 cells. It was hypothesized that the observed mtDNA mutations in 2008 and C13* may be associated with differences in $\Delta\Psi_M$, therefore this variable was measured in cybrid and 143B TK$^-$ ρ^o cells. 2008cyb and C13*cyb cells $\Delta\Psi_M$ values were not significantly different, but were significantly higher than those of 143β TK$^-$ ρ^o which lack mtDNA. The finding that 143B TK$^-$ ρ^o cells maintain a relatively high $\Delta\Psi_M$ was surprising but this observation agrees with results from another study (Loiseau et al. 2002) (see Figure 3.14).

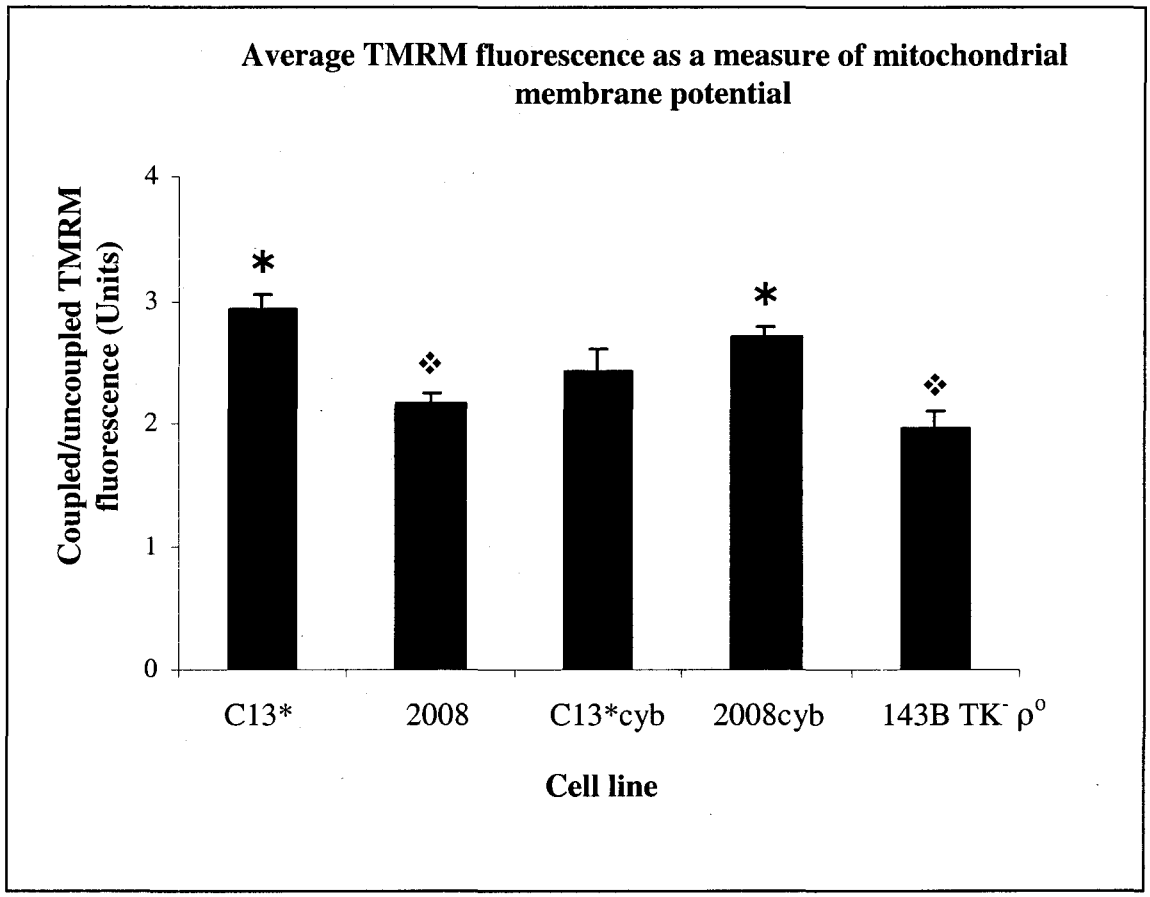

Figure 3.14: Assessment of Mitochondrial Membrane Potential of C13*, 2008, C13*cyb, 2008cyb and 143B TK$^-$ ρ^0 Cell Lines. $\Delta\Psi_M$ measurements are expressed as a ratio of TMRM fluorescence in the absence of inhibitors divided by TMRM fluorescence in the presence of inhibitors. Bars marked with a (✱) indicate values that are significantly different from 2008 cells. Bars marked with a (❖) indicate values that are significantly different from 2008cyb cells. Bars represent the mean ± SEM of at least n=3 independent experiments.

Polarographic Assays

Isolated cells from patients diagnosed with mitochondrial diseases frequently display a decrease in oxygen consumption resulting from inefficient electron transfer to atomic oxygen during OXPHOS (Rungi et al. 2002; Ono et al. 2001; Artuch et al. 2000). Previous investigations have also determined that 2008 cells consume oxygen at a 2-fold higher rate than C13* cells (Doward 1999). In order to verify these results, the oxygen consumption rate of 2008, C13* and RH4 cells were reevaluated. 2008 cells displayed a 1.6 and 1.5-fold higher rate of basal oxygen consumption when compared to C13* or RH4 cells respectively (Table 3.3). Upon stimulation of complex I by glutamate, malate, and ADP, 2008 cells displayed a 1.5 and 1.4-fold increase in oxygen consumption when compared to C13* or RH4 cells respectively. Conversely, C13*cyb cells displayed a 1.5 and 4.8-fold increase in rate of basal oxygen consumption when compared to 2008cyb and 143B TK$^-$ ρ^0 cells respectively. The oxygen consumption rate of C13*cyb cells was increased 1.5-fold when compared to 2008cyb upon stimulation of complex I by glutamate, malate and ADP. There was no significant stimulation of any ETC activity in 143B TK$^-$ ρ^0 cells (Table 3.4).

Oxygen consumption (pmol O_2/s/1x10^6 cells)	Cell Line		
	2008	C13*	RH4
Basal Respiration	49.34±2.92	30.46±2.23❖	34.61±4.45❖
Glutamate and Malate	18.91±4.06	12.09±0.70	9.35±1.38
Glutamate, Malate and ADP	54.70±5.92	37.14±5.18❖	39.58±3.34❖
Succinate and ADP	54.18±12.68	30.38±7.93	35.04±4.11

Table 3.3: Rate of Oxygen Consumption of 2008, C13* and RH4 Cells. Values marked with a (❖) indicate values that are significantly different from 2008 cells. Values represent the mean ± SEM of at least n=3 independent experiments.

Oxygen consumption (pmol O_2/s/1x10^6 cells)	Cell Line		
	C13*cyb	2008cyb	143B TK$^-$ ρ^o
Basal Respiration	66.66±6.44	44.06±6.16❖	15.14±6.28❖
Glutamate and Malate	35.77±4.27	21.69±4.21	7.58±3.39❖
Glutamate, Malate and ADP	65.33±9.63	42.27±5.33❖	7.88±3.47❖
Succinate and ADP	51.50±6.41	39.64±6.69	9.57±4.19❖

Table 3.4: Rate of Oxygen consumption of 2008cyb, C13*cyb and 143B TK$^-$ ρ^o Cells. Values marked with a (❖) indicate values that are significantly different from C13*cyb cells. Values represent the mean ± SEM of at least n=3 independent experiments.

Spectrophotmetric Assays

Patients suffering from mitochondrial diseases show reduced ETC complex activity that is also attributable to inadequate electron transfer to atomic oxygen (Rungi et al. 2002; Chomyn et al. 1991; Chomyn et al. 1992). Spectrophotometeric assays were conducted to determine if the basal oxygen consumption rates observed in mtDNA donor cells (2008 and C13*) and cybrid counterparts was attributable to any obvious ETC dysfunction. 2008 cells displayed a 1.8-fold increase in cytochrome c oxidase (COX) activity when compared to C13* and RH4 cells. SCCR (complex II and III) and GCCR (glycerol phosphate dehydrogenase and complex III) activity was also 1.2-fold higher in 2008 cells when compared to RH4 cells. However, if these values are normalized to citrate synthase activity (CS), differences become diminished or reversed (see Table 3.5 and 3.6) as CS activity in 2008 cells is 2-fold that of C13* or RH4 cells. The rate of oxygen consumption also correlated well with complex IV activity in cybrid models. C13*cyb cells displayed a 1.5-fold higher rate of cytochrome c oxidation when compared to 2008cyb cells. 143B TK^- ρ^0 failed to display any COX activity, while the SCCR and GCCR activity was 12% of that detected in cybrid cells indicating that these assays are specific in the assessment of ETC complex functioning (Table 3.6). CS activity was almost identical in cells with a 143B TK^- background, hence differences observed from enzymatic rate measurements were retained when these values were taken as a fraction of CS activity (Table 3.7).

Cell line	Enzyme Activity (nmol/min/mg protein)			
	CS	COX	SCCR	GCCR
2008	128±2.52	30.5±0.914	3.9±0.25	4.6±0.20
C13*	58.3±3.20❖	17.1±1.65❖	3.7±0.17	5.82±0.31❖
RH4	59.2±2.21❖	16.8±0.752❖	3.2±0.36❖	3.76±0.31❖

Table 3.5: Spectrophotometric Analysis of RespiratoryChain Enzymes in 2008, C13* and RH4 cells. Values marked with a (❖) indicate values that are significantly different from 2008 cells. Values represent the mean ± SEM of at least n=3 independent experiments.

Cell line	Ratio of enzyme activity to CS activity			
	CS	COX/CS	SCCR/CS	GCCR/CS
2008	-	0.24±0.018	0.03±0.004	0.04±0.004
C13*	-	0.30±0.035❖	0.07±0.001❖	0.11±0.002❖
RH4	-	0.30±0.055	0.05±0.016	0.06±0.014❖

Table 3.6: Spectrophotometric Analysis of Respiratory Chain Enzymes in 2008, C13* and RH4 Cells as a Fraction of Citrate Synthase Activity. Values marked with a (❖) indicate values that are significantly different from 2008 cells. Values represent the mean ± SEM of at least n=3 independent experiments.

Cell line	Enzyme Activity (nmol/min/mg protein)			
	CS	COX	SCCR	GCCR
2008cyb	65.32.14	12.4±1.43	5.9±0.24	3.6±0.11
C13cyb*	57.8±1.67❖	18.2±0.85❖	5.8±0.27	4.2±0.27❖
143B TK$^-$ ρ^o	68.0±1.35	0.00❖	0.65±0.06❖	0.40±0.06❖

Table 3.7: Spectrophotometric Analysis of Respiratory Chain Enzymes in 2008cyb, C13*cyb and 143B TK$^-$ ρ^o Cells. Values marked with a (❖) indicate values that are significantly different from 2008cyb cells. Values represent the mean ± SEM of at least n=3 independent experiments.

Cell line	Ratio of enzyme activity to CS activity			
	CS	COX/CS	SCCR/CS	GCCR/CS
2008cyb	-	0.19±0.0418	0.09±0.011	0.06±0.006
C13cyb*	-	0.33±0.007❖	0.10±0.014	0.07±0.005
143B TK$^-$ ρ^o	-	0.00❖	0.01±0.001❖	0.006±0.001❖

Table 3.8: Spectrophotometric Analysis of Respiratory Chain Enzymes in 2008cyb C13*cyb and 143B TK$^-$ ρ^o Cells. Values marked with a (❖) indicate values that are significantly different from 2008cyb cells. Values represent the mean ± SEM of at least n=3 independent experiments.

Electrophoretic Mobility Shift Assay (EMSA)

The d-loop is integral in mtDNA replication and transcription. These activities are chiefly regulated by mtDNA-binding proteins that interact with the mitochondrial genome. Perhaps most notable are proteins such as γ DNA polymerase and mtTFA which initiate replication and transcription, respectively (Tully and Levin 2000). Another protein termed mt4 was observed to bind to a nine base pair portion of the d-loop containing position 379 that is mutated in C13* cells (Suzuki et al. 1991; Suzuki et al. 1995). In order to elucidate if the mutated sequence was capable of modulating mt4 binding, an EMSA was employed using double stranded wildtype and mutated pieces of mtDNA as probes. However, after several trials, results of these assays were difficult to interpret. Observations between trials and even within trials were highly variable (See Figure 3.15). Multiple proteins appear to interact with the labeled probes unlike the single DNA-protein interaction identified in Suzuki et al. (1991). Cold competitor DNA was capable of competing with labeled probe thus reducing probe-protein interaction and resultant signal. It should also be noted that the lack of an antibody towards mt4 made super-shifting experiments to identify true mt4 probe interactions impossible.

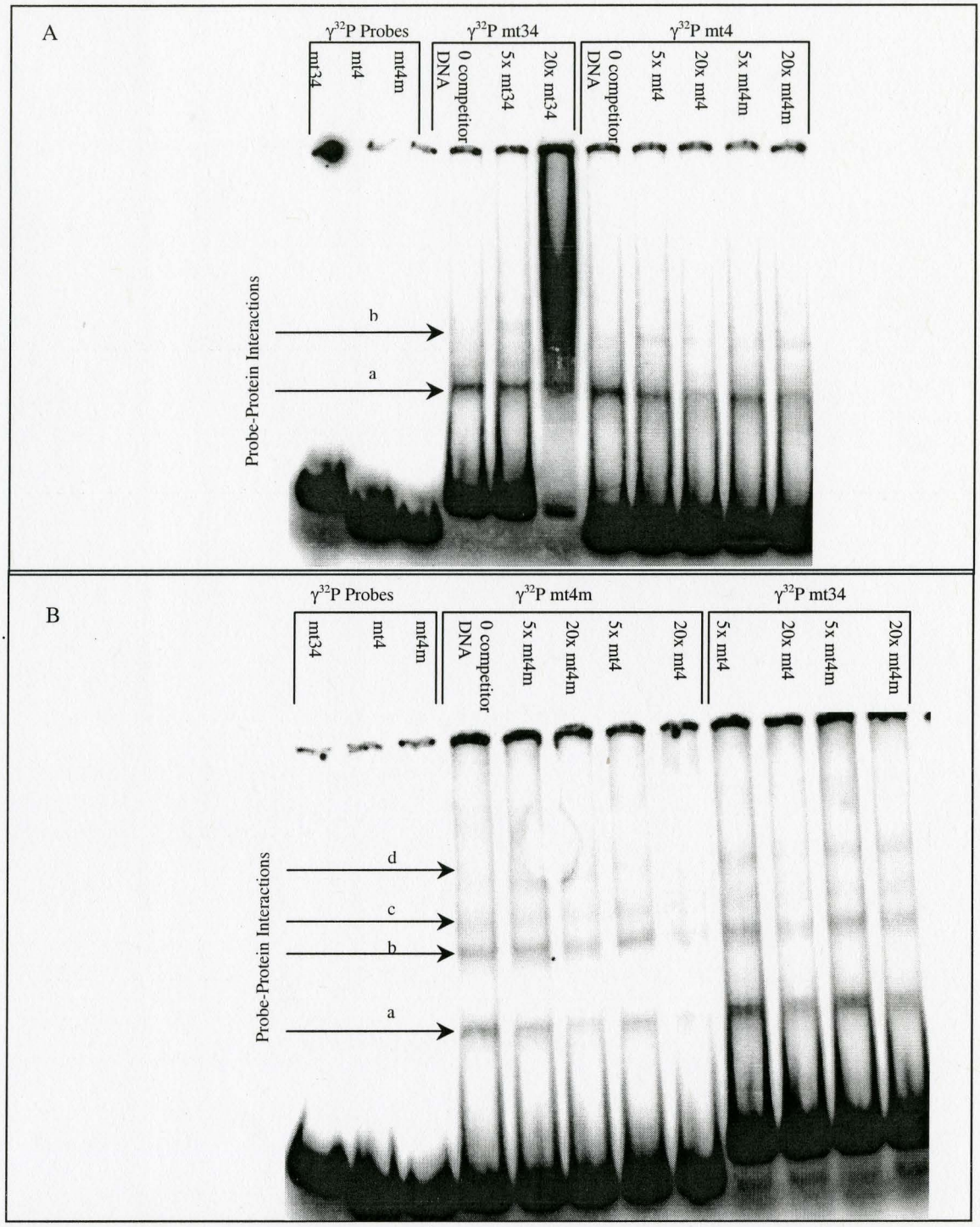

Figure 3.15: Electromobility Shift Assay. Probe-protein interactions of $\gamma^{32}P$ labeled double stranded DNA probes. Bands in the lanes above (a-d) represent probe binding with proteins under non-reducing conditions. mt34 contains two previously identified protein binding sites (mt3 and mt4) while mt4 and mt4m contains only one site (mt4). Gel A and B were run simultaneously in the same apparatus.

4.0 Discussion

4.1 mtDNA Mutations in Carcinogenesis and Utilization of a Cybrid Model

A number of recent reports have indicated that a large proportion of neoplastic cells display mtDNA mutations when compared to tissue adjacent to the tumour (Parrella et al. 2001; Jones et al. 2001; Penta et al. 2001). Proponents of the selective advantage model of mtDNA mutation acquisition believe that a subset of these aberrations arise because they offer some benefit to the cell (Mambo et al. 2003). Mitochondrial defects in the context of mtDNA diseases are known to result in the upregualtion of ROS. If mutations found in tumour cells result in a similar outcome it may prove advantageous, as ROS is known to play a role in the initiation of cancer, and encourage cell proliferation at low levels (Wei 1998; Martindale and Holbrook 2002). Furthermore, some mtDNA molecules appear to have dominance over others, indicating that mitochondrial or nuclear genomic factors influence the mtDNA compliment of a cell (Polyak et al. 1998). Conversely, others have hypothesized that a model of random drift may explain the occurrence of these mutations. In this scenario a mutation would arise during development and reach homoplasmy through "population genetics" alone. Mathematical modeling has predicted that the occurrence of homoplasmic mutations through a process of random drift is possible, and quite probable when a number of individual mtDNA molecules harbour mutations (Jones et al. 2001).

In terms of carcinogenesis, controversy exists between these two mtDNA mutation acquisition models because sufficient evidence does not exist to support one theory, and for good reason. Selecting potential cell lines to test either hypothesis is

difficult as the majority of cancer cells display characteristics reminiscent of mtDNA diseases including an increased rate of glycolysis and ROS production, as well as decreased OXPHOS. In this study, the 2008 human ovarian cancer cell line and its CDDP resistant C13* variant were choosen to determine if mtDNA mutations impact specific phenotypes as differences in mitochondrial morphology, mitochondrial ROS production, rate of O_2 consumption, $\Delta\Psi_M$, and Rh123 resistance have all been previously described between these cells (Doward 1999; Andrews and Albright 1992). Furthermore, RH4 cells displayed Rh123 resistance, a slightly higher $\Delta\Psi_M$, and a 2-3 fold increase in CDDP resistance when compared to 2008 cells, strengthening the theory that mitochondrial properties contribute to the phenotypic variance between these cells (Zinkewich-Peotti and Andrews 1992). Speculations were made not only by us but by others that these changes were the result of a mtDNA mutation brought about during CDDP exposure, a drug which is known to damage mtDNA (Andrews and Albright 1992; Chang et al. 2002).

To test this hypothesis mtDNA genomic differences first needed to be identified. A nested primer strategy was used to PCR amplify portions of the mitochondrial genome of 2008 and C13* cells. Direct sequence analysis of the entire mitochondrial genome revealed three sequence variations between 2008 and C13* cells. The first was a heteroplasmic mutation detected only in 2008 cells, occurring within COXII. This mutation converted an asparigine to an aspartic acid residue close to a α-helix transmembrane domain (Tsukihara et al. 1996). The second adenine to thymine mutation was homplasmic and occurred within a portion of the d-loop in C13* cells which binds

the poorly characterized protein mt4 (Suzuki et al. 1991). This region of the genome is also extremely important in the production of an R-loop that later primes mtDNA replication(Fernandez-Silva et al. 2003). A third mutation was detected in both 2008 and C13* cells, converting a phenylalanine to a leucine residue at position 181 of cytochrome b. This residue is directly beside a histidine that anchors cytochrome b_{566} within cytochrome b. All of these mutations were novel by sequence comparison to a mtDNA database (www.mitomap.org) and to sequences listed in pubmed.

The functional consequences of these mutations were not obvious and any hypotheses as to their effects would have to be tested in a cytoplasmic hybrid model that neutralizes the phenotypic impact of nDNA. 2008 and C13* cells were enucleated through centrifugation and fused to 143B TK^- (thymidine kinase deficient) ρ^o cells which lack mitochondrial DNA. Resultant cybrids were selected through both BRDU resistance (a characteristic of 143B TK^- cells) and for the ability to divide in media that was not supplemented with uridine. RT-PCR for the absence of thymidine kinase cDNA was used to verify that cybrid clones contained the correct 143B TK^- nuclear background. Direct sequence analysis of the mitochondrial genome of cybrid cells confirmed that the full mitochondrial genomic complement was transferred from 2008 and C13* mtDNA donor cells to 143B $TK^- \rho^o$ cells.

4.2 Phenotypic Impact of mtDNA Mutations in the Context of Carcinogenesis

To elucidate if the observed mtDNA sequence variation between 2008 and C13* cells were responsible for observed phenotypic changes, assays that yielded different responses in both cells were repeated in cybrid cell lines. Electron micrographs

revealed that 2008cyb mitochondria displayed morpholgical features of their mtDNA donor 2008 cell with very pronounced cristae (Figure 3.4). Likewise, C13*cyb mitochondria also resembled those of C13* mtDNA donor cells with very compact irregular cristae (Figure 3.5). Fixation techniques used prior to electron microscopic analysis raises concerns that differences in mitochondrial morphology might be the result of fixation artifacts as opposed to true structural variance. However, the structural differences observed between 2008 and C13* cells as well as the organization of the cristae in ρ^0 cells have been previously reported and are confirmed by our results (Figure 3.6) (Andrews and Albright 1992; Gilkerson et al. 2000).

The most obvious explanation for these morphological changes lies with mtDNA differences between donor cells. C13* mtDNA differs from 2008 mtDNA at only two positions, one within COXII and the other within the d-loop (Table 3.2). Polarographic and spectrophotometric analysis implies that these sequence variations do not produce detectable functional changes in the electron transport since decreases in complex I and IV activity in C13* cells were not observed in C13*cyb cells (Tables 3.3 to 3.8). However, the mutation in the d-loop occurs within a sequence that is conserved in a number of species and has also demonstrated the ability to bind a protein designated mt4 (Suzuki et al. 1995).

Mt4 protein binding sequences are also found within the 5' flanking region of human cytochrome c, ubiquinone binding protein, and F_0F_1 ATPase β subunit genes in the nucleus (Suzuki et al. 1991). Site directed mutagenesis studies have determined that this sequence has a functional role, acting as an enhancer element in the F_0F_1 ATPase β

subunit and mt4 protein has been isolated from both human nuclear and mitochondrial fractions (Suzuki et al. 1995; Tomura et al. 1990). The presence of these conserved binding sequences in both nuclear and mtDNA have led to the hypothesis that this protein may play an important role in the expression of nuclear and mitochondrial genes (Suzuki et al. 1991). Other proteins such as nuclear respiratory factor 1 (NRF1) and nuclear respiratory factor 2 (NRF2) are already known to partially coordinate expression of nuclear and mitochondrial encoded genes, although the overall regulation of mtDNA and nDNA encoded proteins are poorly understood (Virbasius and Scarpulla 1994).

The potential role of mt4 in the coordinate expression of nuclear and mitochondrial genes may explain how a mutation within the Mt4 binding sequence would effect mitochondrial morphology. Sequence variations between Mt4 binding sites present within the human cytochrome c gene and mtDNA appear to affect protein binding of mt4, with mt4 having an increased affinity for the cytochrome c binding sequence (Suzuki et al. 1991). Likewise, if the mutation at position 379 increases or decreases binding of mt4 to mtDNA the result could be a modulation of mtDNA encoded gene products and a resultant change in morphology such as that which occurs in ρ^o cells following depletion of mtDNA (Gilkerson et al. 2000). We attempted to use an EMSA to determine if the mutation at mtDNA position 379 affected binding of mt4 with inconclusive results. *In vitro* reporter transcription assays have also been attempted in ρ^o to test the hypothesis that Mt4 elements play a role in transcription. Although these results are negative so far, the authors intend to repeat these experiments in ρ^+ cells (Sewards et al. 1994). The Mt4 binding sequence on mtDNA is 8 nucleotides away from conserved sequence block III

(CSBIII). CSBIII is one of three conserved sequence blocks in mtDNA and although their exact function is unknown, there is speculation that CSBIII along with CSBII aids in the replication of mtDNA (Sbisa et al. 1997). Morphological changes may also result if the mutation effected mt4 binding and the function of CSBIII. However, these resultant morphological changes do not appear to effect overall cell mitochondrial inner membrane content as measured by NAO staining.

The morphological changes observed between 2008 and C13* cells and their cybrid counterpart appear to be unrelated to CDDP growth inhibition. C13* cells demonstrated substantial resistance to growth inhibition following CDDP exposure when compared 2008 and RH4 cells, in accordance with previous findings (Figure 3.8) (Andrews and Albright 1992; Zinkewich-Peotti and Andrews 1992). C13* mtDNA transfer to a 143B TK^- nuclear background did not convey concurrent resistance to CDDP and the 143B TK^- nuclear background alone appears to make cells approximately 2.5-fold more resistant to the effects of CDDP when compared to 2008 cells (Figure 3.9). The 143B TK^- nuclear background may afford elevated levels of glutathione (GSH), a decreased plasma membrane potential, or a mutation in ras or p53, all of which have demonstrated the ability to increase resistance to CDDP, or some other as yet unknown resistance processes may be at work (Andrews et al. 1988; Kartalou and Essigmann 2001; Sato et al. 1999).

C13*cyb cells may have been the most susceptible to CDDP treatment when compared to other cells with a 143B TK^- nuclear background because they were under the greatest amount of oxidative stress. As depicted in Figure 3.13, C13*cyb cells displayed

a 1.6-fold increase in intracellular ROS as measured by DCF fluorescence. Additionally, CDDP is known to cause an increase in intracellular ROS, which can be reversed by treatment with antioxidants(Yoshida et al. 2003; Biroccio et al. 2001; Miyajima et al. 1999). The antioxidant defenses of C13*cyb cells may have been overwhelmed by the added ROS from CDDP treatment imposing a state of oxidative stress, sufficient enough to elicit an apoptotic response.

Surprisingly, 143B TK$^-$ ρ^0 cells demonstrated the greatest resistance to CDDP induced growth inhibition of all lines tested with a 143 TK$^-$ nuclear background (Figure 3.9). The absence of a mitochondrial genome may impact sensitivity to CDDP treatment as CDDP is known to create a greater number of lesions in mtDNA than in nDNA (Murata et al. 1990; Olivero et al. 1997). Furthermore, fewer platinum adducts are removed from mtDNA, likely because mitochondria lack nucleotide excision repair mechanisms, believed to be the main pathway by which these lesions are removed (Kartalou and Essigmann 2001; Olivero et al. 1997; Tully and Levin 2000). However, overall experimental evidence does not suggest an obvious functional relationship between mtDNA and CDDP resistanace. One study has observed that U937 cells which lack mtDNA are actually more susceptible to CDDP induced apoptosis, while another study indicates that mtDNA in cells from particular tissues of the body may be more susceptible to the genotoxic effects of this drug (Giurgiovich et al. 1997; Liang and Ullyatt 1998).

It was hypothesized that an elevation in $\Delta\Psi_M$ was responsible for the CDDP resistance phenotype of C13* cells (Andrews and Albright 1992). A subsequent report

utilizing RH4 cells derived from exposing C13* cells to 4 rounds of Rh123 treatment strengthened this hypothesis. When compared to 2008 cells, both RH4 and C13* cells contained equally increased levels of GSH, accumulated less CDDP, and had similar mitochondrial morphology (Zinkewich-Peotti and Andrews 1992). However, RH4 cells display a 1.2 fold higher $\Delta\Psi_M$, a 2-3 fold increase in CDDP resistance, and a very slight sensitivity to RH123 when compared to 2008 cells (Zinkewich-Peotti and Andrews 1992). Assays conducted in our lab verify these results although TMRM fluorescence based $\Delta\Psi_M$ measurements indicate a 1.4 fold increase in C13* mitochondrial membrane potential when compared to that of the 2008 line. It is not obvious why we were unable to detect a 2-fold difference in $\Delta\Psi_M$ values between 2008 and C13* cells, but these results may reflect differences in assay methods used (Figure 3.14). Conversely, C13*cyb and 2008cyb displayed equal $\Delta\Psi_M$ values, indicating C13* mtDNA sequence variations alone are not responsible for the increased $\Delta\Psi_M$ in C13* cells. An elevated $\Delta\Psi_M$ appears to be integral in the CDDP resistance phenotype of cells C13* cells and the inability of C13* mtDNA to confer an increased $\Delta\Psi_M$ to a 143B TK^- nucleus might explain why no increase in CDDP resistance was observed in C13*cyb cells (See Figure 3.14).

The assay procedure used in our lab to measure mitochondrial membrane potential utilizes the fluorescent properties of TMRM, a dye that is internalized within cells and organelles in proportion to membrane potential. In normal cells, transmembrane proton pumping by the ETC is mainly responsible for the $\Delta\Psi_M$ (Loiseau et al. 2002). In order to evaluate TMRM fluorescence due to the proton gradient across the inner membrane, the

protonophore CCCP and complex V inhibitor oligomycin were added to some samples effectively "uncoupling" respiration within mitochondria. Samples that contained CCCP and oligomycin had reduced fluorescence values, indicating that the mitochondrial membrane potential resulting from the proton gradient alone had been dissipated.

TMRM fluorescence in 143B TK$^-$ ρ^o cells could be reduced by the addition of CCCP and oligomycin indicating that these cells maintain a $\Delta\Psi_M$ that is at least partially dependent on a proton gradient across the inner membrane (Figure 3.14). CCCP reduced TMRM fluorescence in 143B TK$^-$ ρ^o cells by 50% while reducing fluorescence in cells with mtDNA by 50-60%, indicating a comparable proportion of the membrane potential in ρ^o or ρ^+ cells is due a proton gradient. Although these results may be hard to comprehend, these findings are corroborated by another study that also detected a mitochondrial membrane potential that was dissipated by 50% upon addition of CCCP in three ρ^o cell lines including 143B TK$^-$ ρ^o (Loiseau et al. 2002). Surprising, this study also observed that ρ^o lines derived from HepG2 and Hela cells displayed fluorescence values in the absence of inhibitors that were comparable to those of parental lines. Although the entire functional significance of a $\Delta\Psi_M$ in ρ^o cells remains to be elucidated, its maintenance is required for their growth (Loiseau et al. 2002).

These observations are perplexing as ρ^o cells lack a functional ETC that is (or was) believed to contribute to the vast majority of the mitochondrial membrane potential in normal cells through the pumping of protons to the outer membrane space (Loiseau et al. 2002). Loiseau *et al.* (2002) contend that the proton pumping could be produced through the oxidation of NADH at complex III and IV. However, spectrophotmetric

assays conducted in our lab detected minute amounts of complex III activity and absolutely no complex IV activity in 143B TK^- ρ^o cells, which correspond well to the finding that Molt-4 ρ^o lack complex IV activity (Olivero et al. 1997). These low levels of complex III activity are probably insufficient to explain the resultant high proton gradient across the mitochondrial membrane of 143B TK^- ρ^o cells.

Perhaps a phase transition of matrix protiens upon addition of CCCP could explain dissipation of the proton gradient portion of the mitochondrial membrane in 143B TK^- ρ^o cells. In this scenario the protein composition of the inner matrix forms a gel that would naturally exclude hydrogen ions from the matrix via the physical properties of the matrix gel alone. Under these conditions, the pH would be higher in the inner matrix and lower in the outer membrane space even in the presence or absence of an ETC, which occurs in both ρ^o and ρ^+ cells. However, upon addition of CCCP a phase transition occurs in which the physical properties of the proteins in the mitochondrial inner matrix gel change, to now permit the adsorption of hydrogen ions, thus decreasing the pH and dissipating the mitochondrial membrane potential. As you can see, the phase transition model has no reliance on the ETC, but however results in both the maintenance and collapse of the mitochondrial membrane associated proton gradient under certain circumstances. The identical model may also function to allow the modulation of K^+ ions in mitochondria upon the addition of valinomycin. For more information on the extremely controversial phase transition theory of membrane potential generation please refer to the text entitled Cells, **Gels and the Engines of Life** (2001) by G.H. Pollock.

Rhodamine 123 (Rh123) is a xenobiotic that accumulates within the mitochondria of cells in proportion to their mitochondrial membrane potential. The growth inhibitory effects of Rh123 correlated quite well to the observed mitochondrial membrane potential of each individual cell line. C13* cells which have an elevated membrane potential when compared to 2008 or RH4 cells showed a decreased resistance to the growth inhibitory effects of Rh123, presumably because more accumulated in the mitochondria (Figure 3.10). Likewise, 2008cyb or C13*cyb cells displayed elevated membrane potentials and increased sensitivity to Rh123 when compared to their mtDNA deficient 143B TK^- ρ^o counterpart.

However, the energy derivation pathway of a particular cell may also play an important role in Rh123 resistance. Rh123 is reported to exert its main toxic effect through inhibition of the F_0F_1-ATPase portion of complex V, which is responsible for the production of ATP in OXPHOS (Modica-Napolitano and Aprille 1987). Therefore, ρ^o cells, which rely solely on glycolysis for energy production, would be less affected by exposure to Rh123, while cells that have a functional ETC and rely to some degree on OXPHOS would be more sensitive. Cells that have to derive a given proportion of their ATP from OXPHOS may be less able to induce glycolytic pathways to make up for a drop in OXPHOS derived ATP following the administration of Rh123. As a result the minimal energy requirements of the cell are not met and growth inhibition or death of the cell ensues. This may be why C13* and C13*cyb cells display an equal membrane potential when compared to 2008cyb cells but show increased sensitivity to this drug. Rh123 must also exert its toxic effects through other means as 143B TK^- ρ^o are sensitive

to this drug albeit at very high concentrations when compared to the other cell lines, which may also explain why cells with an equal mitochondrial membrane potential show a variance in sensitivity.

4.3 mtDNA Mutations and Enzymatic Consequences

Some pathogenic mtDNA mutations cause an inefficiency in the ETC which results in decreased ETC function, and rate of oxygen consumption, and concomitant increased ROS production (Swerdlow et al. 1997; Sheehan et al. 1997; Pang et al. 2001). Experiments utilizing electron transport chain inhibitors determined that ROS of mitochondrial origin was elevated in C13* cells and the rate of oxygen consumption was lower when compared to 2008 cells, which implied the presence of a mtDNA mutation (Doward 1999). To determine if aberrations between 2008 and C13* mtDNA were responsible for this increased ROS production, this parameter was measured in cybrid cells as well as 143B TK$^-$ ρ^o cells. Like C13* cells, C13*cyb cells displayed a significant increase in ROS production when compared to 2008cyb cells or 143B TK$^-$ ρ^o, which both produced equivalent amounts of ROS (Figure 3.13). 143B TK$^-$ ρ^o cells produce mitochondrial ROS from a functional complex II whose proteins are entirely of nuclear origin (Leach et al. 2001). However, one study has reported that 143B TK$^-$ ρ^o produce only half of the ROS of their ρ^+ parental line, which unfortunately was not included in our study (Leach et al. 2001).

Concerns may be raised that elevated levels of mitochondrial generated ROS in C13* cells may be the result of increased numbers of mitochondria number or a greater amount mitochondrial inner membrane per cell. A previous study found no observable

difference in number of mitochondria per cell through qualitative examination of C13* and 2008 electron micrographs (Andrews and Albright 1992). Cardiolipin, which is present exclusively within the mitochondiral inner membrane and at inner membrane contact sites, was stained with NAO to indirectly assess inner membrane content per cell (McMillin and Dowhan 2002; Maftah et al. 1989; Petit et al. 1992). NAO fluorescence values between C13* and 2008 cells were not significantly different indicating equal quantities of inner mitochondrial membrane per cell (Figure 3.12). Furthermore, NAO fluorescence values were significantly higher in cells with a 143B TK^- nuclear background when compared to 2008 or C13* cells, but these values were not significantly different between cybrid cells. 143B TK^- ρ^0 cells possessed the highest mitochondrial mass of all cell lines, which is not entirely surprising as an increase in mitochondrial mass has been reported in cybrid cells harbouring the 4977 bp deletion (Wei et al. 2001). These results provide evidence that the measured levels of ROS are not a result of increased numbers of mitochondria or increased inner mitochondrial membrane content in cells that contain mtDNA.

When evaluating ROS levels it is also important to assess detoxification systems that exist within the cell to combat oxidative stress. MnSOD, CuZnSOD and catalase protein levels were evaluated in 2008 and C13* cells as well as in cells with a 143B TK^- background. 2008 cells displayed the highest levels of all antioxidants investigated, which may partially explain why they produced the smallest amount of ROS (Figure 3.13). C13* cells had considerably lower levels of MnSOD and catalase when compared to 2008 cells, which may partially explain why they produce a greater amount of ROS.

Likewise, cells with a 143B TK$^-$ nuclear background contained considerably lower levels of MnSOD, CuZnSOD and catalase when compared to 2008 cells (Figure 3.13). These lowered levels of antioxidant defences likely play a role in the elevated ROS levels when compared to 2008 or C13* cells. It should also be noted that MnSOD protein levels were increased in C13*cyb cells, possibly indicating an increase in antioxidant defences in response to increased ROS production. Studies evaluating antioxidant enzymes within tissues harbouring mitochondrial disease have determined that MnSOD staining corresponded well to RRF staining (Ohkoshi et al. 1995). However, the induction of MnSOD, CuZnSOD and GPx do not correlate well with biochemical abnormalities, clinical phenotype, or duration of disease (Filosto et al. 2002). In the case of breast, stomach and heptocarcinoma, MnSOD levels correlate inversely to tumour aggressiveness (Korenaga et al. 2003; Soini et al. 2001; Cullen et al. 2003). Conversely, MnSOD expression in colorectal cancer appears to directly correlate with tumour invasiveness and decreased survival time, indicating that the role of antioxidant defences in tumour aggressiveness may be tissue specific. As mentioned earlier, ROS and in particular H_2O_2 are known to be mitogenic and promote cell growth through a number of different pathways(Dong-Yun et al. 2003; Cheng et al. 2003). However, the JNK pathway is involved in both ROS induced proliferation and events leading to cell death, indicating that the level of oxidative stress dictates which outcome occurs(Martindale and Holbrook 2002).

Some pathogenic mtDNA mutations reduce the rate of oxygen consumption within cells through inefficient transfer of electrons to atomic oxygen to form water at

complex IV of the ETC (Pang et al. 2001). Previous experiments have observed that 2008 cells have twice the oxygen consumption rate of C13* cells (Doward 1999). Our experimental findings corroborate previous ones. However, RH4 cells, which are similar to 2008 cells with respect to Rh123 and CDDP resistance as well as $\Delta\Psi_M$, displayed a rate of oxygen consumption almost equal to that of C13* cells (Table 3.3). These findings would imply that the decreased rate of oxygen consumption alone is not sufficient to confer Rh123 sensitivity or CDDP resistance.

C13*cyb cells produced a greater amount of ROS when compared to 2008cyb cells suggesting that mitochondrial genomic differences might confer this phenotype (Figure 3.13). In order to test this hypothesis the rate of oxygen consumption was evaluated in all cells with a 143B TK^- nuclear background. Contrary to C13* cells, the rate of oxygen consumption in C13*cyb cells was 1.5-fold higher than that of 2008cyb cells (Table 3.4). Furthermore, activation of complex I by glutamate, malate, and ADP sustained the oxygen consumption difference between C13*cyb and 2008cyb, indicating an overall increase in ETC activity. This data might indicate that the increased rate of ROS production observed in C13*cyb cells is due to an increased ETC activity and resultant rate of oxygen consumption as opposed to mtDNA genomic differences. However, many pathogenic mtDNA mutations that result in a decrease in ETC function also cause a concomitant increase in ROS making it difficult to correlate ROS production and ETC function. The use of digitonin in this assay may raise concerns that the concentration used might result in rupture of the inner mitochondrial membrane, giving oxygen consumption rates that are not truly reflective of ETC function. In order to address this

issue, oxidized cytochrome c was added following the activation of complex I with no significant increase in rate of oxygen consumption, indicating the inner mitochondrial membrane was intact (data not shown) (Chowdhury et al. 2000). The substrates and inhibitors used in this assay also appear to be specific for the electron transport chain as 143B TK$^-$ ρ^0 cells rate of oxygen consumption did not change upon the addition of any reagents.

A spectrophotometric analysis of ETC function was carried out to determine if observed variances between the mitochondrial genome of 2008 and C13* cells were sufficient to effect enzymatic activity. 2008 cells displayed a 1.8-fold higher COX (complex IV) activity when compared to C13* or RH4 cells (Table 3.5). These results correlated well with oxygen consumption data, implying that the decrease in oxygen consumption in C13* and RH4 cells is due to a reduction in ETC activity. Similar levels of COX activity in C13* and RH4 cells would also lead to the conclusion that depressed ETC activity alone is not sufficient to confer the observed phenotype of C13* cells. The transfer of C13* mtDNA to a 143B TK$^-$ ρ^0 background did not result in a subsequent decrease in COX activity, indicating that mtDNA variances between 2008 and C13* cells do not effect complex IV function (Table 3.7). In fact, C13*cyb cells displayed a 1.5-fold higher COX activity when compared to 2008cyb cells, implying that the observed increase in ROS production in C13*cyb cells is due in part to an increased ETC activity and subsequent elevated rate of oxygen consumption. However, this may not be the case as some pathological mtDNA mutations result in decreased rates of oxygen consumption and COX activity, but increased ROS production, making it difficult to correlate all three

factors. COX activity was completely absent in 143B TK$^-$ ρ^o cells indicating that the assay methods used to evaluate complex IV activity are specific to the ETC and are not affected by other enzymatic reactions in the lysate.

Succinate cytochrome c reductase (SCCR, complex II and III), as well as glycrophosphate cytochrome c reductase activity (GCCR, glycerophosphoshate dehydrogenase and complex III) was also evaluated. SCCR activity was not significantly different between 2008 and C13* cells, however, GCCR activity was 1.2-fold higher in C13* cells (Table 3.5). Cybrid cells demonstrated equal SCCR activity, while GCCR activity was also 1.2-fold higher in C13*cybrid cells when compared to 2008 cells. SCCR and GCCR activity was detectable in 143B TK$^-$ ρ^o, however the activity of both were approximately 10-fold lower than that of C13*cyb cells, indicating that these enzymatic assays are also highly specific to electron transport chain function (Table 3.7). Residual SCCR and GCCR activity has also been noted in other mtDNA deficient cells, providing evidence that readings in 143B TK$^-$ ρ^o cells were not anomalous(Loiseau et al. 2002).

Diagnosis of a mitochondrial disease involves a comparison of patient respiratory chain activities to those obtained from normal control subjects. However, Rustin *et al.* (1994) observed that enzyme activities obtained from control subjects were scattered over almost 2 orders of magnitude depending on the specific enzyme and tissue tested. This observation posed a problem in that respiratory chain activities obtained from patients would fall within the range of control subjects and appear to be normal. In an attempt to normalize enzymatic activities and reduce false negatives Rustin *et al.* (1994) divided the

rate of COX activity by the rate of SCCR activity, giving a number in the range of 2.5 to 3.5 depending on the control tissue measured. These authors state that if the value obtained from a patient is outside or low on the normal distribution curve for that tissue the individual can be unambiguously diagnosed as COX deficient. However, the ratio of COX to SCCR seems to be tissue specific as this ratio was reported to be 4.75 in aminocytes (Chowdhury et al. 2000). This method obviously will not hold true for generalized respiratory defects in which the activities of all enzyme complexes are reduced. In this case it was proposed that enzyme activities could be expressed as a ratio of a Krebs cycle enzyme such as citrate synthase, which was evaluated in our study. This ratio has also been reported to reflect the proportion of inner mitochondrial membrane and matrix compartment (Chowdhury et al. 2000). However, Rustin *et al.* (1994) states that these ratios are not as conserved as ratios within the respiratory complex (i.e. COX activity:SCCR activity).

In our study we compared the rate of enzymatic activity from one cell line to another without being expressed as a ratio for several reasons. Because C13* cells were derived from 2008 cells, and RH4 cells were derived from C13* cells, we compared ETC enzymatic activity to 2008 cells, which served as our parental control cells. Secondly, there was some conflicting data concerning the mitochondrial inner membrane. NAO fluorescence readings and electron micrographs detected the presence of an inner membrane in 143B TK^- ρ^o cells, however they displayed no COX activity. If the ratio of COX to CS activity reflects the inner mitochondrial membrane to matrix proportion it would appear that ρ^o cells contain absolutely no inner mitochondrial membrane.

Furthermore, the citrate synthase activity was 2-fold higher in 2008 cells, which is interesting as this enzymatic activity was determined to be equal in either the presence or absence of mtDNA and a functional ETC (Tables 3.5 and 3.7). Finally, if the enzymatic activity is expressed as a ratio of CS activity the ETC enzymatic activity of 2008 cells appears lower than C13*or RH4 cells, which does not correspond to observed rates of oxygen consumption in these respective cell lines.

To summarize, the mtDNA genomic differences in C13* cells when compared to 2008 cells do not appear to confer CDDP resistance, an increase in mitochondrial membrane potential, or a decrease in O_2 consumption and ETC activity to C13*cyb cells. However, these genomic differences do appear to be responsible for mitochondrial morphological, Rh123 sensitivity and ROS production differences observed between 2008 and C13* cells, most likely resulting from the mutation within the d-loop at position 379. The data from this study provides some evidence to support the selective advantage mode of mtDNA mutation acquisition. However, the mechanism through which these morphological changes occur or the advantage that they provide to the overall cell biology remains to be elucidated. More study is required with a larger sample of neoplastic cells from human patients to determine exactly what advantage a broad range of mtDNA mutations provide to tumour cells.

4.4 Future dierections

Previous studies have demonstrated that the nuclear genomic compliment is capable of affecting the mutational load of mtDNA. It is also quite possible that a number of the phenotypic differences observed between 2008, C13* and RH4 cells are

related to the combined characteristics of both the nDNA and mtDNA compliment. Removal of the mtDNA from its native nDNA environment may have abolished its phenotypic properties. Ideally it would have been most advantageous to produce cybrids with a 2008 nDNA compliment and C13* mtDNA. This would have allowed us to elucidate if C13* mtDNA transplantation was sufficient to invoke observed characteristics in a closely related 2008 nucleus. Conversely, this experiment could involve the transfer of 2008 mtDNA to a C13* nDNA background. We attempted this experimental procedure by depleting the mtDNA of 2008 and C13* cells with Rhodamine 6G which would not have the nDNA genotoxic effects associated with the use of ethidium bromide. However, this process was evidently unsuccessful and no cells survived. Perhaps mtDNA depletion with ethidium bromide may prove more effective although the potential mutagenic effect it may have on nDNA must be realized. If ρ^0 cells with a 2008 or C13* nDNA background can be isolated it would also be possible to determine definitively what effect the mtDNA compliment of each cell contributes to both $\Delta\Psi_M$ and CDDP resistance.

A number human tumours contain the common 4977 bp deletion of the mitochondrial genome that has also been implicated in mtDNA disease resulting in conditions such as CPEO, KSS, and Pearson's syndrome (Maximo et al. 2001). Furthermore, this mutation has been detected in individuals in an age dependent manner and correlates with mtDNA lesions resulting from oxidative stress (Lu et al. 1999). Despite these findings, the phenotypic relevance of this mutation in the context of carcinogenesis has yet to be elucidated. Human tumours could be screened for the

presence of this mutation. Tumour cells containing the deletion could be fused to human platelets that lack a nucleus, but contain normal mtDNA. The cells containing both platelet and native tumour mtDNA could be evaluated to determine if a larger proportion of full-length mtDNA is capable of modulating mitochondrial function. It is quite possible that phenotypic differences will not be observed in cells, which only harbour a small proportion of the 4977 bp deletion, so cells with a high proportion of this defect may be preferred for fusion studies.

The D310 d-loop insertion or deletion mutation is also observed frequently in a number of tumour cells and has recently been shown to occur following mtDNA damage (Mambo et al. 2003). This region of the d-loop lies within CSBII that is proposed to be involved in some aspect of mtDNA replication and transcription (Ghivizzani et al. 1994). Cells with D310 insertions or deletions could be identified and *in vitro* mtDNA transcription and replication studies could be performed to determine if these mutations do indeed have a phenotypic impact. These assays should also include the evaluation of d-loop and R-loop structures present within each cell, which may also be affected by mutations within the D310 stretch.

The mutation located within the d-loop within C13* cells is also intriguing as it appears to elicit a mitochondrial morphological change upon transfer to a 143B TK^- nuclear background. As mentioned earlier, this portion of the d-loop has been reported to bind a protein named mt4 (Suzuki et al. 1995). EMSAs outlined in Suzuki et al. (1995) were attempted in this study, but with inconclusive results. The mutation occurs 8 nucleotides from CSBIII, which is also hypothesized to have some role in d-loop

production as well as in replication of the mtDNA genome. Experiments used to determine if the D310 mutation have a phenotypic impact could also be used to evaluate the mutation at 379 in C13* cells.

Maintenance of a proton gradient across the inner membrane of cells which lack mtDNA and hence a functional electron transport chain also deserves further investigation. It is currently believed that normal cells produce and maintain the majority of this charge differential by ETC complex proton pumping out of the inner mitochondrial matrix (Loiseau et al. 2002). However, in the case of ρ^0 cells it is believed that residual complex III and IV activity is capable of generating a proton gradient and resultant mitochondrial membrane potential (Loiseau et al. 2002). Complex III and IV inhibitors such as antimycin A and potassium cyanide could possibly be used to determine if these complexes are responsible for the generation of a proton gradient in cells devoid of mtDNA. However, there is a portion of complex IV activity that is potassium insensitive, which may pose problems to this experimental approach(Rustin et al. 1994). If these complexes prove incapable of generating a sufficient proton gradient, investigations into a phase transition mode of mitochondrial membrane potential dissipation by CCCP may be warranted.

5.0 References

Anderson C. T. and Friedberg E. C. (1980) The presence of nuclear and mitochondrial uracil-DNA glycosylase in extracts of human KB cells. *Nucleic Acids Res* **8,** 875-888.

Andrews P. A. and Albright K. D. (1992) Mitochondrial defects in cis-diamminedichloroplatinum(II)-resistant human ovarian carcinoma cells. *Cancer Res* **52,** 1895-1901.

Andrews P. A., Murphy M. P., and Howell S. B. (1985) Differential potentiation of alkylating and platinating agent cytotoxicity in human ovarian carcinoma cells by glutathione depletion. *Cancer Res* **45,** 6250-6253.

Andrews P. A., Velury S., Mann S. C., and Howell S. B. (1988) cis-Diamminedichloroplatinum(II) accumulation in sensitive and resistant human ovarian carcinoma cells. *Cancer Res* **48,** 68-73.

Artuch R., Colome C., Playan A., Alcaine M. J., Briones P., Montoya J., Vilaseca M. A., and Pineda M. (2000) Oxygen consumption measurement in lymphocytes for the diagnosis of pediatric patients with oxidative phosphorylation diseases. *Clin Biochem* **33,** 481-485.

Attardi G. and Schatz G. (1988) Biogenesis of mitochondria. *Annu Rev Cell Biol* **4,** 289-333.

Ballinger S. W., Patterson C., Yan C. N., Doan R., Burow D. L., Young C. G., Yakes F. M., Van Houten B., Ballinger C. A., Freeman B. A., and Runge M. S. (2000) Hydrogen peroxide and peroxynitrite induced mitochondrial DNA damage and dysfuction in vascular endothelial and smooth muscle cells. *Circ Res* **86,** 960-966.

Ballinger S. W., Van Houten B., Jin G. F., Conklin C. A., and Godley B. F. (1999) Hydrogen peroxide causes significant mitochondrial DNA damage in human RPE cells. *Exp Eye Res* **68,** 765-772.

Bass D. A., Parce J. W., Dechatelet L. R., Szejda P., Seeds M. C., and Thomas M. (1983) Flow cytometric studies of oxidative product formation by neutrophils: a graded response to membrane stimulation. *J Immunol* **130,** 1910-1917.

Beal M. F. (2003) Mitochondria, oxidative damage, and inflammation in Parkinson's disease. *Ann N Y Acad Sci* **991,** 120-131.

Bell R. M., Maddock H. L., and Yellon D. M. (2003) The cardioprotective and mitochondrial depolarising properties of exogenous nitric oxide in mouse heart. *Cardiovasc Res* **57,** 405-415.

Bijur G. N., Davis R. E., and Jope R. S. (1999) Rapid activation of heat shock factor-1 DNA binding by H2O2 and modulation by glutathione in human neuroblastoma and Alzheimer's disease cybrid cells. *Brain Res Mol Brain Res* **71,** 69-77.

Biroccio A., Benassi B., Amodei S., Gabellini C., Del Bufalo D., and Zupi G. (2001) c-Myc down-regulation increases susceptibility to cisplatin through reactive oxygen species-mediated apoptosis in M14 human melanoma cells. *Mol Pharmacol* **60,** 174-182.

Bogenhagen D. F. (1999) Repair of mtDNA in vertebrates. *Am J Hum Genet* **64,** 1276-1281.

Bogenhagen D. F., Applegate E. F., and Yoza B. K. (1984) Identification of a promoter for transcription of the heavy strand of human mtDNA: in vitro transcription and deletion mutagenesis. *Cell* **36,** 1105-1113.

Borisov V. B. (2002) Defects in mitochondrial respiratory complexes III and IV, and human pathologies. *Mol Aspects Med* **23,** 385-412.

Brown M. D. and Wallace D. C. (1994) Molecular basis of mitochondrial DNA disease. *J Bioenerg Biomembr* **26,** 273-289.

Brown T. A. and Clayton D. A. (2002) Release of replication termination controls mitochondrial DNA copy number after depletion with 2',3'-dideoxycytidine. *Nucleic Acids Res* **30,** 2004-2010.

Brown W. M., George M., Jr., and Wilson A. C. (1979) Rapid evolution of animal mitochondrial DNA. *Proc Natl Acad Sci U S A* **76,** 1967-1971.

Buck C. R., Jurynec M. J., Gupta D. K., Law A. K., Bilger J., Wallace D. C., and McKeon R. J. (2003) Increased adenine nucleotide translocator 1 in reactive astrocytes facilitates glutamate transport. *Exp Neurol* **181,** 149-158.

Burdon R. H. (1995) Superoxide and hydrogen peroxide in relation to mammalian cell proliferation. *Free Radic Biol Med* **18,** 775-794.

Carew J. S. and Huang P. (2002) Mitochondrial defects in cancer. *Mol Cancer* **1,** 9.

Carlsson L. M., Jonsson J., Edlund T., and Marklund S. L. (1995) Mice lacking extracellular superoxide dismutase are more sensitive to hyperoxia. *Proc Natl Acad Sci U S A* **92,** 6264-6268.

Castellani R., Hirai K., Aliev G., Drew K. L., Nunomura A., Takeda A., Cash A. D., Obrenovich M. E., Perry G., and Smith M. A. (2002) Role of mitochondrial dysfunction in Alzheimer's disease. *J Neurosci Res* **70,** 357-360.

Cathcart R., Schwiers E., and Ames B. N. (1983) Detection of picomole levels of hydroperoxides using a fluorescent dichlorofluorescein assay. *Anal Biochem* **134,** 111-116.

Chang B., Nishikawa M., Sato E., Utsumi K., and Inoue M. (2002) L-Carnitine inhibits cisplatin-induced injury of the kidney and small intestine. *Arch Biochem Biophys* **405,** 55-64.

Chen J. Z., Gokden N., Greene G. F., Mukunyadzi P., and Kadlubar F. F. (2002) Extensive somatic mitochondrial mutations in primary prostate cancer using laser capture microdissection. *Cancer Res* **62,** 6470-6474.

Chen X., Prosser R., Simonetti S., Sadlock J., Jagiello G., and Schon E. A. (1995) Rearranged mitochondrial genomes are present in human oocytes. *Am J Hum Genet* **57,** 239-247.

Cheng C. M., Hong H. J., Liu J. C., Shih N. L., Juan S. H., Loh S. H., Chan P., Chen J. J., and Cheng T. H. (2003) Crucial role of extracellular signal-regulated kinase pathway in reactive oxygen species-mediated endothelin-1 gene expression induced by endothelin-1 in rat cardiac fibroblasts. *Mol Pharmacol* **63,** 1002-1011.

Chinnery P. F., Brown D. T., Andrews R. M., Singh-Kler R., Riordan-Eva P., Lindley J., Applegarth D. A., Turnbull D. M., and Howell N. (2001) The mitochondrial ND6 gene is a hot spot for mutations that cause Leber's hereditary optic neuropathy. *Brain* **124,** 209-218.

Chinnery P. F., Howell N., Lightowlers R. N., and Turnbull D. M. (1997) Molecular pathology of MELAS and MERRF. The relationship between mutation load and clinical phenotypes. *Brain* **120 (Pt 10),** 1713-1721.

Chomyn A. and Attardi G. (2003) MtDNA mutations in aging and apoptosis. *Biochem Biophys Res Commun* **304,** 519-529.

Chomyn A., Martinuzzi A., Yoneda M., Daga A., Hurko O., Johns D., Lai S. T., Nonaka I., Angelini C., and Attardi G. (1992) MELAS mutation in mtDNA binding site for transcription termination factor causes defects in protein synthesis and in respiration but no change in levels of upstream and downstream mature transcripts. *Proc Natl Acad Sci U S A* **89,** 4221-4225.

Chomyn A., Meola G., Bresolin N., Lai S. T., Scarlato G., and Attardi G. (1991) In vitro genetic transfer of protein synthesis and respiration defects to mitochondrial DNA-less cells with myopathy-patient mitochondria. *Mol Cell Biol* **11,** 2236-2244.

Chowdhury S. K., Drahota Z., Floryk D., Calda P., and Houstek J. (2000) Activities of mitochondrial oxidative phosphorylation enzymes in cultured amniocytes. *Clin Chim Acta* **298,** 157-173.

Christianson T. W. and Clayton D. A. (1988) A tridecamer DNA sequence supports human mitochondrial RNA 3'-end formation in vitro. *Mol Cell Biol* **8,** 4502-4509.

Clayton D. A. (1982) Replication of animal mitochondrial DNA. *Cell* **28,** 693-705.

Clayton D. A. (1991) Nuclear gadgets in mitochondrial DNA replication and transcription. *Trends Biochem Sci* **16,** 107-111.

Clayton D. A., Doda J. N., and Friedberg E. C. (1974) The absence of a pyrimidine dimer repair mechanism in mammalian mitochondria. *Proc Natl Acad Sci U S A* **71,** 2777-2781.

Coenen M. J., van den Heuvel L. P., and Smeitink J. A. (2001) Mitochondrial oxidative phosphorylation system assembly in man: recent achievements. *Curr Opin Neurol* **14,** 777-781.

Coller H. A., Khrapko K., Bodyak N. D., Nekhaeva E., Herrero-Jimenez P., and Thilly W. G. (2001) High frequency of homoplasmic mitochondrial DNA mutations in human tumors can be explained without selection. *Nat Genet* **28,** 147-150.

Cullen J. J., Weydert C., Hinkhouse M. M., Ritchie J., Domann F. E., Spitz D., and Oberley L. W. (2003) The role of manganese superoxide dismutase in the growth of pancreatic adenocarcinoma. *Cancer Res* **63,** 1297-1303.

Davis C. A., Nick H. S., and Agarwal A. (2001) Manganese superoxide dismutase attenuates Cisplatin-induced renal injury: importance of superoxide. *J Am Soc Nephrol* **12,** 2683-2690.

Di Giovanni S., Mirabella M., Papacci M., Odoardi F., Silvestri G., and Servidei S. (2001) Apoptosis and ROS detoxification enzymes correlate with cytochrome c oxidase deficiency in mitochondrial encephalomyopathies. *Mol Cell Neurosci* **17,** 696-705.

Diaz F., Bayona-Bafaluy M. P., Rana M., Mora M., Hao H., and Moraes C. T. (2002) Human mitochondrial DNA with large deletions repopulates organelles faster than full-length genomes under relaxed copy number control. *Nucleic Acids Res* **30,** 4626-4633.

DiMauro S. and Andreu A. L. (2000) Mutations in mtDNA: are we scraping the bottom of the barrel? *Brain Pathol* **10,** 431-441.

Doersen C. J., Guerrier-Takada C., Altman S., and Attardi G. (1985) Characterization of an RNase P activity from HeLa cell mitochondria. Comparison with the cytosol RNase P activity. *J Biol Chem* **260,** 5942-5949.

Dong-Yun S., Yu-Ru D., Shan-Lin L., Ya-Dong Z., and Lian W. (2003) Redox stress regulates cell proliferation and apoptosis of human hepatoma through Akt protein phosphorylation. *FEBS Lett* **542,** 60-64.

Doward, A. M. Hydrogen peroxide production and autocrine proliferation control. 1999. McMaster University.

Dunbar D. R., Moonie P. A., Zeviani M., and Holt I. J. (1996) Complex I deficiency is associated with 3243G:C mitochondrial DNA in osteosarcoma cell cybrids. *Hum Mol Genet* **5,** 123-129.

Eds.Attardi, G. M. and Chomyn, A. Methods in Enzymology. Volume 264 Mitochondrial Biogenesis and Genetics. 304-334. 1996. United States of America, Acedemic Press.
Ref Type: Generic

El Meziane A., Lehtinen S. K., Hance N., Nijtmans L. G., Dunbar D., Holt I. J., and Jacobs H. T. (1998a) A tRNA suppressor mutation in human mitochondria. *Nat Genet* **18,** 350-353.

El Meziane A., Lehtinen S. K., Holt I. J., and Jacobs H. T. (1998b) Mitochondrial tRNALeu isoforms in lung carcinoma cybrid cells containing the np 3243 mtDNA mutation. *Hum Mol Genet* **7,** 2141-2147.

Esposti M. D., De Vries S., Crimi M., Ghelli A., Patarnello T., and Meyer A. (1993) Mitochondrial cytochrome b: evolution and structure of the protein. *Biochim Biophys Acta* **1143,** 243-271.

Esworthy R. S., Ho Y. S., and Chu F. F. (1997) The Gpx1 gene encodes mitochondrial glutathione peroxidase in the mouse liver. *Arch Biochem Biophys* **340,** 59-63.

Fernandez-Silva P., Enriquez J. A., and Montoya J. (2003) Replication and transcription of mammalian mitochondrial DNA. *Exp Physiol* **88,** 41-56.

Filosto M., Tonin P., Vattemi G., Spagnolo M., Rizzuto N., and Tomelleri G. (2002) Antioxidant agents have a different expression pattern in muscle fibers of patients with mitochondrial diseases. *Acta Neuropathol (Berl)* **103,** 215-220.

Flint D. H., Tuminello J. F., and Emptage M. H. (1993) The inactivation of Fe-S cluster containing hydro-lyases by superoxide. *J Biol Chem* **268,** 22369-22376.

Floryk D. and Houstek J. (1999) Tetramethyl rhodamine methyl ester (TMRM) is suiTable for cytofluorometric measurements of mitochondrial membrane potential in cells treated with digitonin. *Biosci Rep* **19,** 27-34.

Fridovich I. (1995) Superoxide radical and superoxide dismutases. *Annu Rev Biochem* **64,** 97-112.

Geromel V., Kadhom N., Cebalos-Picot I., Ouari O., Polidori A., Munnich A., Rotig A., and Rustin P. (2001) Superoxide-induced massive apoptosis in cultured skin fibroblasts harboring the neurogenic ataxia retinitis pigmentosa (NARP) mutation in the ATPase-6 gene of the mitochondrial DNA. *Hum Mol Genet* **10,** 1221-1228.

Ghivizzani S. C., Madsen C. S., Nelen M. R., Ammini C. V., and Hauswirth W. W. (1994) In organello footprint analysis of human mitochondrial DNA: human mitochondrial transcription factor A interactions at the origin of replication. *Mol Cell Biol* **14,** 7717-7730.

Ghosh S. S., Swerdlow R. H., Miller S. W., Sheeman B., Parker W. D., Jr., and Davis R. E. (1999) Use of cytoplasmic hybrid cell lines for elucidating the role of mitochondrial dysfunction in Alzheimer's disease and Parkinson's disease. *Ann N Y Acad Sci* **893,** 176-191.

Gilkerson R. W., Margineantu D. H., Capaldi R. A., and Selker J. M. (2000) Mitochondrial DNA depletion causes morphological changes in the mitochondrial reticulum of cultured human cells. *FEBS Lett* **474,** 1-4.

Giurgiovich A. J., Diwan B. A., Olivero O. A., Anderson L. M., Rice J. M., and Poirier M. C. (1997) Elevated mitochondrial cisplatin-DNA adduct levels in rat tissues after transplacental cisplatin exposure. *Carcinogenesis* **18,** 93-96.

Goto Y. (1995) Clinical features of MELAS and mitochondrial DNA mutations. *Muscle Nerve* **3,** S107-S112.

Goto Y., Nonaka I., and Horai S. (1990) A mutation in the tRNA(Leu)(UUR) gene associated with the MELAS subgroup of mitochondrial encephalomyopathies. *Nature* **348,** 651-653.

Graves S. W., Johnson A. A., and Johnson K. A. (1998) Expression, purification, and initial kinetic characterization of the large subunit of the human mitochondrial DNA polymerase. *Biochemistry* **37,** 6050-6058.

Gregoire M., Morais R., Quilliam M. A., and Gravel D. (1984) On auxotrophy for pyrimidines of respiration-deficient chick embryo cells. *Eur J Biochem* **142,** 49-55.

Grossman L. I. (1995) Mitochondrial mutations and human disease. *Environ Mol Mutagen* **25 Suppl 26,** 30-37.

Gu M., Cooper J. M., Taanman J. W., and Schapira A. H. (1998) Mitochondrial DNA transmission of the mitochondrial defect in Parkinson's disease. *Ann Neurol* **44,** 177-186.

Hatefi Y. (1985) The mitochondrial electron transport and oxidative phosphorylation system. *Annu Rev Biochem* **54,** 1015-1069.

Hayashi J., Ohta S., Kikuchi A., Takemitsu M., Goto Y., and Nonaka I. (1991) Introduction of disease-related mitochondrial DNA deletions into HeLa cells lacking mitochondrial DNA results in mitochondrial dysfunction. *Proc Natl Acad Sci U S A* **88,** 10614-10618.

Holt I. J., Harding A. E., and Morgan-Hughes J. A. (1988) Deletions of muscle mitochondrial DNA in patients with mitochondrial myopathies. *Nature* **331,** 717-719.

Huang C. C., Kuo H. C., Chu C. C., Liou C. W., Ma Y. S., and Wei Y. H. (2002) Clinical phenotype, prognosis and mitochondrial DNA mutation load in mitochondrial encephalomyopathies. *J Biomed Sci* **9,** 527-533.

Ito S., Ohta S., Nishimaki K., Kagawa Y., Soma R., Kuno S. Y., Komatsuzaki Y., Mizusawa H., and Hayashi J. (1999) Functional integrity of mitochondrial genomes in human platelets and autopsied brain tissues from elderly patients with Alzheimer's disease. *Proc Natl Acad Sci U S A* **96,** 2099-2103.

Jones J. B., Song J. J., Hempen P. M., Parmigiani G., Hruban R. H., and Kern S. E. (2001) Detection of mitochondrial DNA mutations in pancreatic cancer offers a "mass"-ive advantage over detection of nuclear DNA mutations. *Cancer Res* **61,** 1299-1304.

Jun A. S., Brown M. D., and Wallace D. C. (1994) A mitochondrial DNA mutation at nucleotide pair 14459 of the NADH dehydrogenase subunit 6 gene associated with maternally inherited Leber hereditary optic neuropathy and dystonia. *Proc Natl Acad Sci U S A* **91,** 6206-6210.

Jun A. S., Trounce I. A., Brown M. D., Shoffner J. M., and Wallace D. C. (1996) Use of transmitochondrial cybrids to assign a complex I defect to the mitochondrial DNA-encoded NADH dehydrogenase subunit 6 gene mutation at nucleotide pair 14459 that causes Leber hereditary optic neuropathy and dystonia. *Mol Cell Biol* **16,** 771-777.

Kartalou M. and Essigmann J. M. (2001) Mechanisms of resistance to cisplatin. *Mutat Res* **478,** 23-43.

Kimura E., Enns R. E., Thiebaut F., and Howell S. B. (1993) Regulation of HSP60 mRNA expression in a human ovarian carcinoma cell line. *Cancer Chemother Pharmacol* **32,** 279-285.

King M. P. and Attardi G. (1989) Human cells lacking mtDNA: repopulation with exogenous mitochondria by complementation. *Science* **246,** 500-503.

Kluza J., Lansiaux A., Wattez N., Hildebrand M. P., Leonce S., Pierre A., Hickman J. A., and Bailly C. (2002) Induction of apoptosis in HL-60 leukemia and B16 melanoma cells by the acronycine derivative S23906-1. *Biochem Pharmacol* **63,** 1443-1452.

Korenaga D., Yasuda M., Honda M., Nozoe T., and Inutsuka S. (2003) MnSOD expression within tumor cells is closely related to mode of invasion in human gastric cancer. *Oncol Rep* **10,** 27-30.

Kunkel T. A. and Loeb L. A. (1981) Fidelity of mammalian DNA polymerases. *Science* **213,** 765-767.

Lai H. and Singh N. P. (1995) Selective cancer cell cytotoxicity from exposure to dihydroartemisinin and holotransferrin. *Cancer Lett* **91,** 41-46.

Larsson N. G., Eiken H. G., Boman H., Holme E., Oldfors A., and Tulinius M. H. (1992) Lack of transmission of deleted mtDNA from a woman with Kearns-Sayre syndrome to her child. *Am J Hum Genet* **50,** 360-363.

Leach J. K., Van Tuyle G., Lin P. S., Schmidt-Ullrich R., and Mikkelsen R. B. (2001) Ionizing radiation-induced, mitochondria-dependent generation of reactive oxygen/nitrogen. *Cancer Res* **61,** 3894-3901.

Lebovitz R. M., Zhang H., Vogel H., Cartwright J., Jr., Dionne L., Lu N., Huang S., and Matzuk M. M. (1996) Neurodegeneration, myocardial injury, and perinatal death in mitochondrial superoxide dismutase-deficient mice. *Proc Natl Acad Sci U S A* **93,** 9782-9787.

LeDoux S. P., Driggers W. J., Hollensworth B. S., and Wilson G. L. (1999) Repair of alkylation and oxidative damage in mitochondrial DNA. *Mutat Res* **434,** 149-159.

Lehninger, A. L., Nelson, D. L., and Cox, M. M. Principles of bichemistry. 1-1013. 1997. United States of America, Worth Publisher Inc.

Leprat P., Ratinaud M. H., Maftah A., Petit J. M., and Julien R. (1990) Use of nonyl acridine orange and rhodamine 123 to follow biosynthesis and functional assembly of mitochondrial membrane during L1210 cell cycle. *Exp Cell Res* **186,** 130-137.

Lestienne P. and Bataille N. (1994) Mitochondrial DNA alterations and genetic diseases: a review. *Biomed Pharmacother* **48,** 199-214.

Li Y., Huang T. T., Carlson E. J., Melov S., Ursell P. C., Olson J. L., Noble L. J., Yoshimura M. P., Berger C., Chan P. H., and . (1995) Dilated cardiomyopathy and neonatal lethality in mutant mice lacking manganese superoxide dismutase. *Nat Genet* **11,** 376-381.

Liang B. C. and Ullyatt E. (1998) Increased sensitivity to cis-diamminedichloroplatinum induced apoptosis with mitochondrial DNA depletion. *Cell Death Differ* **5,** 694-701.

Liu V. W., Shi H. H., Cheung A. N., Chiu P. M., Leung T. W., Nagley P., Wong L. C., and Ngan H. Y. (2001) High incidence of somatic mitochondrial DNA mutations in human ovarian carcinomas. *Cancer Res* **61,** 5998-6001.

Loiseau D., Chevrollier A., Douay O., Vavasseur F., Renier G., Reynier P., Malthiery Y., and Stepien G. (2002) Oxygen consumption and expression of the adenine nucleotide translocator in cells lacking mitochondrial DNA. *Exp Cell Res* **278,** 12-18.

Lombes A., Diaz C., Romero N. B., Ziegler F., and Fardeau M. (1992) Analysis of the tissue distribution and inheritance of heteroplasmic mitochondrial DNA point mutation by denaturing gradient gel electrophoresis in MERRF syndrome. *Neuromuscul Disord* **2,** 323-330.

Lu C. Y., Lee H. C., Fahn H. J., and Wei Y. H. (1999) Oxidative damage elicited by imbalance of free radical scavenging enzymes is associated with large-scale mtDNA deletions in aging human skin. *Mutat Res* **423,** 11-21.

Lu H., Forbes R. A., and Verma A. (2002) Hypoxia-inducible factor 1 activation by aerobic glycolysis implicates the Warburg effect in carcinogenesis. *J Biol Chem* **277,** 23111-23115.

Luo X., Pitkanen S., Kassovska-Bratinova S., Robinson B. H., and Lehotay D. C. (1997) Excessive formation of hydroxyl radicals and aldehydic lipid peroxidation products in cultured skin fibroblasts from patients with complex I deficiency. *J Clin Invest* **99,** 2877-2882.

Maftah A., Petit J. M., Ratinaud M. H., and Julien R. (1989) 10-N nonyl-acridine orange: a fluorescent probe which stains mitochondria independently of their energetic state. *Biochem Biophys Res Commun* **164,** 185-190.

Mambo E., Gao X., Cohen Y., Guo Z., Talalay P., and Sidransky D. (2003) Electrophile and oxidant damage of mitochondrial DNA leading to rapid evolution of homoplasmic mutations. *Proc Natl Acad Sci U S A* **100,** 1838-1843.

Mandavilli B. S., Santos J. H., and Van Houten B. (2002) Mitochondrial DNA repair and aging. *Mutat Res* **509,** 127-151.

Manfredi G., Fu J., Ojaimi J., Sadlock J. E., Kwong J. Q., Guy J., and Schon E. A. (2002) Rescue of a deficiency in ATP synthesis by transfer of MTATP6, a mitochondrial DNA-encoded gene, to the nucleus. *Nat Genet* **30,** 394-399.

Marchington D. R., Macaulay V., Hartshorne G. M., Barlow D., and Poulton J. (1998) Evidence from human oocytes for a genetic bottleneck in an mtDNA disease. *Am J Hum Genet* **63,** 769-775.

Martindale J. L. and Holbrook N. J. (2002) Cellular response to oxidative stress: signaling for suicide and survival. *J Cell Physiol* **192,** 1-15.

Mason P. A., Matheson E. C., Hall A. G., and Lightowlers R. N. (2003) Mismatch repair activity in mammalian mitochondria. *Nucleic Acids Res* **31,** 1052-1058.

Mathupala S. P., Rempel A., and Pedersen P. L. (1995) Glucose catabolism in cancer cells. Isolation, sequence, and activity of the promoter for type II hexokinase. *J Biol Chem* **270,** 16918-16925.

Maximo V., Soares P., Seruca R., Rocha A. S., Castro P., and Sobrinho-Simoes M. (2001) Microsatellite instability, mitochondrial DNA large deletions, and mitochondrial DNA mutations in gastric carcinoma. *Genes Chromosomes Cancer* **32,** 136-143.

McMillin J. B. and Dowhan W. (2002) Cardiolipin and apoptosis. *Biochim Biophys Acta* **1585,** 97-107.

Melov S., Doctrow S. R., Schneider J. A., Haberson J., Patel M., Coskun P. E., Huffman K., Wallace D. C., and Malfroy B. (2001) Lifespan extension and rescue of spongiform encephalopathy in superoxide dismutase 2 nullizygous mice treated with superoxide dismutase-catalase mimetics. *J Neurosci* **21,** 8348-8353.

Mirabella M., Di Giovanni S., Silvestri G., Tonali P., and Servidei S. (2000) Apoptosis in mitochondrial encephalomyopathies with mitochondrial DNA mutations: a potential pathogenic mechanism. *Brain* **123 (Pt 1),** 93-104.

Miyajima A., Nakashima J., Tachibana M., Nakamura K., Hayakawa M., and Murai M. (1999) N-acetylcysteine modifies cis-dichlorodiammineplatinum-induced effects in bladder cancer cells. *Jpn J Cancer Res* **90,** 565-570.

Miyajima A., Nakashima J., Yoshioka K., Tachibana M., Tazaki H., and Murai M. (1997) Role of reactive oxygen species in cis-dichlorodiammineplatinum-induced cytotoxicity on bladder cancer cells. *Br J Cancer* **76,** 206-210.

Modica-Napolitano J. S. and Aprille J. R. (1987) Basis for the selective cytotoxicity of rhodamine 123. *Cancer Res* **47,** 4361-4365.

Mohanan P. V. and Yamamoto H. A. (2002) Preventive effect of melatonin against brain mitochondria DNA damage, lipid peroxidation and seizures induced by kainic acid. *Toxicol Lett* **129,** 99-105.

Montoya J., Christianson T., Levens D., Rabinowitz M., and Attardi G. (1982) Identification of initiation sites for heavy-strand and light-strand transcription in human mitochondrial DNA. *Proc Natl Acad Sci U S A* **79,** 7195-7199.

Montoya J., Gaines G. L., and Attardi G. (1983) The pattern of transcription of the human mitochondrial rRNA genes reveals two overlapping transcription units. *Cell* **34,** 151-159.

Murata T., Hibasami H., Maekawa S., Tagawa T., and Nakashima K. (1990) Preferential binding of cisplatin to mitochondrial DNA and suppression of ATP generation in human malignant melanoma cells. *Biochem Int* **20,** 949-955.

Nakabeppu Y. (2001) Regulation of intracellular localization of human MTH1, OGG1, and MYH proteins for repair of oxidative DNA damage. *Prog Nucleic Acid Res Mol Biol* **68,** 75-94.

Nakamura T. and Sakamoto K. (2001) Reactive oxygen species up-regulates cyclooxygenase-2, p53, and Bax mRNA expression in bovine luteal cells. *Biochem Biophys Res Commun* **284,** 203-210.

Nakashima R. A., Paggi M. G., and Pedersen P. L. (1984) Contributions of glycolysis and oxidative phosphorylation to adenosine 5'-triphosphate production in AS-30D hepatoma cells. *Cancer Res* **44,** 5702-5706.

Novotny E. J., Jr., Singh G., Wallace D. C., Dorfman L. J., Louis A., Sogg R. L., and Steinman L. (1986) Leber's disease and dystonia: a mitochondrial disease. *Neurology* **36,** 1053-1060.

Ohkoshi N., Mizusawa H., Shiraiwa N., Shoji S., Harada K., and Yoshizawa K. (1995) Superoxide dismutases of muscle in mitochondrial encephalomyopathies. *Muscle Nerve* **18,** 1265-1271.

Ojala D., Montoya J., and Attardi G. (1981) tRNA punctuation model of RNA processing in human mitochondria. *Nature* **290,** 470-474.

Oldfors A., Holme E., Tulinius M., and Larsson N. G. (1995) Tissue distribution and disease manifestations of the tRNA(Lys) A-->G(8344) mitochondrial DNA mutation in a case of myoclonus epilepsy and ragged red fibres. *Acta Neuropathol (Berl)* **90,** 328-333.

Olivero O. A., Chang P. K., Lopez-Larraza D. M., Semino-Mora M. C., and Poirier M. C. (1997) Preferential formation and decreased removal of cisplatin-DNA adducts in Chinese hamster ovary cell mitochondrial DNA as compared to nuclear DNA. *Mutat Res* **391,** 79-86.

Ono T., Isobe K., Nakada K., and Hayashi J. I. (2001) Human cells are protected from mitochondrial dysfunction by complementation of DNA products in fused mitochondria. *Nat Genet* **28,** 272-275.

Pang C. Y., Lee H. C., and Wei Y. H. (2001) Enhanced oxidative damage in human cells harboring A3243G mutation of mitochondrial DNA: implication of oxidative stress in the pathogenesis of mitochondrial diabetes. *Diabetes Res Clin Pract* **54 Suppl 2,** S45-S56.

Papermaster B. W., Pincus J. H., Lincoln P., and Reisfeld R. A. (1974) Probit analysis of cytotoxicity data. *Transplantation* **18,** 541-544.

Parrella P., Seripa D., Matera M. G., Rabitti C., Rinaldi M., Mazzarelli P., Gravina C., Gallucci M., Altomare V., Flammia G., Casalino B., Benedetti-Panici P. L., and Fazio V. M. (2003) Mutations of the D310 mitochondrial mononucleotide repeat in primary tumors and cytological specimens. *Cancer Lett* **190,** 73-77.

Parrella P., Xiao Y., Fliss M., Sanchez-Cespedes M., Mazzarelli P., Rinaldi M., Nicol T., Gabrielson E., Cuomo C., Cohen D., Pandit S., Spencer M., Rabitti C., Fazio V. M., and Sidransky D. (2001) Detection of mitochondrial DNA mutations in primary breast cancer and fine-needle aspirates. *Cancer Res* **61,** 7623-7626.

Penso J. and Beitner R. (1998) Clotrimazole and bifonazole detach hexokinase from mitochondria of melanoma cells. *Eur J Pharmacol* **342,** 113-117.

Penta J. S., Johnson F. M., Wachsman J. T., and Copeland W. C. (2001) Mitochondrial DNA in human malignancy. *Mutat Res* **488,** 119-133.

Petit J. M., Maftah A., Ratinaud M. H., and Julien R. (1992) 10N-nonyl acridine orange interacts with cardiolipin and allows the quantification of this phospholipid in isolated mitochondria. *Eur J Biochem* **209,** 267-273.

Pieri C., Moroni F., and Recchioni R. (1992) Glutathione influences the proliferation as well as the extent of mitochondrial activation in rat splenocytes. *Cell Immunol* **145,** 210-217.

Pitkanen S. and Robinson B. H. (1996) Mitochondrial complex I deficiency leads to increased production of superoxide radicals and induction of superoxide dismutase. *J Clin Invest* **98,** 345-351.

Plas D. R. and Thompson C. B. (2002) Cell metabolism in the regulation of programmed cell death. *Trends Endocrinol Metab* **13,** 75-78.

Polyak K., Li Y., Zhu H., Lengauer C., Willson J. K., Markowitz S. D., Trush M. A., Kinzler K. W., and Vogelstein B. (1998) Somatic mutations of the mitochondrial genome in human colorectal tumours. *Nat Genet* **20,** 291-293.

Porteous W. K., James A. M., Sheard P. W., Porteous C. M., Packer M. A., Hyslop S. J., Melton J. V., Pang C. Y., Wei Y. H., and Murphy M. P. (1998) Bioenergetic consequences of accumulating the common 4977-bp mitochondrial DNA deletion. *Eur J Biochem* **257,** 192-201.

Preston T. J., Woodgett J. R., and Singh G. (2003) JNK1 activity lowers the cellular production of H2O2 and modulates the growth arrest response to scavenging of H2O2 by catalase. *Exp Cell Res* **285,** 146-158.

Pryor W. A. (1986) Oxy-radicals and related species: their formation, lifetimes, and reactions. *Annu Rev Physiol* **48,** 657-667.

Raha S., McEachern G. E., Myint A. T., and Robinson B. H. (2000) Superoxides from mitochondrial complex III: the role of manganese superoxide dismutase. *Free Radic Biol Med* **29,** 170-180.

Raha S. and Robinson B. H. (2001) Mitochondria, oxygen free radicals, and apoptosis. *Am J Med Genet* **106,** 62-70.

Rhee S. G., Kim K. H., Chae H. Z., Yim M. B., Uchida K., Netto L. E., and Stadtman E. R. (1994) Antioxidant defense mechanisms: a new thiol-specific antioxidant enzyme. *Ann N Y Acad Sci* **738,** 86-92.

Rossmanith W., Tullo A., Potuschak T., Karwan R., and Sbisa E. (1995) Human mitochondrial tRNA processing. *J Biol Chem* **270,** 12885-12891.

Rungi A. A., Primeau A., Nunes C. L., Gordon J. W., Robinson B. H., and Hood D. A. (2002) Events upstream of mitochondrial protein import limit the oxidative capacity of fibroblasts in multiple mitochondrial disease. *Biochim Biophys Acta* **1586,** 146-154.

Rustin P., Chretien D., Bourgeron T., Gerard B., Rotig A., Saudubray J. M., and Munnich A. (1994) Biochemical and molecular investigations in respiratory chain deficiencies. *Clin Chim Acta* **228,** 35-51.

Sanchez-Cespedes M., Parrella P., Nomoto S., Cohen D., Xiao Y., Esteller M., Jeronimo C., Jordan R. C., Nicol T., Koch W. M., Schoenberg M., Mazzarelli P., Fazio V. M., and Sidransky D. (2001) Identification of a mononucleotide repeat as a major target for mitochondrial DNA alterations in human tumors. *Cancer Res* **61,** 7015-7019.

Sato S., Kigawa J., Minagawa Y., Okada M., Shimada M., Takahashi M., Kamazawa S., and Terakawa N. (1999) Chemosensitivity and p53-dependent apoptosis in epithelial ovarian carcinoma. *Cancer* **86,** 1307-1313.

Satoh M., Kashihara N., Fujimoto S., Horike H., Tokura T., Namikoshi T., Sasaki T., and Makino H. (2003) A novel free radical scavenger, edarabone, protects against cisplatin-induced acute renal damage in vitro and in vivo. *J Pharmacol Exp Ther* **305,** 1183-1190.

Saybasili H., Yuksel M., Haklar G., and Yalcin A. S. (2001) Effect of mitochondrial electron transport chain inhibitors on superoxide radical generation in rat hippocampal and striatal slices. *Antioxid Redox Signal* **3,** 1099-1104.

Sbisa E., Tanzariello F., Reyes A., Pesole G., and Saccone C. (1997) Mammalian mitochondrial D-loop region structural analysis: identification of new conserved sequences and their functional and evolutionary implications. *Gene* **205,** 125-140.

Schatz G. (1995) Mitochondria: beyond oxidative phosphorylation. *Biochim Biophys Acta* **1271,** 123-126.

Schmiedel J., Jackson S., Schafer J., and Reichmann H. (2003) Mitochondrial cytopathies. *J Neurol* **250,** 267-277.

Schon, E. A. Mitochondria. In:Mitochondrial DNA in Human Pathology. 1-7. 1993. New York: Raven Press Ltd. DiMauro, S. and Wallace, D. C.
Ref Type: Generic

Schon E. A., Bonilla E., and DiMauro S. (1997) Mitochondrial DNA mutations and pathogenesis. *J Bioenerg Biomembr* **29,** 131-149.

Schwartz M. and Vissing J. (2002) Paternal inheritance of mitochondrial DNA. *N Engl J Med* **347,** 576-580.

Sewards R., Wiseman B., and Jacobs H. T. (1994) Apparent functional independence of the mitochondrial and nuclear transcription systems in cultured human cells. *Mol Gen Genet* **245,** 760-768.

Sheehan J. P., Swerdlow R. H., Miller S. W., Davis R. E., Parks J. K., Parker W. D., and Tuttle J. B. (1997) Calcium homeostasis and reactive oxygen species production in cells transformed by mitochondria from individuals with sporadic Alzheimer's disease. *J Neurosci* **17,** 4612-4622.

Shoffner J. M., Brown M. D., Stugard C., Jun A. S., Pollock S., Haas R. H., Kaufman A., Koontz D., Kim Y., Graham J. R., and . (1995) Leber's hereditary optic neuropathy plus dystonia is caused by a mitochondrial DNA point mutation. *Ann Neurol* **38,** 163-169.

Shoffner J. M., Fernhoff P. M., Krawiecki N. S., Caplan D. B., Holt P. J., Koontz D. A., Takei Y., Newman N. J., Ortiz R. G., Polak M., and . (1992) Subacute necrotizing encephalopathy: oxidative phosphorylation defects and the ATPase 6 point mutation. *Neurology* **42,** 2168-2174.

Shoffner, J. M. and Wallace, D. C. In: The Metabolic and Molecular Basis of Disease. Eds.Scriver, C. R. Beaudet A. L. W. S. Sly Valle D. 1535-1609. 1995. New York, McGraw Hill.
Ref Type: Generic

Simonnet H., Alazard N., Pfeiffer K., Gallou C., Beroud C., Demont J., Bouvier R., Schagger H., and Godinot C. (2002) Low mitochondrial respiratory chain content correlates with tumor aggressiveness in renal cell carcinoma. *Carcinogenesis* **23,** 759-768.

Singh G., Sharkey S. M., and Moorehead R. (1992) Mitochondrial DNA damage by anticancer agents. *Pharmacol Ther* **54,** 217-230.

Soini Y., Vakkala M., Kahlos K., Paakko P., and Kinnula V. (2001) MnSOD expression is less frequent in tumour cells of invasive breast carcinomas than in in situ carcinomas or non-neoplastic breast epithelial cells. *J Pathol* **195,** 156-162.

Sousa S. C., Maciel E. N., Vercesi A. E., and Castilho R. F. (2003) Ca2+-induced oxidative stress in brain mitochondria treated with the respiratory chain inhibitor rotenone. *FEBS Lett* **543,** 179-183.

Staniek K., Gille L., Kozlov A. V., and Nohl H. (2002) Mitochondrial superoxide radical formation is controlled by electron bifurcation to the high and low potential pathways. *Free Radic Res* **36,** 381-387.

Suzuki H., Hosokawa Y., Nishikimi M., and Ozawa T. (1991) Existence of common homologous elements in the transcriptional regulatory regions of human nuclear genes and mitochondrial gene for the oxidative phosphorylation system. *J Biol Chem* **266,** 2333-2338.

Suzuki H., Suzuki S., Kumar S., and Ozawa T. (1995) Human nuclear and mitochondrial Mt element-binding proteins to regulatory regions of the nuclear respiratory genes and to the mitochondrial promoter region. *Biochem Biophys Res Commun* **213,** 204-210.

Swerdlow R. H., Parks J. K., Cassarino D. S., Maguire D. J., Maguire R. S., Bennett J. P., Jr., Davis R. E., and Parker W. D., Jr. (1997) Cybrids in Alzheimer's disease: a cellular model of the disease? *Neurology* **49,** 918-925.

Swerdlow R. H., Parks J. K., Miller S. W., Tuttle J. B., Trimmer P. A., Sheehan J. P., Bennett J. P., Jr., Davis R. E., and Parker W. D., Jr. (1996) Origin and functional consequences of the complex I defect in Parkinson's disease. *Ann Neurol* **40,** 663-671.

Tan D. J., Bai R. K., and Wong L. J. (2002) Comprehensive scanning of somatic mitochondrial DNA mutations in breast cancer. *Cancer Res* **62,** 972-976.

Tatuch Y., Christodoulou J., Feigenbaum A., Clarke J. T., Wherret J., Smith C., Rudd N., Petrova-Benedict R., and Robinson B. H. (1992) Heteroplasmic mtDNA mutation (T----G) at 8993 can cause Leigh disease when the percentage of abnormal mtDNA is high. *Am J Hum Genet* **50,** 852-858.

Tomura H., Endo H., Kagawa Y., and Ohta S. (1990) Novel regulatory enhancer in the nuclear gene of the human mitochondrial ATP synthase beta-subunit. *J Biol Chem* **265,** 6525-6527.

Torroni A., Stepien G., Hodge J. A., and Wallace D. C. (1990) Neoplastic transformation is associated with coordinate induction of nuclear and cytoplasmic oxidative phosphorylation genes. *J Biol Chem* **265,** 20589-20593.

Toyokuni S., Okamoto K., Yodoi J., and Hiai H. (1995) Persistent oxidative stress in cancer. *FEBS Lett* **358,** 1-3.

Trounce I., Neill S., and Wallace D. C. (1994) Cytoplasmic transfer of the mtDNA nt 8993 T-->G (ATP6) point mutation associated with Leigh syndrome into mtDNA-less cells demonstrates cosegregation with a decrease in state III respiration and ADP/O ratio. *Proc Natl Acad Sci U S A* **91,** 8334-8338.

Tsukihara T., Aoyama H., Yamashita E., Tomizaki T., Yamaguchi H., Shinzawa-Itoh K., Nakashima R., Yaono R., and Yoshikawa S. (1996) The whole structure of the 13-subunit oxidized cytochrome c oxidase at 2.8 A. *Science* **272,** 1136-1144.

Tully L. A. and Levin B. C. (2000) Human mitochondrial genetics. *Biotechnol Genet Eng Rev* **17,** 147-177.

Virbasius J. V. and Scarpulla R. C. (1994) Activation of the human mitochondrial transcription factor A gene by nuclear respiratory factors: a potential regulatory link between nuclear and mitochondrial gene expression in organelle biogenesis. *Proc Natl Acad Sci U S A* **91,** 1309-1313.

Wallace D. C. (1992) Diseases of the mitochondrial DNA. *Annu Rev Biochem* **61,** 1175-1212.

Wallace D. C. (1997) Mitochondrial DNA in aging and disease. *Sci Am* **277,** 40-47.

Wallace D. C. (1999) Mitochondrial diseases in man and mouse. *Science* **283,** 1482-1488.

Wallace D. C., Singh G., Lott M. T., Hodge J. A., Schurr T. G., Lezza A. M., Elsas L. J., and Nikoskelainen E. K. (1988) Mitochondrial DNA mutation associated with Leber's hereditary optic neuropathy. *Science* **242,** 1427-1430.

Warberg, O. The metabolism of tumors. London ConsTable Co.Ttd. 1930.

Warburg, O. On the origin of cancer cells. *Science* **123**, 309-314. 1956.

Wei Y. H. (1992) Mitochondrial DNA alterations as ageing-associated molecular events. *Mutat Res* **275,** 145-155.

Wei Y. H. (1998) Oxidative stress and mitochondrial DNA mutations in human aging. *Proc Soc Exp Biol Med* **217,** 53-63.

Wei Y. H., Lee C. F., Lee H. C., Ma Y. S., Wang C. W., Lu C. Y., and Pang C. Y. (2001) Increases of mitochondrial mass and mitochondrial genome in association with enhanced oxidative stress in human cells harboring 4,977 BP-deleted mitochondrial DNA. *Ann N Y Acad Sci* **928,** 97-112.

Weiss H., Friedrich T., Hofhaus G., and Preis D. (1991) The respiratory-chain NADH dehydrogenase (complex I) of mitochondria. *Eur J Biochem* **197,** 563-576.

Wong A. and Cortopassi G. A. (2002) High-throughput measurement of mitochondrial membrane potential in a neural cell line using a fluorescence plate reader. *Biochem Biophys Res Commun* **298,** 750-754.

Yamamoto H. A. and Mohanan P. V. (2003) Ganglioside GT1B and melatonin inhibit brain mitochondrial DNA damage and seizures induced by kainic acid in mice. *Brain Res* **964,** 100-106.

Yamamoto K., Okamoto A., Isonishi S., Ochiai K., and Ohtake Y. (2001) Heat shock protein 27 was up-regulated in cisplatin resistant human ovarian tumor cell line and associated with the cisplatin resistance. *Cancer Lett* **168,** 173-181.

Yin Y., Terauchi Y., Solomon G. G., Aizawa S., Rangarajan P. N., Yazaki Y., Kadowaki T., and Barrett J. C. (1998) Involvement of p85 in p53-dependent apoptotic response to oxidative stress. *Nature* **391,** 707-710.

Yoshida M., Fukuda A., Hara M., Terada A., Kitanaka Y., and Owada S. (2003) Melatonin prevents the increase in hydroxyl radical-spin trap adduct formation caused by the addition of cisplatin in vitro. *Life Sci* **72,** 1773-1780.

Zinkewich-Peotti K. and Andrews P. A. (1992) Loss of cis-diamminedichloroplatinum(II) resistance in human ovarian carcinoma cells selected for rhodamine 123 resistance. *Cancer Res* **52,** 1902-1906.

6.0 Appendix

Cell Line	CDDP resistance	$\Delta\Psi_M$	Rh123 resistance	ROS	O_2 consumption	Complex I	COX	CS
2008	+	+	+++	+	+++	+++	+++	+++
C13*	+++	+++	+	+++	+	+	+	+
RH4	++		+++		+	+	+	+

Cell Line	CDDP resistance	$\Delta\Psi_M$	Rh123 resistance	ROS	O_2 consumption	Complex I	COX	CS
2008cyb	++	+++	++	+	++	++	++	+++
C13*cyb	+	+++	+	+++	+++	+++	+++	+++
143B ρ^o	+++	+	+++	+	+	none	none	+++

Table 6.1: Summary of Phenotypic Characteristics of 2008, C13*, RH4, 2008cyb, C13*cyb and 143B ρ^o cells.